Study on Vapor Transfer Processes into the Atmosphere from Vegetated Surface in an Arid Region

Takashi SATOH

200821176

January 2010

A Thesis Submitted to

The Graduate School of Life and Environmental Sciences

The University of Tsukuba

in Partial Fulfillment of the Requirements

for the Degree of Master of Environmental Sciences

Abstract

Although evapotranspiration takes important place of the hydrological cycle especially in the arid region, there are not many studies that considered comprehensively including plant water use strategy. The aim of our study was to investigate the characteristics of soil surface-atmosphere water vapor transfer processes considering soil moisture variability with plant activity in the arid steppe of central Mongolia. The steppe is dominated by shrubs (*Caragana microphylla*) and herbaceous plant (*Allium polyrrhizum*). Distribution of evaporation (EV) and transpiration (TR) was estimated by using chamber measurement from bare soil and dominant species. Measurements were took place for 3 days on early June when the surface was dry, and 22 days on July between successive rainfall events when the upper soil moisture changed significantly. At the same time, stable hydrogen and oxygen isotopes were used to determine water source of transpiration. On the beginning of July when there were no successive rainfalls for about two months, only shrubs were observed. The rate of EV to TR was about 85:15 on this period while vegetation coverage was only 3.12%. After the rainfall, EV and TR from herbaceous plants increased significantly while TR from shrubs did not respond. Isotopic signature of plant and soil samples indicated that shrubs uptake water from around 80cm deep where soil volumetric water content was higher (around 6%) than the surface which contains only 3-4%. The result indicates that even if the vegetation coverage was small, plant activities and hydrologically active soil moisture profiles might be important factor to consider when estimating water vapor transfer from vegetated surface into the atmosphere in arid region.

Key words: evapotranspiration, chamber measurement, stable isotope analysis, arid region

Contents

List of Table

List of Figures

1. Introduction

1. 1 Water Scarcity

Water scarcity has been one of the biggest issues in the 21st century. It is estimated that almost half of the global population will not be able to access fresh water by 2030 (World Water Assessment Programme, 2009). Not only for drinking but it is also a critical issue for whole terrestrial ecosystems which supply foods, goods and many other benefits for human. Especially, in an arid region, ensuring water has been a fatal issue. Mongolia is one of such countries whose water resource is limited where 38% of its citizens could not access to water suitable for drinking in 2002 (United Nations Development Programme, 2004). However, more than 90% of the Mongolian people rely on groundwater (Sugita, 2003). Therefore, it is important to understand the water cycle to evaluate the behavior of the groundwater.

1. 2 Ecosystems in Mongolia

Mongolia is a landlocked country in central East Asia which occupies the largest part of the Mongolian Plateau. The ecosystem of Mongolia varies from the Gobi Desert to the south and to the forested area to the north (Figure 1) (Saandar and Sugita, 2005). However, most of Mongolia consists of steppes. This vegetation distribution follows that of the amount of annual rainfall (Sugita, 2003). Mean annual precipitation in the country is limited and is largest in the northern part (250-400 mm/year) and decreases toward south (less than150 mm/year) with more than 60% falls during summer time (Davaa et al., 2006). Yamanaka et al. (2007a) indicates that part of the source of the precipitation in July is from rice paddy fields in southeast China.

Mongolia is affected by global warming and aridification (Yasunari, 2003; Sato et al., 2007). Sato et al. (2007) indicates that the soil moisture over Mongolia tends to decrease in July and it affect vegetation distribution among the country. As mentioned above, this country is in ecotone that is in general considered to be vulnerable to climatic changes (Stott, 1994). Mongolia has been exposed to overgrazing due to the introduction of market economy in 1990 (Mori, 2003). This is due to the fact that has been the demands for lambs and goats are increasing because of the rising population and incentive to gain more wage income (Mori, 2003). As a result, these natural and social had been a driving force of ecosystem changes in Mongolia (Sugita et al., 2007).

To take measures to solve water scarcity and to understand ecosystem changing, knowledge of the water cycle process is essential. Also, from the hydrological point of view, it is absorbing to reveal how hydrological processes affect those vegetations variability, and to understand the interaction between vegetated surface and atmosphere in arid region.

1. 3. Evapotranspiration

In most of an arid and a semi-arid region, precipitation is the only supplier of the water into to a basin. Evapotranspiration (ET) occupies the greater portion of decrement factor of water in a basin on arid region (Yasunari, 2003; Kurc and Small, 2004; Yamanaka et al., 2007b). Thus, amount and timing of precipitation and ET can strongly affect ground water recharge. Therefore, relation of precipitation and ET rate can be an important factor for understanding the water cycle. Although measurement of precipitation is relatively easy, ET is more difficult to measure and many methodologies have been developed to measure ET. Such measurement techniques for ET include eddy correlation method (Li, 2007), Bowen ratio method (Kurc and Small, 2004), catchment water budget (Wilson et al., 2001), stable isotope tracer (Yepez et al., 2003; Sasaki, 2004; Tsujimura et al., 2007b), compensated heat pulse system (sap flow) (Cohen et al., 1988; Xu and Li, 2006), and chamber method (Heijmans et al., 2004; Yepez et al., 2005: Stannard and Mark, 2006; Nakano et al., 2007). These techniques have spatial and temporal scales in which they are applicable, and also there are difference in whether they measure ET or just one or several of its components, i.e. evaporation (EV) and transpiration (TR) (Wilson et al., 2001). Eddy correlation method, Bowen ratio method and catchment water budget method are suitable for the application on a relatively large spatial scale. But these methods have disadvantage that they can not separate ET components. EV and TR can be partitioned by using stable isotope tracer. But this method is not suitable for observing spatially and temporary small ET processes. For example, it is difficult to discriminate TR from each individual species, or EV and TR interaction with precipitation. To understand detailed ET behavior, compensated heat pulse system and chamber method are more adequate. However, by using compensated heat pulse system, they cause damages to plants because this method has to pierce a sensor into branches. Also, this method is capable of measuring TR but is incapable of measuring EV. On the other hand, chamber method can be used both for EV and TR measurement by applying the same procedure by covering either bare soils or plants without disturbing environment. Although chamber measurement is often criticized for their potential to change the environment of the vegetation or soil surface which could disturb the measured flux (Heijmans et al., 2004), its effect has been minimized by making measurement in a short time period in which temporal environmental changes could be limited (Stannard and Weltz, 2006).

1. 4. Below ground water movement

When we consider the surface-atmosphere vapor transfer processes, not only the surface vapor transfer processes themselves but also the behaviors of soil water and plant water use strategies are important (Gochis et al., 2009). One of the methods to reveal a behavior of the

soil water is to utilize vertical profile of stable isotope ratio of oxygen and hydrogen (Yabusaki, 2007). This method is also capable of determining the depth of soil water which plants uptake because isotopic composition in xylem sap corresponds to the average isotopic composition in soil water they utilizes (Yamanaka et al., in preparation). There are many examples which had studied the water utilization strategy of plants by using this method from a wide range of ecosystems (e.g. Ehleringer et al., 1991; Smith et al., 1997; Weltzin and McPherson, 1997; Zencich et al. 2002; Romero-Saltos et al., 2005).

1. 5 Purpose of the study

In this study, we aim at investigating the characteristics of vegetated surface-atmosphere water vapor transfer processes with consideration of soil water behavior and plant activity in an arid region, using chamber method and stable isotope ratio analysis of oxygen and hydrogen. We also conducted vegetation survey such as vegetation coverage analysis, above and below ground biomass and total upper leaf area for the validation of those experiments.

2. Materials and Methods

2. 1 Study area

The study was conducted at about 4 km north east from Mandalgobi, Dundgobi aimag, Mongolia (Figure 1). The climate in this area is classified as arid (Nakamura et al., 2007). According to the Mandalgobi meteorological station near the Mandalgobi airport (about 5.5km southeast from the study area) operated by the Institute of Meteorology and Hydrology, Mongolia (IMH), mean annual precipitation is 153 mm for the period 1944 - 2007. About 78% of precipitation falls during the summer season (Figure 2). The mean annual air temperature at Mandalgobi is 1.5 °C with January being the coldest month (mean monthly air temperature: -17.7 °C) and July the hottest (mean monthly air temperature: 19.3 °C). The vegetation is predominantly shrub (*Caragana microphylla*, C_3 plant) and herbaceous plant (*Allium polyrrhizum*, C_3 plant) (Figure 3). However, there were only *Caragana* in the beginning of July, 2009 until successive rainfalls in July 17 and 18, 2009. These plants, especially *Allium*, were under grazing pressure from sheep and goat of some nomadic herdsmen. The topography of this area is rugged gentle slope where large size shrubs are forming mounds (Figure 4). Mounds were formed under the shrubs by their trapping wind-blown topsoil particles from the surrounding bare soil surfaces. In these mounds, nutrients such as nitrogen and phosphorus compounds are accumulated because the blown topsoil includes litters (Fu et al., 2007). The field study was conducted during summer seasons of 2008 (July 5^{th} – 11^{th}, August 12^{th} – 17^{th}) and 2009 (May 21^{st} – June 11^{th}, July 9^{th} – August 2^{nd}).

2. 2 Environmental measurement

Two sets of automatic weather station (AWS) MG1 (45°49'11.30"N, 106°17'43.00"E) and MG2 (45°48'34.80"N, 106°16'51.40"E) were installed in the study area (Figure 1). These stations are shown in Figure 5. On the MG1 station, 3-cup anemometer (3101, R.M. Young) was installed at the height of 3 m and just beneath it humidity and temperature probe (HMP45D, Vaisala) housed within a 10-plate radiation shield (41003-5, Campbell Scientific, Inc.) were installed (2.65 m from the ground). A solar panel which supplies power to the station was placed on the top of the pole to prevent direct sunshine to the radiation shield. Upward and downward components of long-wave and short-wave radiation were measured by a 4-component net radiometer (NR01, Hukseflux Thermal Sensors) at 2.5 m from the ground surface and soil heat flux was measured by a soil heat flux plate (HFP01, Hukseflux Thermal Sensors) just below the surface at about 0.01 m deep. Precipitation was measured by a tipping bucket rain gauge (TR-525M, Texas Electronics) at 0.6 m height. This height was selected to prevent dusts and soil particles blown into the sensor. Time domain reflectometry (TDR) (CS-616, Campbell Scientific, Inc.) were placed at 0.05, 0.1, 0.2, 0.3, 0.7 and 1.1 m depth to

measure soil volumetric water content. Soil temperature at 0.1, 0.3 and 0.7 deep were measured by a platinum resistance thermometer (C-PTG-10, Climatec, Inc.) buried at each depth. These sensors for volumetric soil water content and soil temperature were buried under the mounds with shrubs. On the MG2 station, a 2-component radiation sensor (RA01, Hukseflux Thermal Sensors) were installed at 2.5 m above the ground for the measurements of the upward short-wave and long-wave radiation. Downward components are assumed the same as those at the MG1. TDR (CS-616, Campbell Scientific, Inc.) were placed at 0.1, 0.2, 0.3, 0.5 and 0.7 m depth for volumetric soil water content. Soil temperatures at 0.1, 0.2, 0.3, 0.5 and 0.7 depth were measured by a platinum resistance thermometer (C-PTG-10, Climatec, Inc.) buried at each depth. Details are also shown in Table 1. MG1 station started operation on July 7th, 2008 and MG2 on May 3rd, 2009.

During the growing season of 2008 and 2009, volumetric soil water content distribution near the surface was measured several times manually. A handy type TDR sensor (CS620 12cm probe, Campbell Scientific, Inc.) was inserted into soil at 30 to 45 degree from surface to measure soil moisture at twenty points in each of eight directions at a1.5 m interval from the center (Figure 6).

2. 3 Vegetation survey

2. 3. 1 Vegetation coverage

Vegetation coverage was determined by taking photographs of the vegetated surface from waist-height by keeping a camera (EX-Z600, CASIO COMPUTER CO., LTD., Japan) horizontal from the surface on June 2nd, July 11th, 19th, 25th and 29th. On each day, we took 1600 × 1200 pixel photographs at twenty points at 1.5 m interval for each of the eight directions extending from the center. They are the same points used for the measurement of soil surface water content distribution (Figure 6). In the classification procedure, it was found difficult to differentiate shadow from leaves. Therefore, it was decided to take photographs in a cloudy period to prevent shadows. Each digital camera image was then transformed from RGB color image to IHS color image by using a color space-transformation method of ERDAS IMAGINE (Leica Geosystems, ver. 9.1, USA). This was done because it is suggested that the IHS color space system is more suitable for the image processing procedure (Byambakhuu, 2007). Finally, the supervised classification was applied to those IHS images to distinguish bare soil from vegetation and calculate coverage (Figure 7). Details on this procedure can be found in Byambakhuu (2007).

2. 3. 2 Above ground biomass

Nine 50 cm × 50 cm quadrats were established on each corner, midpoint of the side and

center of a 20 m × 20 m square also established near the MG1 station to randomly sample the above ground biomasses (Figure 8). Photographs of each quadrat were taken to determine the vegetation coverage and the correlation with biomass. Plants inside the quadrat were all cut by using pruning clippers and kept in a paper bag. Their weight was measured after drying 24 hours by an oven at 80°C. The above ground biomass was sampled on July 10th, 12th, 20th, 25th and 29th.

2. 3. 3 Below ground biomass

Vertical profile of small sized roots and large sized roots distribution was estimated respectively by determining below ground biomass. Small sized roots were separated by using 500 μm and 211 μm mesh hand sieve from a 1000 cm^3 cubic soil samples which was taken off from the side wall of a 1 m × 2 m wide and 1 m deep trench at 0.1 m interval (Figure 9). Large sized roots were sampled by digging a 1.2 m × 1 m wide and 1 m deep trench just below a mound with shrubs cuts the mound (1.2 m in diameter) so that diameter of the mound corresponds to the trench wall. All exposed taproots were cut and sampled at 0.1 m interval (Figure 10). All samples were put into paper bags and weighted after drying 24 hours by an oven at 80°C. Below ground biomass of fine root was sampled on July 7th, 2008 and on July 13th, 2009 while biomass for taproot was sampled on July 28th, 2009.

2. 3. 4 Total one-sided leaf area

Total upper leaf area which represents total one-sided area of photosynthetic tissue is important to discuss plant activity through photosynthesis. The canopy area of both shrubs and herbaceous plant was also measured on of July 30th and 31st. Thirteen quadrats (15 cm × 15 cm) established for shrubs and 10 for herbaceous plants. These plants were chosen to include various sizes to obtain a functional relation between the total one-sided leaf area and canopy area. The total one-sided leaf area of plants which were subjected for the chamber measurement was also calculated. All the leaves from the plant inside the quadrat were removed and then scanned. Leaf area of scanned image was measured using LIA for Win32 Ver.0.378 (Yamamoto, 2008) a leaf area measuring software. Vegetation coverage was also measured for these plants by applying the procedures described in 2. 3. 1.

2. 4 Soil characteristic analysis

Soil samples for soil characteristic analysis were obtained with a stainless sampling tube and sealed with vinyl tape. Soils were sampled in a vertical direction for the depth of 0 - 100 cm depth at 10 cm interval on July 7th, 2008, June 2nd and July 31st, 2009. On July 7th, 2008 and June 2nd, 2009, 70 - 100 cm soils samples were sampled in horizontally direction from a

trench wall.

Water permeability was measured for each sample by applying the falling head method using a permeameter (DIK-4000, Daiki Rika Kogyo Co., Ltd.). For the June 2nd, 2009 samples, porocity and volumetric water content were determined by measuring the actual volume using a soil three phase meter (DIK-1121, Daiki Rika Kogyo Co., Ltd.) and by weighing samples before and after drying at 105 °C. Also, pF value of the samples was measured by the vacuum method using a pF meter (DIK-3340, Daiki Rika Kogyo Co., Ltd.).

2. 5 Chamber measurements

2. 5. 1 Field observations

The shape of the chamber was cylinder which has height of 0.3 m and 0.4 m in diameter, made of acrylic plastic (5 mm thick). Polyvinylchloride film extension was attached to the bottom edge of the chamber to minimize the effect of wind blowing into the chamber (Figure 11). Note that collar type chamber (Urano, 2004) was not applied for this study because it damages plants root. A fan was installed on the top center of the chamber which circulates and mixes the air inside chamber by air speed of 1.8 m/s. The wind speed at the middle part (10 cm above base) of the chamber was 0.7 - 0.9 m/s in a longitudinal direction and 0.2 m/s in a transverse direction. It was attached on that place of the chamber to make the condition inside the chamber close to natural (Heijmans et al., 2004) The chamber was connected to an air pump (MP-Σ300, Shibata Scientific Technology LTD.) which makes 1 L/min steady flow and a CO_2/H_2O gas analyzer (LI-840, LI-COR Biosciences) with a vinyl tube. The flow rate was monitored by connecting a flow meter (RK1700, Kojima Instruments Inc.) between the chamber and the air pump. Temperature of air inside the chamber, top soil surface (5 cm) inside and outside of the chamber was measured at the same time. Outside sensor readings were used as a reference. Incident photosynthetically active radiation (400-700 nm wavebands) was also measured with a quantum sensor (LI-190, LI-COR Biosciences) to provide photosynthetic photon flux density (PPFD) (Figure 11). It is an estimate of the number of photons in the 400-700 nm wavebands which are available for plants to produce sugars. It was measured outside the chamber at the height of 1.35 m. Because the chamber was not completely transparent, PPFD was modified with its transmittance of 83% which was determined experimentally by comparing PPFD inside and outside the chamber by the quantum sensor. All data were collected by a data logger (CR23X Micrologger, Campbell Scientific, Inc.) every second. System diagram is shown in Figure 12. Chamber measurements were carried out during daytime period for 3 days in early June (June 1st, 3rd and 4th) and 22 days in July (10th – 14th and 16th – 31st) in 2009 to determine the amount of evapotranspiration (ET) and its component, evaporation (EV) and transpiration (TR). In June, five individual shrubs (CA1,

CA2, CA3d, CA3 and CA4) and two herbaceous plants were chosen for TR measurement and five points of bare ground were chosen for EV measurement. The same individual shrubs selected in the June observing period were chosen in the beginning of July when herbaceous plants were not present. Because one shrub (CA3d) stands were dead on July 16th, another shrub (CA5) was added for the measurement. After the sufficient rainfall of July 17th (6.4 mm), five newly grown up herbaceous plants were added for the measurement. The chamber was covered about two minutes for each measurement. It was carried out at least 3 cycles (3 times for each individual) and it includes the time span between 11:00 to 15:00 to compare the ET day-by-day. On June 4th, July 14th, 18th (shortly after the sufficient rainfall), 21st and 25th, measurement started from sunrise to see a diurnal water vapor transfer changes. The same procedures as deriving vegetation coverage were applied for the determination of bare soil and canopy area inside the chamber (Figure 13).

Although as nomadic herdsmen live near the study site, plants which had chosen for the chamber measurement were not affected by grazing during the measuring period of June and July.

2. 5. 2 Data analysis

Water flux was derived from measured H_2O gas density variation. Thirty seconds data from gas density were picked out after its variation had been stabilized（Figure 14）. Water flux was derived by the following equation:

$$E = \Delta E \times \frac{v}{a} \times \frac{PM}{RT} \times \frac{1}{\rho_v} \times 60 \times 60 \qquad (1)$$

where E is the water flux (mm h^{-1}), ΔE is the variation of H_2O gas density (ppt s^{-1}), v is the volume of the chamber (m^3), a is the area of base of the chamber (m^2), P is the pressure (atm), M is the molar weight (g mol^{-1}), R is the gas constant (atm m^3 mol^{-1} K^{-1}), T is the absolute temperature (K) and ρ_v is water density (g m^{-2}) which was given as ρ_v = 1000. Because pressure was not measured, the daily average data from Mandalgovi meteorological station (IMH) was used instead. This was acceptable because there was only 1.2% difference on the result of water flux when pressure changed 10 hPa.

2. 6 Stable isotope analysis

2. 6. 1 Precipitation and groundwater sampling

Precipitation samples were continuously collected every month by the Mandalgobi center of the Institute of Meteorology and Hydrology, Mongolia from May through September, 2009.

Also, it was collected at Dalanzadagad, Omungobi province (about 270 km south from Mandaligobi. See Figure 1). During the same period by Dalanzadagad center of Institute of Meteorology and Hydrology, Mongolia. The precipitation samples from Dalanzadagad were collected for comparison. Rain water was collected with a funnel of 120 mm in diameter attached to a polyethylene tank containing a Ping-Pong ball to prevent evaporation (Yamanaka et al., 2007a) (Figure 15). It was fixed with some pegs and strings so as not to be blown away by a strong wind. The rain water accumulated in the tank was collected in a polyethylene bottle at the end of each month and groundwater was collected manually during the plant and soil sample collection periods from the MG1 site on June 1st and 20th and from the MG2 site on June 1st, July 11th, 18th and August 1st, 2009. Both rain water and groundwater samples were collected and stored in 100 ml polyethylene bottles.

2. 6. 2 Plant and soil sampling

Plant and soil samples were collected at the same time on July 7th, 2008, June 2nd, July 13th, 19th, 25th, and 28th, 2009. On July 13th only shrubs were sampled because herbaceous plants were no present. On July 22nd, only plant samples were collected. For *Caragana*, we collected randomly selected stems and roots fully covered with periderm which we peeled off from each individual and the remaining parts were stored in 100 ml fully sealed test tube and kept refrigerated. Soil samples were collected from depths of 5, 10, 20, 30, 40, 50, 60, 70, 80, 90 and 100 cm by digging a 1 m × 2 m wide and 1 m deep trench. Three samples from each depth were collected and placed into 200 ml glass vials double sealed with polyethylene and polypropylene caps. Soil samples were stored at ordinary temperature.

2. 6. 3 Water extractions from plant and soil samples

Water from plant samples were extracted using the cryogenic vacuum distillation method (Iizuka et al., 2004) (Figure 16). A 100-ml test tube which contains plant samples and an empty tube were connected to a branching tubule with silicon grease coated on the joints (Figure 16 (A)). The tube which contains plant samples was then submerged into liquid nitrogen to freeze plants completely with cock closed to make a closed system (Figure 16 (B)). To reduce the pressure inside the system, the branching tubule was connected to a vacuum pump and the cock is opened until it was sufficiently reduced (Figure 16 (C)). The water inside the plant will not scattered and lost because the test tube with plants was kept in liquid nitrogen during this process. After the pressure inside was sufficiently reduced, it was disconnected from the vacuum pump and then the test tube with the plant inside was put into a hot tub of 80 °C. At the same time, the empty test tube was put into liquid nitrogen (Figure 16 (D)). The water inside plants melts and evaporates immediately to move into the chilled tube

and trapped there by sublimation.

Ordinary temperature distillation method (Yamanaka and Shimada, 1997) was used to extract water from soil samples. The layout sketch is shown in Figure 17. This method was adopted because it is suitable for soil samples which contain a little soil water and also because it will not extract water from hydrated minerals. Such water cannot be utilized by plants. A sealed up polyethylene container with soil sample inside was connected to the cold trap chilled by -40 °C ethanol connected with fluorine-contained tube. The air inside the closed system was steadily circulated by electromagnetic pump (MV-6005 VP, Enomoto Micro Pump Mfg. Co., LTD.) which makes 4 L/min steady flow. The water was collected after 24 hours of operation.

2. 6. 4 Stable isotope ratio measurements

Hydrogen and oxygen stable isotope ratio was measured using an isotope ratio mass spectrometer (Finnigan MAT252, Thermo Fisher Scientific Inc.). Hydrogen stable isotope ratio was determined with the gaseous hydrogen equilibration method (Coplen, 1991) using hydrophobic platinum catalyst, while oxygen isotope ratio was determined with the carbon dioxide equilibration method (Socki et al., 1999). The stable isotope ratio of water sample was expressed in delta notation (‰) relative to the V-SMOW standard (Vienna-Standard Mean Ocean Water) by the following equation:

$$\delta_{Sample} = \left[\frac{R_{sample} - R_{SMOW}}{R_{SMOW}} \right] \times 1000 \qquad (2)$$

where R represents the heavy to light isotope ratio (D/H or $^{18}O/^{16}O$). The precision of the analysis by spectrometer was approximately ±1‰ for δD and ±0.1‰ for $\delta^{18}O$.

Table 1　List of installed sensors for Automatic Weather Station (AWS).

Item	Location	Installation height (m above ground)	Sensor	Sampling interval	Statistical strategy
Temperature (°C) Relative humidity (%)	MG1	2.65	Humidity and temperature probe (HMP45D, Vaisala) with 10-Plate Radiation Shield (41003-5, Campbell Scientific, Inc.)	10 min.	Instantaneous
Wind speed	MG1	3	Gill 3-Cup Anemometer (3101,　R. M. Young)	10 sec.	10 min. average
Upward and downward long-wave and short-wave radiation	MG1	2.5	4-component net radiation sensor (NR01, Hukseflux Thermal Sensors)	10 sec.	10 min. average
Upward long-wave and short-wave radiation	MG2	2.5	2-component radiation sensor (RA01, Hkseflux Thermal Sensors)	10 sec.	10 min. average
Soil volumetric water content	MG1 MG2	-0.05, -0.1, -0.2, -0.3, -0.7, -1.1 -0.1, -0.2, -0.3, -0.5, -0.7	Time domain reflectomery (CS-616, Campbell Scientific, Inc.)	1 min.	10 min. average
Soil heat flux	MG1	-0.01	Soil heat flux plate (HFP01, Hukseflux Thermal Sensors)	1 min.	10 min. average
Precipitation	MG1	0.6	Tipping Bucket Rain Gauge (TR-525M, Texas Electronics)	10 sec.	10 min. total
Soil temperature	MG1 MG2	-0.1, -0.3, -0.7 -0.1, -0.2, -0.3, -0.5, -0.7	Platinum resistance thermometer (C-PTG-10, Climatec, Inc.)	10 min.	Instantaneous

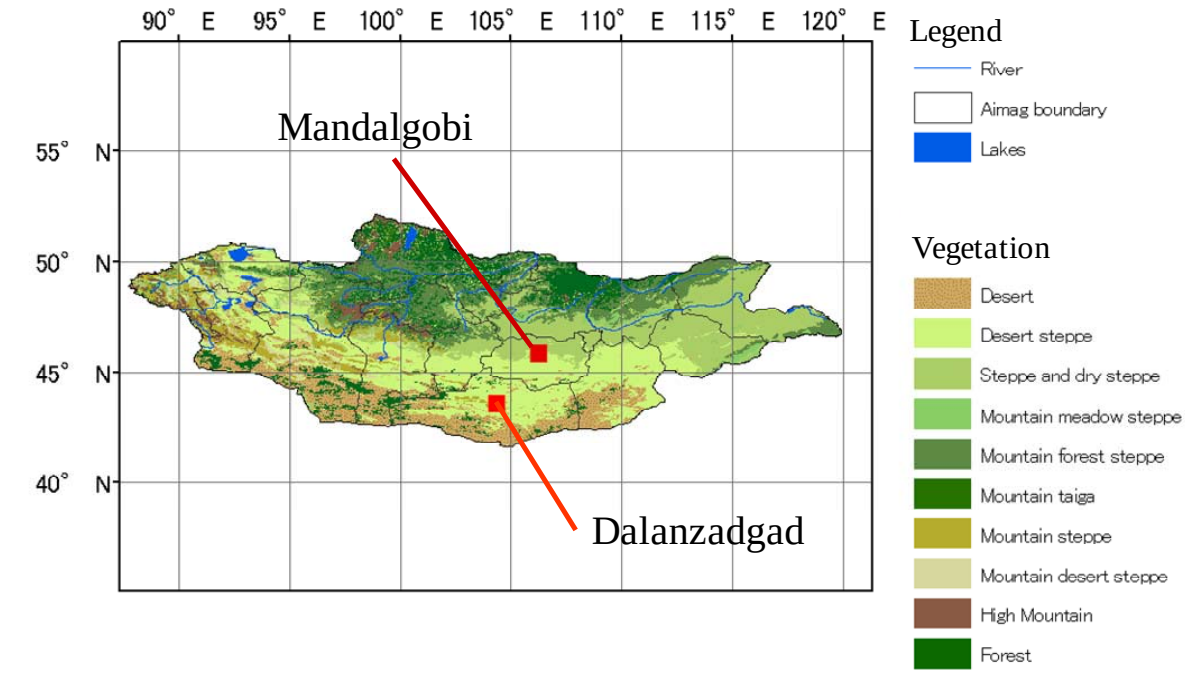

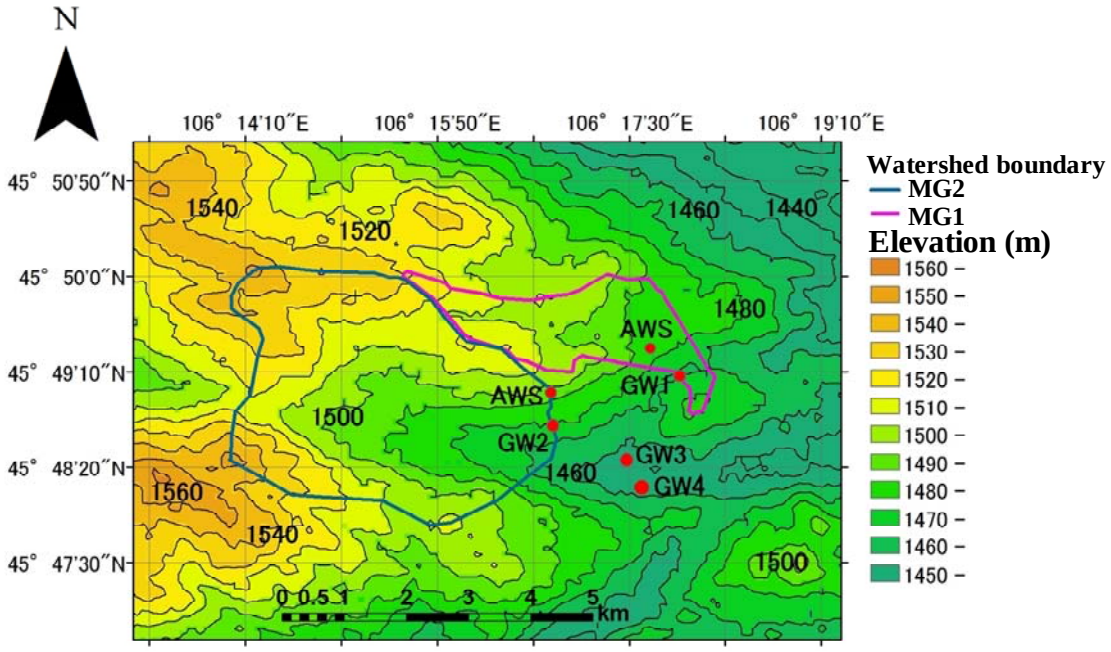

Figure 1 Location of Mandalgovi, Dundgovi aimag and Dalanzadagad, Omunogobi aimag (province), Mongolia (top) (data source: Saandar and Sugita, 2005) and topography of the study area (below) (Yoshizawa, 2010). Red closed circle in below map indicates the locations of Automatic Weathering Station (AWS) and wells (GW1 – GW4).

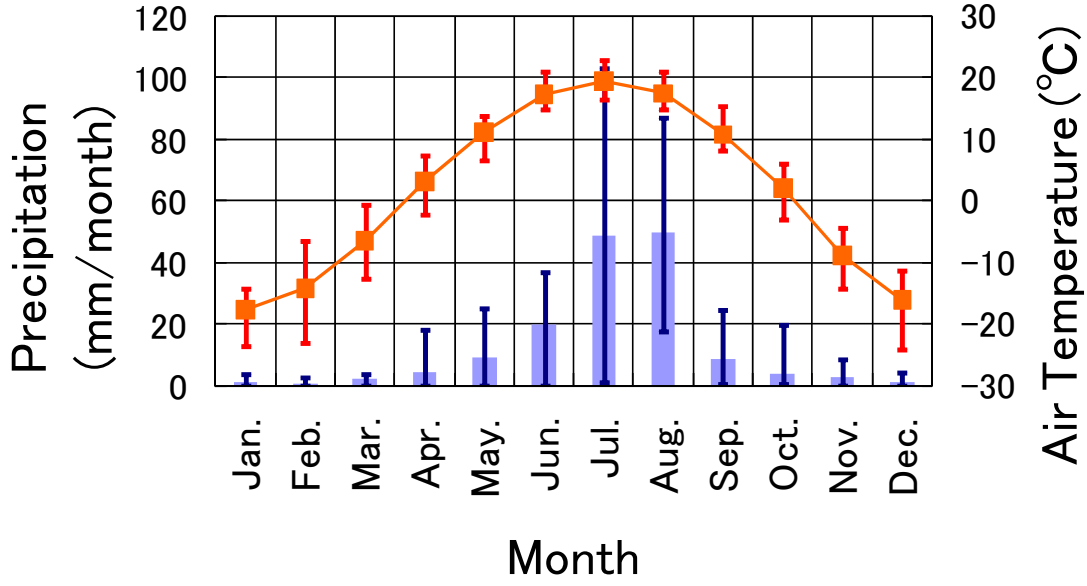

Figure 2　Mean monthly precipitation and mean monthly air temperature of 1993-2003 from Mandalgovi meteorological station operated by Institute of Hydrology and Meteorology, Mongolia.　Error bar shows the maximum and minimum values of each data.

A

B

Figure 3 Dominant species around study area, shrub and herbaceous plant. A: *Caragana microphylla*, C_3 plant (MG1, June 2nd, 2009). B: *Allium polyrrhizum*, C_3 plant (MG1, July 31st, 2009).

A

B

Figure 4 Landscape view of the study area (A) and shrubs with mound (B). Red dashed line shows the shape of the mound. It was formed under the shrubs by trapping wind-blown particles from the surrounding bare soil surfaces.

A

B

Figure 5 The MG1 station (A) and the MG2 station (B).

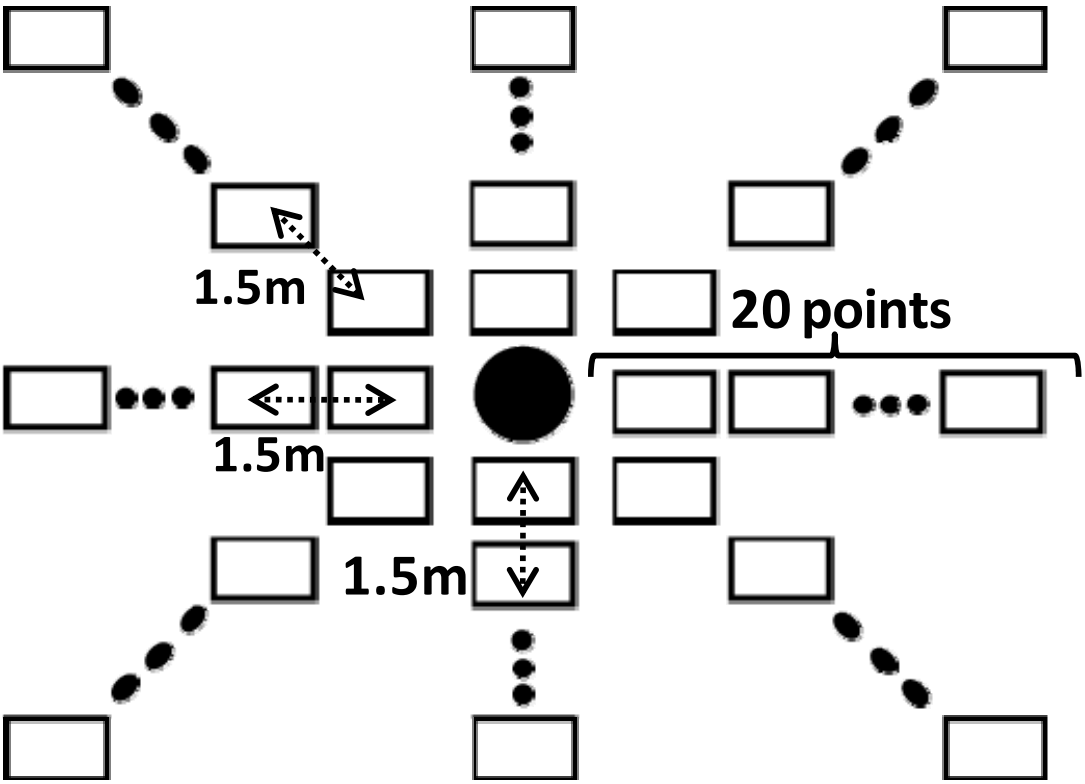

Figure 6 Position relations of sites of which the surface volumetric water condition was measured and surface pictures were taken. Both procedures were done at twenty points in each of eight directions at a1.5 m interval from the center as a total of 160 points.

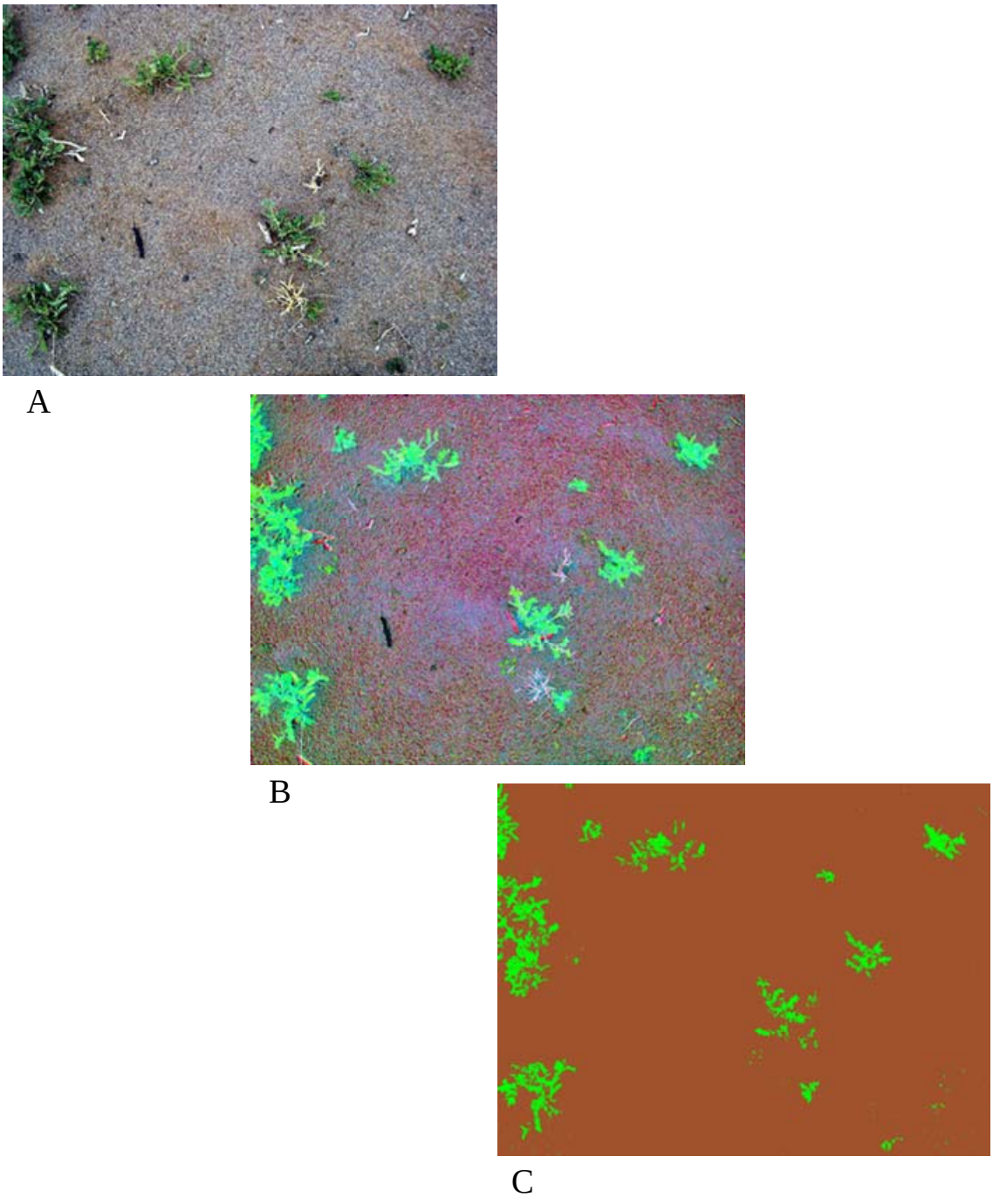

Figure 7　Process of deriving vegetation coverage using ERDAS IMAGINE ver.9.1. A Digital camera image was transformed from RGB color image (A) to IHS color image (B) because this color space system is more suitable for the image processing procedure.　Finally, the supervised classification was applied and obtain classified image (C).

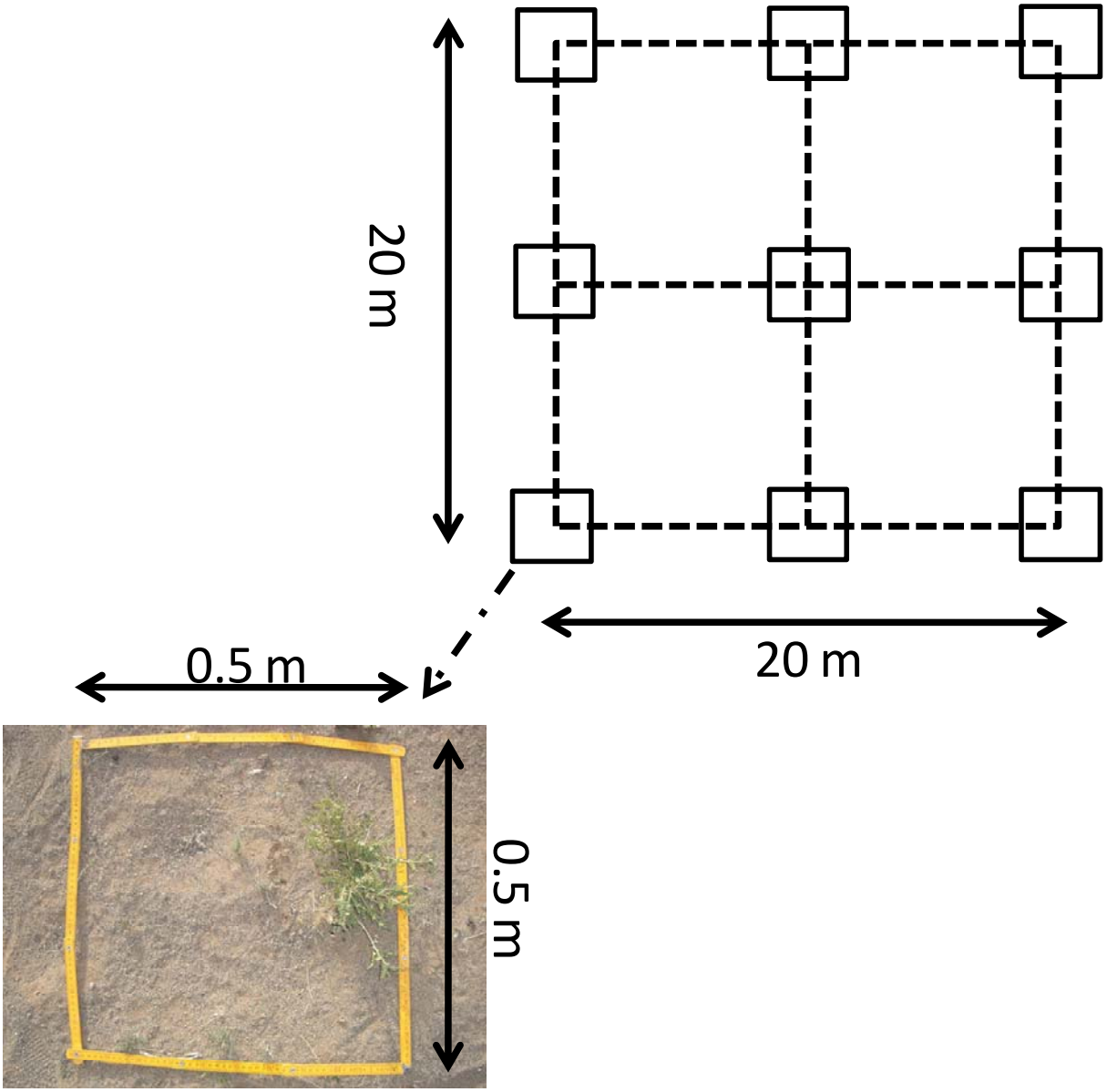

Figure 8 Alignment and top view of quadrat. Nine 0.5 m × 0.5 m quadrats were established on each corner, midpoint of the side and center of a 20 m × 20 m square to randomly samples the above ground biomass.

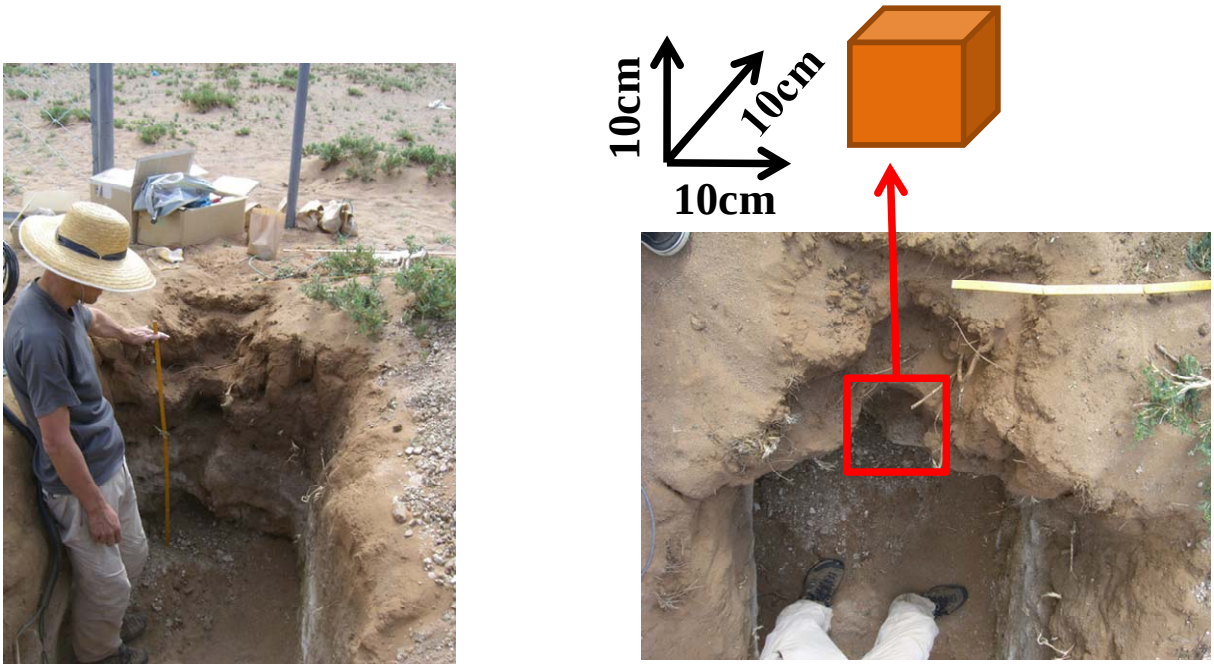

A. B.

Figure 9　A: Side wall of the trench. B: Top view of the side wall after cube was collected. Samples for below ground biomass of fine root were collected from the side wall of the trench. The soil cube including roots of 10 cm side was cut off for each 10 cm deep by using shovels. Cubes were hand sheaved to pick up roots.

A

B

Figure 10 A mound with shrubs was cut into half (A) and excavated for about 50 cm deep (B) to collect the large sized roots of the shrub. It was collected in 10cm interval.

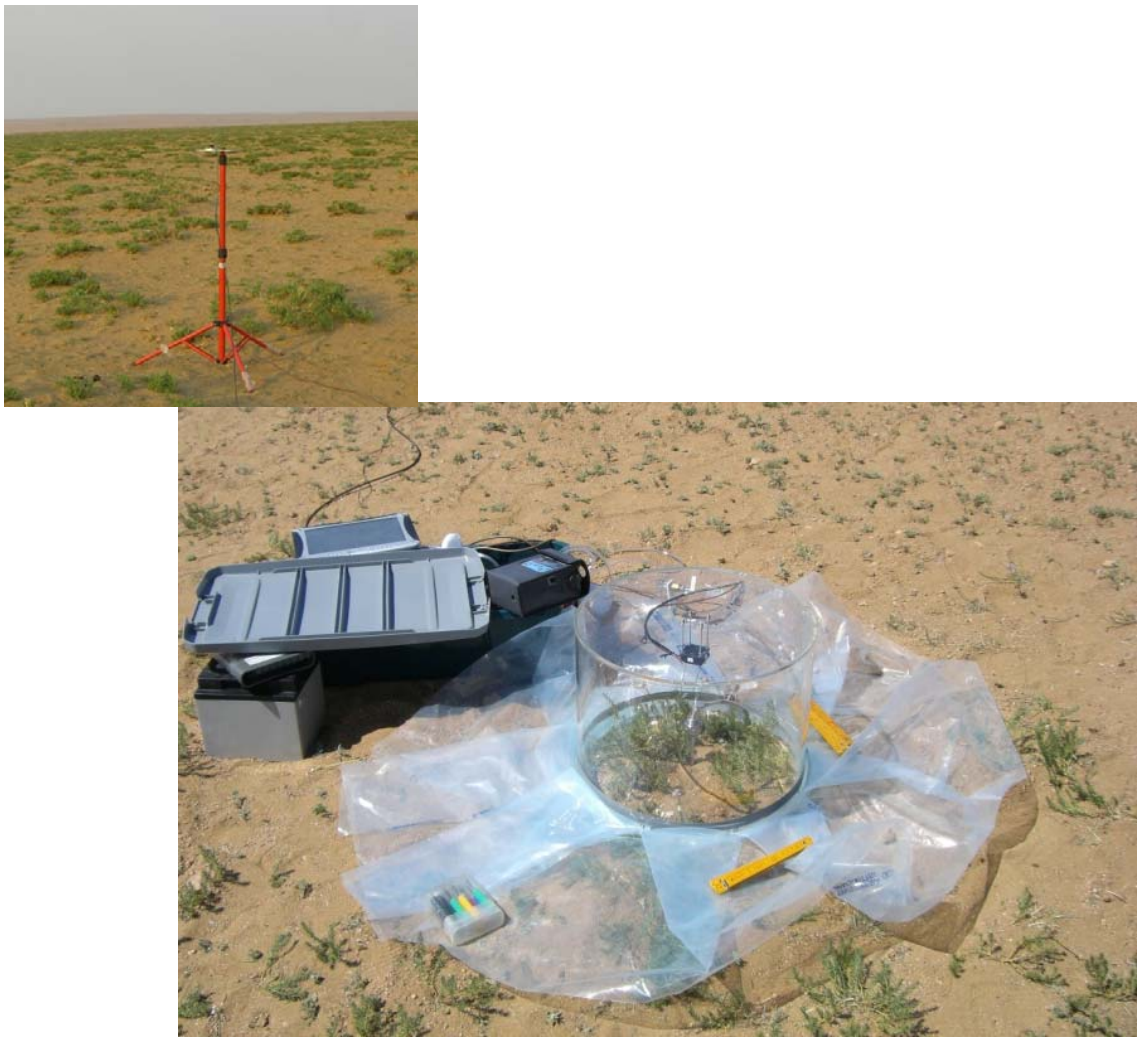

Figure 11 The Acrylic plastic chamber used for the H_2O flux measurements (below) and quantum sensor which measured incident photosynthetically active radiation with tripod stand (Above). A polyvinylchloride film extension was attached to the bottom edge of the chamber to prevent a wind blowing into chamber. The fan was installed on the top of the chamber to provide some air mixing necessary to make condition inside it to natural condition (Heijmans et al., 2004).

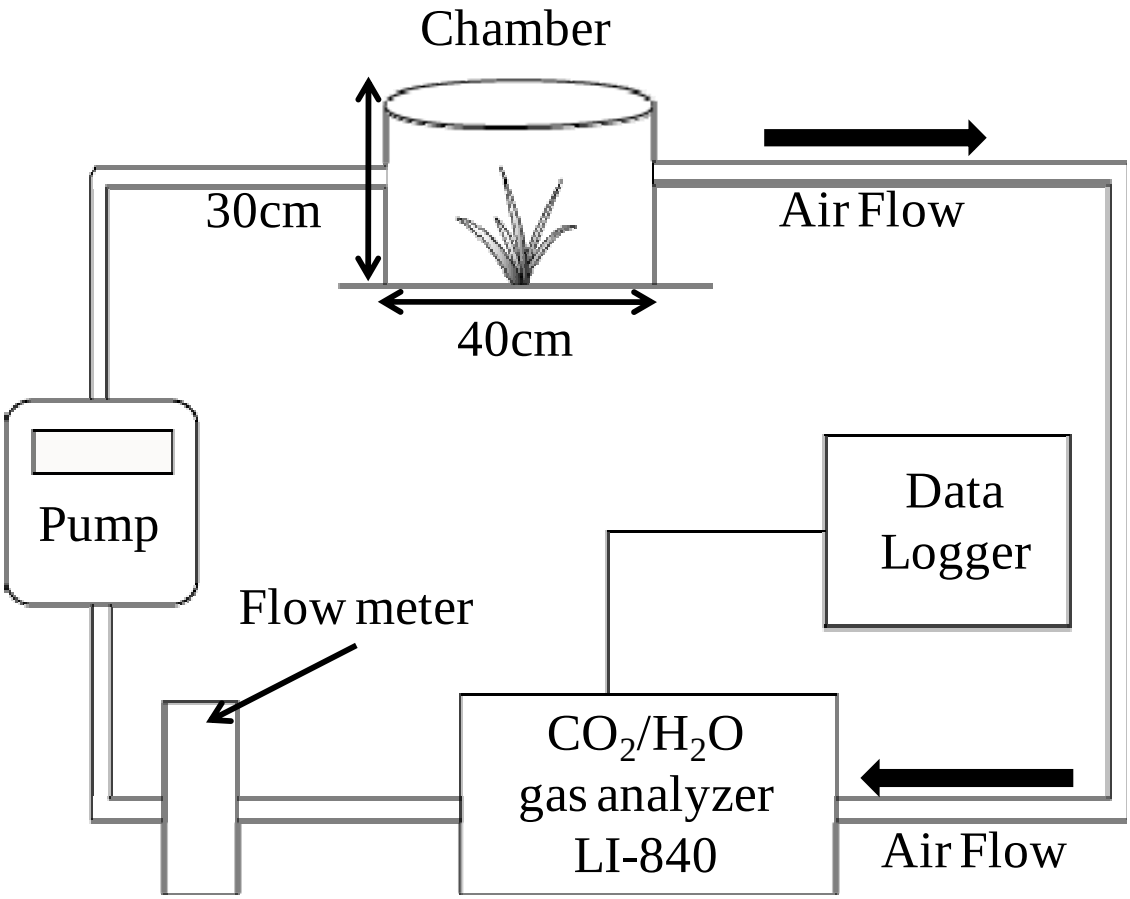

Figure 12　A system diagram of the chamber measurement. The chamber was connected to gas analyzer with vinyl tube.　The air was circulated by an air pump by 1 L/min which were monitored by a flow meter.

A

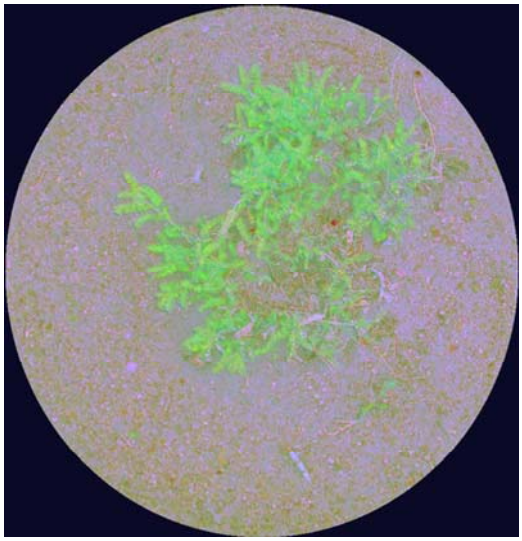

B

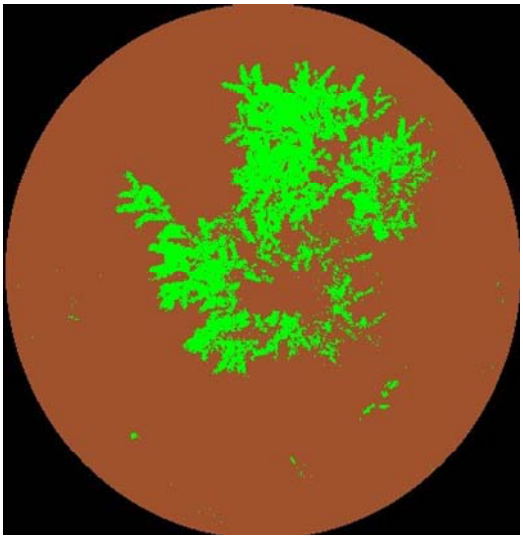

C

Figure 13　Images used for vegetation coverage analysis for the vegetated surface inside the chamber. The same procedures were conducted as coverage analysis of study basin. RGB color image (A) was translated into HIS color image (B).　Image was cut into chamber bottom aspect size with this procedure.　Then, the image was classified into canopy area and bare soil (C).

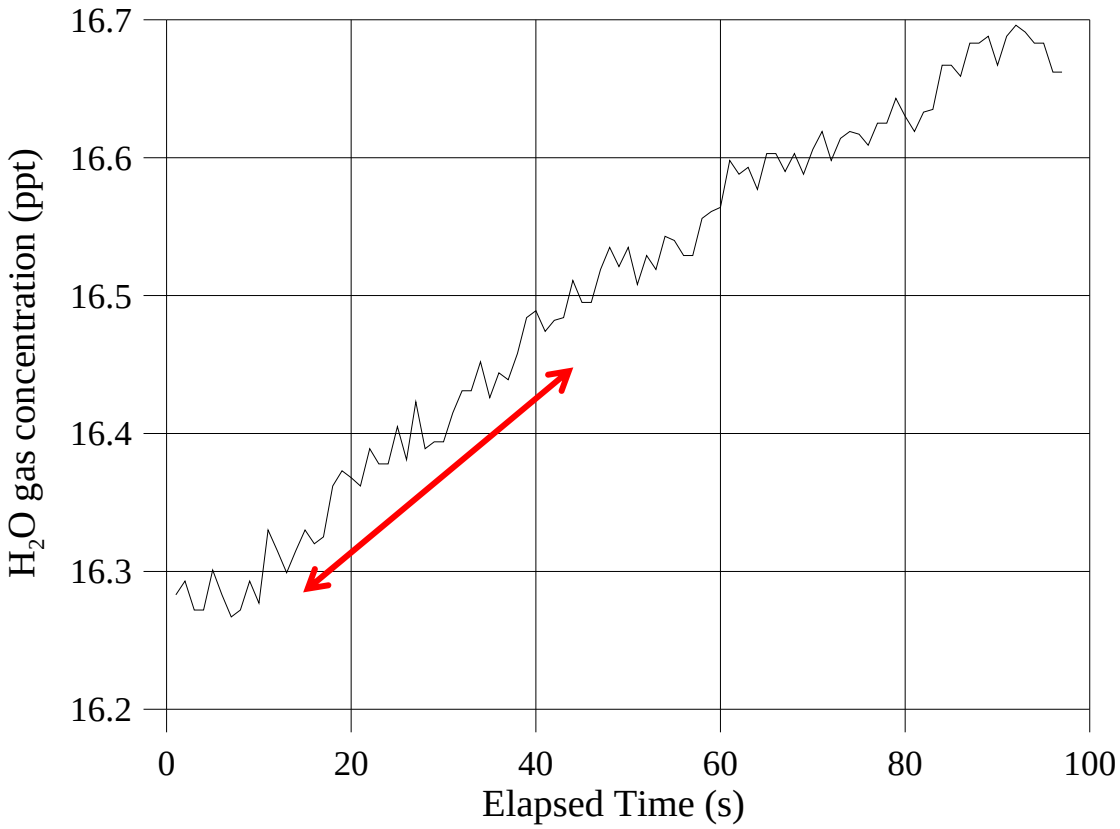

Figure 14 Measured H_2O gas concentration as a function of elapsed time. The interval between the red arrows was picked up for deriving the water flux.

A.

B.

Figure 15 Pictures of the rain sample collector. A funnel with 120 mm in diameter was attached to a polyethylene tank. A Ping-Pong ball was put inside the funnel to prevent evaporation from the tank (A). It was fixed with pegs and strings so as not to be blown away by a strong wind. The collector was set inside the premises of the branch office of Institute of Meteorology and Hydrology, Mongolia, at Mandalgobi and Dalanzadagad.

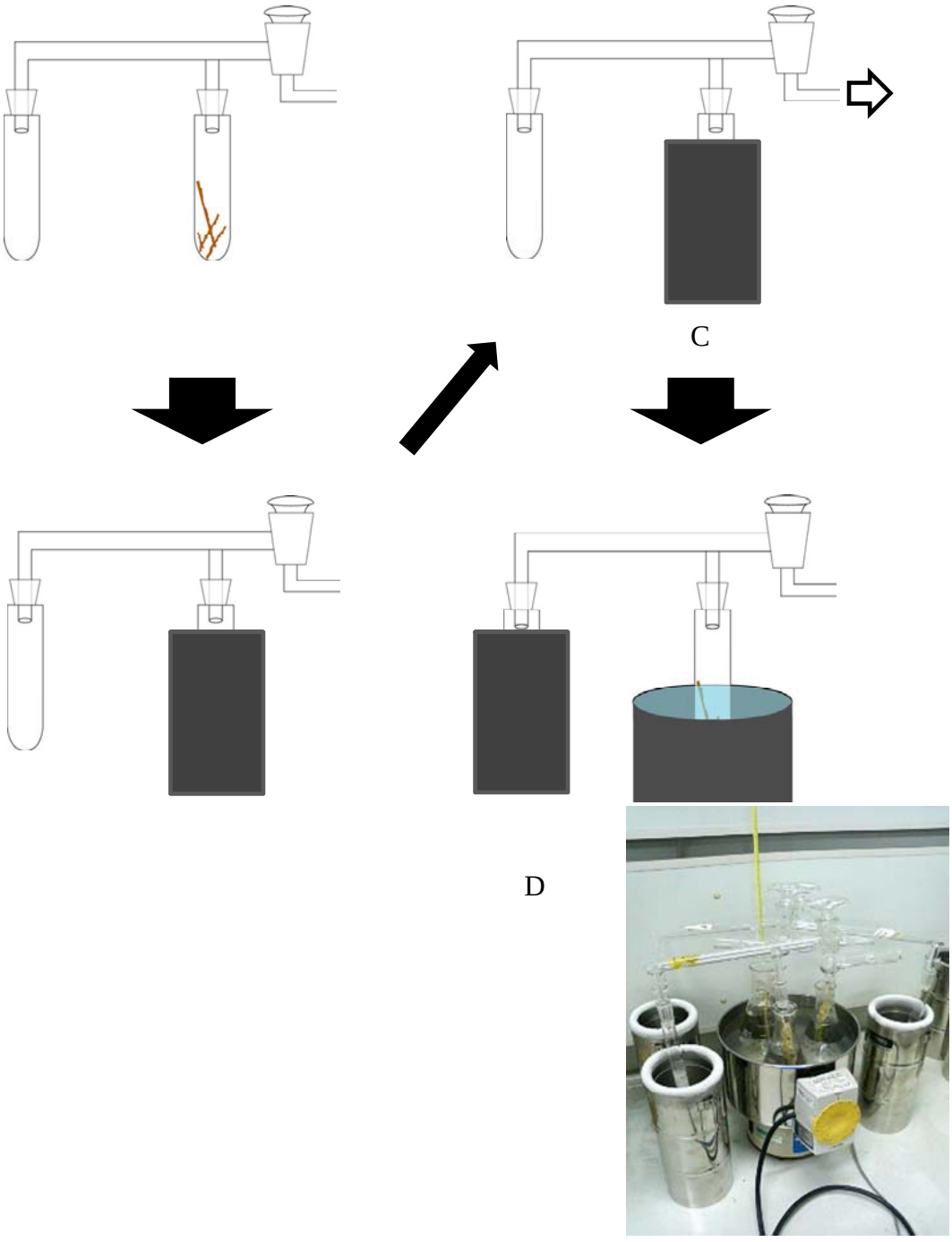

Figure 16 Procedure of the cryogenic vacuum distillation method. Empty test tube and sample contained one were connected to branching tubule (A). Test tube with sample inside was put into vessel of liquid nitrogen (B) and then pressure inside the system was reduced by connecting it to vacuum pump with vinyl tube (C). Finally, plant sample contained test tube was put into 80 °C hot tub and empty one was cooled with liquid nitrogen to collect water inside the plant samples (D).

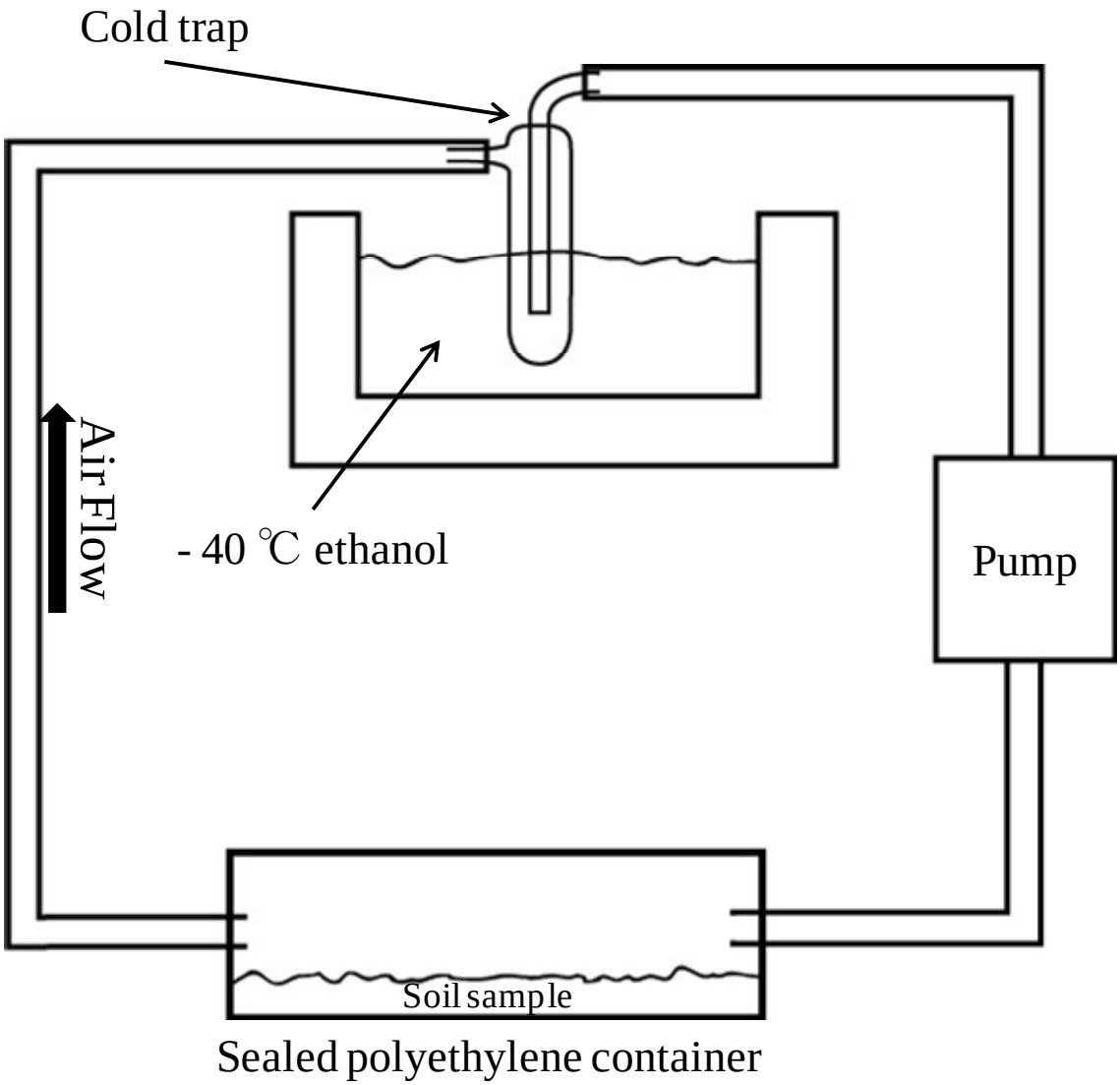

Figure 17　A frame format of ordinary temperature distillation method.　The air inside the system was circulated by pump with 4 L/min.　The soil was put into sealed polyethylene container on room temperature.　Soil water was collected in cold trap which was chilled by -40 ℃ ethanol.

3. Results

3. 1. Environments

3. 1. 1 Weather condition of the observing period

Figure 18 shows the comparison of monthly means of temperature and precipitation data derived from observation for 1944 – 2007 by IMH Mandalgobi branch office and those observed by the MG1 station from July, 2008 through July, 2009. Although mean air temperature agrees with each other, the mean precipitation at the MG1 was smaller than the long-term means especially in June and July. Thus the observed period can be considered somewhat drier than the long-term means.

3. 1. 2 Volumetric soil water content distribution

Shallower sensors were affected by the soil temperature. Therefore, an empirical model based on temperature, water content, and soil texture parameters was applied to correct the temperature dependency of TDR which was buried at shallower depth than 30 cm from the surface (Yamanaka et al., 2003). The compensation formula is given as follows:

$$\theta_c = \theta_{uc} - C_T (T - T_{ref}) \tag{3}$$

where θ_c (m^3/m^3) represents the corrected value of volumetric soil water content and θ_{uc} (m^3/m^3) represents the uncorrected value measured at temperature T (°C). T_{ref} is the reference temperature given as T_{ref} = 20. C_T represents the variation of the measured volumetric soil water content with respect to the change in temperature ($= \partial\theta / \partial T$) given by a multiple regression analysis.

$$C_T = (0.759\theta_{da} - 0.109\log(k_s) - 0.450) \times 10^{-2} \tag{4}$$

where θ_{da} (m^3/m^3) represents the daily averaged volumetric soil water content and k_s represents the saturated hydraulic conductivity. An example of volumetric water content profile with time before and after the correction is shown in Figure 19. Relation between daily precipitations, soil temperature at 10 cm depth and time-depth variation of volumetric soil water content measured by the MG1 station is shown in Figure 20. Increment of volumetric soil water content near the surface at the end of March, 2009 can be explained by the frozen soil and resulting infiltration melted or/and snow cover melted accumulated above the surface during winter period because volumetric soil water content increased despite of absence of precipitation while soil temperature rose above 0 °C. The relatively large and intensive rainfall on April 19th, 2009 saturated soil immediately to the depth of about 70 cm (Figure 21).

The volumetric soil water content at 20 cm depth decreased faster than the other layers. There was similar layer where the soil water content was smaller observed by the MG2 station (Figure 22). Table 1 shows the date, time duration and amount of precipitation of relatively large rainfall event from March through July, 2009, when the soils were not frozen. These rainfall events were chosen when there were precipitations of more than 1.0 mm. Each event was defined as one successive event when the rainfall restarted within an hour. Time variation of these rainfall events are shown in Figure 23. This table shows that the rainfall on April 19th, 2009 was heavy intensive rainfall since there were 4.7 mm of precipitation within one hour and twenty minutes. The figure shows the time variation of the rainfall events heavier than 3 mm per event. Figure 24 shows the daily precipitation of July, 2009. There was relatively heavy rainfall on July 17th, 26th and 27th. It was confirmed by the field observation that soils were wet at about 10 cm depth after the rainfall on July 17th (Figure 25). In this month, TDRs buried at shallower depth at the MG1 station did not respond to the rainfall events so that the TDR sensors at the MG2 station were used instead for discussions in this study. The reason why TDRs at the MG1 station did not respond was probably because they were buried beneath the mounds formed by shrubs. The profile of hourly averaged volumetric soil water content measured by the TDRs at the MG1 and MG2 station and hourly averaged precipitation are shown in Figure 26. Horizontal distributions of surface volumetric soil water content are shown in Figure 27 and its average and standard deviation of 160 plots for each day are shown in Table 3. It shows that there was little spatial variability especially when the surface was dry. After the rainfall of July 17th, the water content had returned to its former dry condition by 25th. This trend was corresponded to the value of 10cm depth on MG2 station.

3. 2 Vegetation distribution (above and below ground)

Vegetation covered 3.12% of the land surface in the beginning of July when there was no sufficient rainfall for more than two months. This ratio is just from shrubs because there were no herbaceous plants present until July 18th after sufficient rainfalls on 17th. The vegetation covered measured on July 29th showed that the shrubs covered about 3.59% and herbaceous plants covered about 0.689%. The relation between rainfall and the length of tallest herbaceous plant within each community used for the chamber measurement are shown in Figure 28. It shows that the herbaceous plant grew rapidly after the sufficient rainfall on July 17th. The growth rate decreased after three days from the rainfall and it started to decrease gradually at about one week after the event. It had started to grow out again after the sufficient rainfall on July 26th.

Vertical distribution of below ground biomass is show in Figure 29. Both fine root and

taproot was observed continuously from the surface to 100 cm deep soil. Distribution of taproot tends to decreases with distance from the surface. Although biomass of fine roots also had similar distribution with that of the taproot, the amount was largest at the 20-30 cm deep. Roots of herbaceous plants were only found at shallower depth than 30 cm by field observation.

The results of above ground biomass are shown in Table 4 which includes sampling date and average amount of biomass from each quadrats and standard deviation. It shows that when the average amount was relatively large, the standard deviation was also large. This was caused by the presence of shrubs in the quadrat. Although the quadrats were placed randomly at nine plots, shrubs distributed sparse and intense that more quadrats should be placed to take averaged above ground biomass.

3. 3 Correlation of total one-sided leaf area with biomass and canopy area

Correlation between total one-sided leaf area and canopy area (the area of green coverage when viewed vertically from above the ground surface) is shown in Figure 30. Canopy areas of both shrubs and herbaceous plants were well correlated with the total upper leaf areas. It suggests that there was shape similarity on both plants. Relationship between the biomass and the total one-sided leaf area is shown in Figure 31 which also shows good correlatation.

3. 4 Soil characteristics

Figure 32 shows the overview of the trench and its side-wall. There was clear change of the soil color at layer at 30 – 70 cm depth. Above the layer, soil consists of fine to medium sand with gravels. Several roots of shrubs and herbaceous plant were observed in this layer while herbaceous plant roots were found only below 15 cm deep. The color below the layer changed clearly from brown to white. This white layer is the calcium carbonate accumulated layer which is called Calcic horizon (Tamura, 2003). This layer is harder than the layer above and there was a little fine root (about 1 mm in diameter) of shrubs in it. This Calcic horizon gradually changes to rocky layer with the depth.

Volumetric soil water content, porosity and field capacity of soils sampled on June 2nd, 2009 and saturated hydraulic conductivity are shown in Table 5. Volumetric soil water content was largest at the depth of 50 – 60 cm which also had the highest porosity and the smallest saturated hydraulic conductivity on June 2nd, 2009. Volumetric soil water content was small at the shallow layer. There seems to be boundary within 40 cm to 60 cm depth where the saturated hydraulic conductivity drastically decreased. This depth range corresponds to the layer where Calcic horizon appeared. Relation between volumetric soil water content and pF rate is shown in Figure 33. Water-retaining capacity of soil at 0 – 10

cm depth were higher than the other layers while 10 – 40 cm depth layer had low capability.

3. 5 Relation between PPFD and solar radiation

Figure 34 represents relation between independently measured PPFD measured by the quantum sensor and solar radiation measured by the 4-component net radiometer at the MG1 station. PPFD was measured each second when the camber measurements were conducted. On the other hand, the solar radiation was logged whole day by the MG1 station every 10 minutes (average of the data measured every 10 seconds). They are well correlated to each other with correlation coefficients of 96%. The equation derived from the regression line is:

$$\text{PPFD } (\mu \text{ mol } m^{-2} s^{-1}) = 1.98 \times \text{Solar radiation } (Wm^{-1}) \quad (5)$$

This ratio of PPFD to solar radiation is similar to the result of Udo and Aro (1991). The average ratio of PPFD to solar radiation over a year was 2.08 in their study. PPFD was measured only during the chamber measurement so that the solar radiation was derived from PPFD values with this estimation (equation (5)) for the EV discussion in this study.

3. 6 Water fluxes

3. 6. 1 Evaporation

Relationship between the solar radiation and the evaporation (EV) measured on June 1st to 4th, 2009 is shown in Figure 35. They are well correlated to each other with linear relation. Figure 36 represents the relation between the solar radiation and EV from the chamber measurement covered on the bare soil from July 11th through 31st, 2009. Unlike the trend of EV measured in June, the correlation between these two components was not as good. However, there seems to be a linear relation when the EV is smaller than about 0.1 mm/h. Figure 37 shows the relation between daily precipitation and the EV measured from 11:00 a.m. to 15:00 a.m. on each day. This period of time was chosen to compare the daily variation of the EV under the same condition. This figure indicates that EV increased rapidly after the rainfall event and then gradually dropped back. Figure 38 represents the relation between PPFD and EV in the vicinity of rainfall event on July 17th and 26th-27th. The gradual decrease of EV after the rainfall event can be also seen in this figure. The trend of EV with solar radiation on the day after several days from the rainfall corresponds to the trend on the day before the event. There is a linear relation between the solar radiation and EV except for the day when there was rainfall on July 17th. Figure 39 shows the time variation of solar radiation and EV on the day before the rainfall event (July 14th) and shortly after the event (July 18th). This figure represents that those negative EV fluxes (i.e., condensation) occurred in the early

morning. One-day EV variation follows that of solar radiation on both days.

3. 6. 2 Evapotranspiration

Evapotranspiration (ET) was measured by covering the chamber on soil surface with plants. Details of those plants on each sites such as biomass, total one-sided leaf area and vegetation coverage are shown in Table 6. CA represents sites with shrubs and AL represents sites with herbaceous plants. Shrubs in CA1 and CA2 sites were larger than shrubs in other three sites. An amount of herbaceous plants in AL sites were very small compared to the shrubs. Relation between PPFD (solar radiation) and ET measured on July 25th is shown in Figure 40 as an example. EV from bare ground measurements are also shown in the figure for comparison. ET from all sites had linear correlation with solar radiation or PPFD. ET from shrub sites (CA) was larger than herbaceous plant sites (AL). Especially ET from CA1 and CA2 was larger than ET from the others.

3. 6. 3 Transpiration

Transpiration (TR) was estimated from the ET measurement by subtracting the EV. Vegetation coverage was used to separate TR and EV from ET. The equation is given as follows:

$$ET = aTR + (1 - a)EV \tag{6}$$

$$TR = \frac{ET - (1 - a)EV}{a} \tag{7}$$

where *a* represents the vegetation coverage (%). EV measurements (chamber covered on a bare soil) immediately before or after each ET measurement were used as the EV in the equation. The results are shown in Figure 41 with the relation between PPFD and TR on July 25th. TR of shrubs agreed very well among all sites while TR of herbaceous plant varied among sites. TR of shrubs had linear correlation with PPFD when the PPFD was less than about 1200 (μ mol m^{-2} s^{-1}). Although TR of shrub on CA1 site kept rising over 1200 (μ mol m^{-2} s^{-1}), the others were stable or decreased. This trend was also seen in TR of herbaceous plats that TR decreased when the PPFD was high. Figure 42 shows the relation between PPFD and TR of shrubs in the vicinity of rainfall event. The TR varied widely on the day when there was rainfall and shortly after it. However, TR of shrubs did not change among the rainfall event. Time variations of PPFD and TR on July 14th are shown in Figure 43. TR variation followed the PPFD variation in the morning and the evening but it varied in daytime

when the PPFD was higher. Figure 44 shows the relation between PPFD and TR measured on June 1st to 4th, 2009. They also had liner correlation as observed in the July measurement. However, the TR was relatively larger than July.

The relation between PPFD and TR of herbaceous plants in the vicinity of rainfall event on July 26th and 27th is shown in Figure 45. TR varied widely on the day and after several days from rainfall event. This was because EV was large and the vegetation coverage in each AL site was very small so that the observed EV from bare ground and ET from AL sites were almost the same (Figure 46). Therefore, subtraction of EV from ET at AL sites by using equation (7) tends to result in a large error of TR. Figure 47 shows the relation between PPFD and TR of herbaceous plants on those days when the EV was small (day after several days from rainfall event). The relations between solar radiation and EV over the same period are also shown for comparison. The TR varied day by day while the EV did not change. The TR increased with PPFD on the days when the magnitude of TR is larger (hereafter it is referred to as A trend). On the other hand, TR increased with PPFD until PPFD reached to about 1400 (μ mol m^{-2} s^{-1}), and then TR decreases with PPFD increment (hereafter it is referred to as B trend). Figure 48 shows the time variation of PPFD and TR of herbaceous plants the A and B trend day, July 22nd and 25th, 2009 respectively. It indicates that on July 25th, TR of herbaceous plants decreased after 11:00 a.m.

3.6 Stable isotope composition

Stable isotope ratio of soil waters was corrected because soil water was not fully recovered from the soil samples by the ordinary temperature distillation. They were corrected by the method of Yamanaka and Shimada (1997). When the liquid water with δ_0 evaporates and separates into water vapor with δ_v and remaining liquid water with δ_l, the following relation would result:

$$\delta_0 = f\delta_l + (1-f)\delta_v \tag{8}$$

where f represents the residual ratio of the water, given by $f = 1 - r/100$ where r represents collection ratio (%). The δ_l is derived from the following Rayleigh distillation formula when the residual ratio is f:

$$\delta_l = \left\{ f^{\frac{1}{\alpha}-1}(1+10^{-3}\delta_0) - 1 \right\} \times 1000 \tag{9}$$

where α represents fractionation factor. δ_0 is then derived by eliminating δ_l:

$$\delta_0 = \frac{(1-f)\delta_v + 1000(f^{\frac{1}{\alpha}} - f)}{1 - f^{\frac{1}{\alpha}}} \quad (10)$$

The α was determined by substituting stable isotope ratio of the water (δ_0) which was added on completely dried soil (dried 24 hours at 105 °C) and its collected water (δ_v) from ordinary temperature distillation to the equation. The results are shown in Table 7. The fractionation factor for δ ^{18}O and δ D where obtained as α_O = 1.02465 and α_D = 1.0946, respectively. Figure 49 shows the relationship between δ ^{18}O and δ D values for soil water, well water and precipitation of Mandalgobi in 2009. Precipitations of Dalanzadagad are also shown for comparison. Precipitation values are monthly mean data because accumulated rainfall was collected once in a month except for July when it was sampled twice. The volume weighted mean value of rain water at Mandalgobi was determined using the amount of monthly precipitation measured by the MG1 station. A Global Meteoric Water Line (GMWL) is a regression line determined from stable isotope ratios of hydrogen and oxygen in monthly precipitation on global scale (Craig, 1961). On a local scale, Local Meteoric Water Line (LMWL) is derived from local precipitation isotopic value. The LMWL in the figure was determined using all the precipitation data at Mandalgobi. The slope of LMWL was 7.36 with intercept of 6.19. This corresponds well with the result from Yamanaka et al. (2007a) which had slope of 7.75 (±0.77) and intercept of 1.47 (±14.19). They derived LMWL from rain samples collected from October 2002 to September 2003 at Mandaigobi. All the data from well water was plotted along the LMWL which suggests that well water should be originated from precipitation. Deviations of soil water regression line from LMWL suggest that the soil water was affected by evaporation process (Schwartz and Zhang, 2002; Gat and Airey, 2006; Gibson et al., 2008). The soil water regression lined had the slope of 2.97. It agreed well with the value which Gibson et al. (2008) had indicated that the slopes were less than 3. This value of slope indicates that the soil water was evaporated mainly through the molecular diffusion (Gibson et al., 2008). The soil water above about 20 cm depth was more affected by evaporation than the deeper soil water. Cross point of regression line derived from a certain water pools isotope ratio values and LMWL indicates the source of the water in the water pool (Schwartz and Zhang, 2002). Thus, the cross point of soil water regression line and LMWL indicates that the soil water was cultivated by ground water or precipitations in April.

The vertical profiles of δ ^{18}O in soil water sampled on June 2nd, July 13th, 18th 25th, 29th

and August 1st 2009 are shown in Figure 50. The $\delta^{18}O$ values in the shallow soil water tend to be higher than those of deeper soil water. It suggests that shallower soil water was more affected by evaporation than deeper soil water. Although there was sufficient rainfall on July 17th, there was not much difference in soil water isotopic value. A $\delta^{18}O$ value of the water inside the xylem sap of shrubs and herbaceous plants, and well water are also shown in Figure 50. It indicates that shrubs utilize water from about 70 cm to 90 cm depth soil water before rainfall and gradually shift to shallower depth after the sufficient rainfall event while herbaceous plants utilize the very surface soil water.

Table 2 Information of the sufficient rainfall (more than 1 mm per event) event on 2009. The event was defined as one event when the rainfall restarted within an hour.

Date	Time	Duration	Precipitation (mm)
4/19	11:00-12:20	1 h. 20 min.	4.7
4/23	3:50-9:30	8 h. 40 min.	1.7
5/8	9:30-14:10	4 h. 40 min.	5.7
6/7	10:40-11:30	50 min.	1.2
7/3	11:50-12:40	50 min.	1.0
7/12	16:50-17.20	30 min.	1.7
7/16	22:50-24:50	2 h.	1.5
7/17	4:40-6:00	1 h. 20 min.	4.4
7/26	7:00-9:40	2 h. 40 min.	3.5
7/27	1:50-2:20	30 min.	2.7

Table 3　Information of horizontal soil surface volumetric water content measured on July, 2009.　Averages and standard deviations are derived from 160 measurement plots on each day.

Date	Average (%)	Standard deviation
7/10	4.11	0.31
7/17	7.87	1.44
7/18	7.22	1.01
7/21	5.52	0.76
7/25	4.36	0.66
7/26	7.88	1.14
7/27	7.41	1.19
7/31	6.24	0.80

Table 4　Information of above ground biomass.　Averages and standard deviations are derived from 9 quadrats on each sampling day.

Date	Average (g/ m^2)	Standard deviation
2009/7/10	82.4	28.4
2009/7/12	45.2	14.1
2009/7/20	44.8	14.8
2009/7/25	20.0	6.0
2009/7/29	24.4	3.0

Table 5 Information of hydraulic soil characteristics. Volumetric soil water content, porosity and field capacity represented are from samples of June 2nd, 2009.

Depth (cm)	Volumetric soil water content (%)	Porosity (%)	Field capacity (%)	Saturated hydraulic conductivity (cm/s)		
				July 7th, 2008	June 2nd, 2009	July 31st, 2009
0-10	2.68	41.3	35.09	1.00×10^{-3}	2.40×10^{-3}	9.29×10^{-4}
10-20	5.19	37.4	28.96	1.93×10^{-4}	6.82×10^{-4}	8.57×10^{-4}
20-30	4.95	31.7	24.2	1.46×10^{-4}	1.60×10^{-4}	5.86×10^{-4}
30-40	4.43	25.2	20.96	1.01×10^{-4}	3.69×10^{-4}	2.50×10^{-4}
40-50	4.12	33.3	23.94	1.70×10^{-4}	2.31×10^{-6}	1.46×10^{-3}
50-60	6.33	43.8	21.19	6.07×10^{-5}	2.90×10^{-3}	5.82×10^{-3}
60-70	4.8	42.1	25.98	4.85×10^{-5}	8.21×10^{-4}	8.24×10^{-5}
70-80	3.55	42.2	23.88	5.17×10^{-4}	1.41×10^{-3}	1.55×10^{-5}
80-90				2.08×10^{-3}		2.89×10^{-4}
90-100				2.37×10^{-4}		9.71×10^{-3}

Table 6　Information of plants for the chamber measurement where CA represents of chamber site with *Caragana microphylla* and AL represents that with *Allium polyrrhizum*.

Site ID	Biomass (g)	Total One-sided Leaf Area (m^2)	Vegetation coverage ratio (%)
CA1	64.76	1.61×10^{-1}	41.9
CA2	56.93	1.46×10^{-1}	44.6
CA3	19.74	5.16×10^{-2}	21.5
CA4	19.92	3.87×10^{-2}	13.6
CA5	16.85	3.78×10^{-2}	15.0
AL1	0.58	5.64×10^{-3}	1.2
AL2	1.09	1.10×10^{-2}	4.3
AL3	0.56	4.62×10^{-3}	2.6
AL4	0.93	9.57×10^{-3}	2.4
AL5	0.6	4.00×10^{-3}	2.0

Table 7 Information of the calibration for ordinary temperature distillation.

	δD	$\delta^{18}O$	Collection ratio r (%)	Residual ratio $f = 1-r/100$
Added water (δ_0)	-40	-6.4		
Collected water 1 (δ_v)	-63	-12.1	92.6	0.0743
Collected water 2 (δ_v)	-60	-11.3	93.1	0.0686
Collected water 3 (δ_v)	-57	-10.9	94.0	0.0596
Collected water 4 (δ_v)	-58	-11.0	92.9	0.0714
Collected water 5 (δ_v)	-56	-11.0	93.5	0.0646
Average (δ_v)	-58.7	-11.2675		0.0677
Fractionation factor	$\alpha_D = 1.0946$	$\alpha_O = 1.02465$		

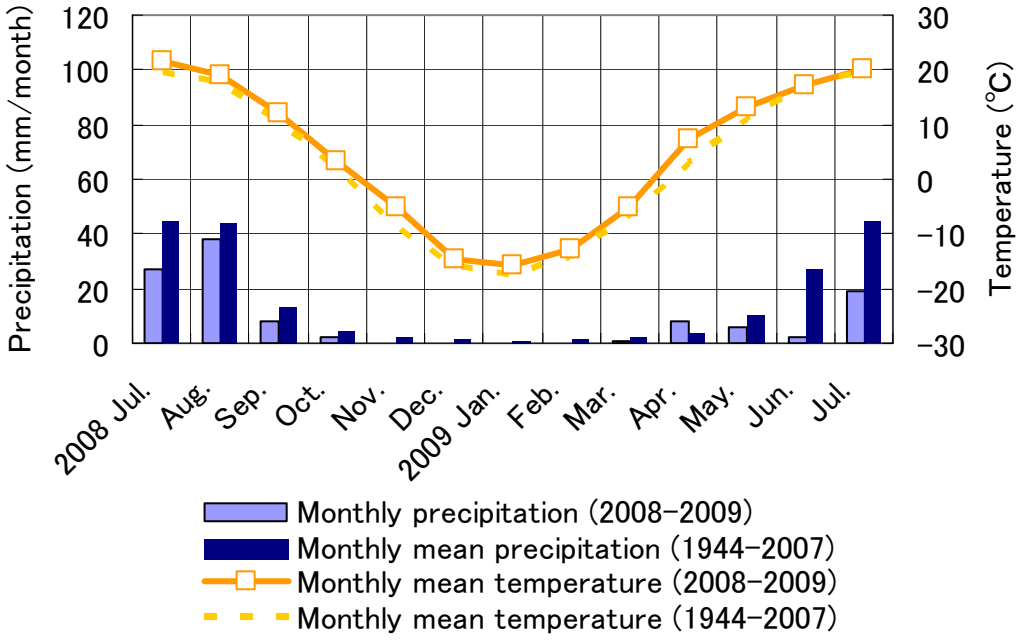

Figure 18　Comparison between average data from 1993-2003 and observed data of monthly precipitation and monthly mean temperature of growing season (Institute of Meteorology and Hydrology, Mongolia).

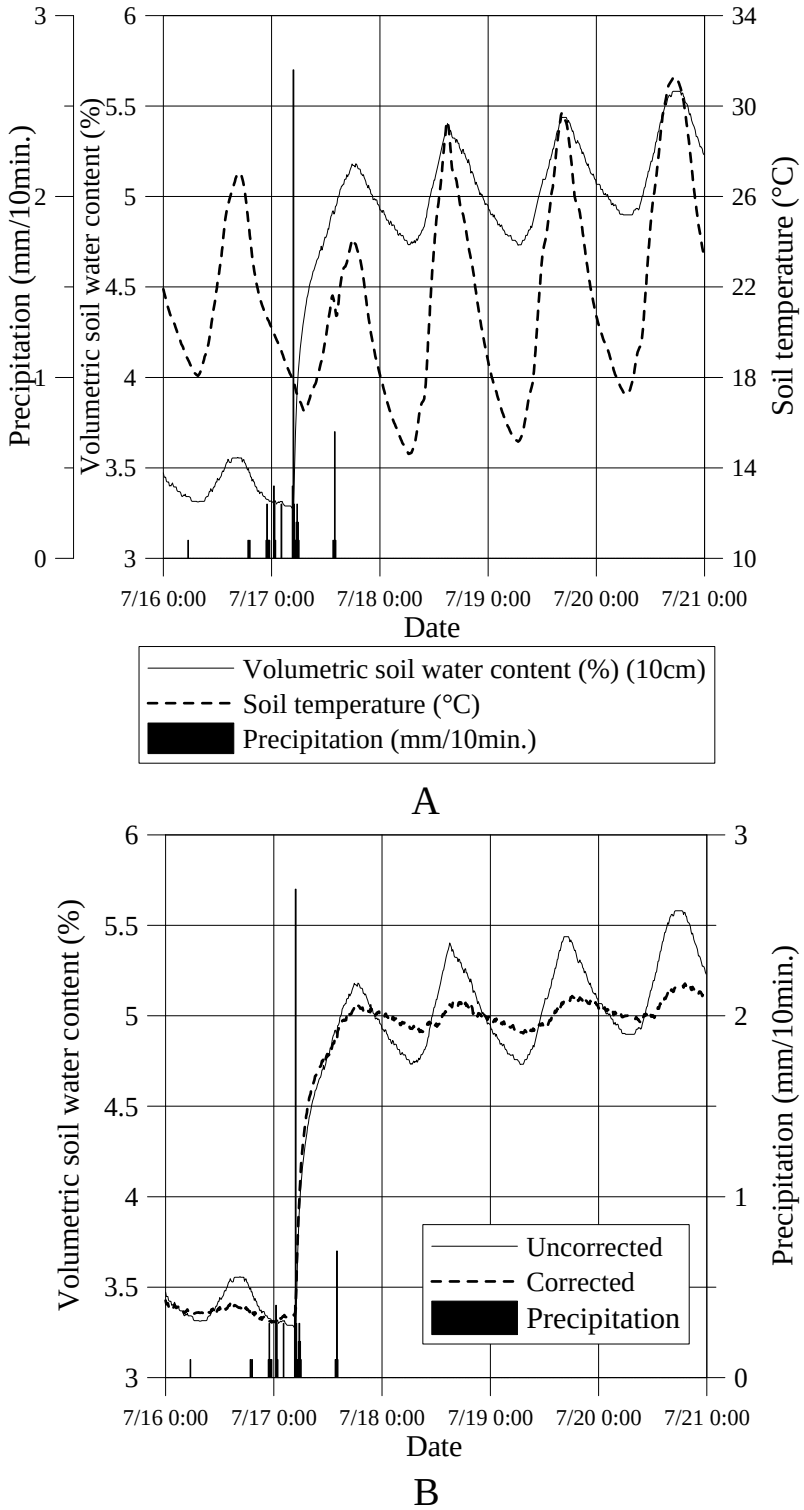

Figure 19 A: Relation between raw volumetric soil water content as measured by a TDR sensor and soil temperature at 10 cm depth at MG2. B: Comparison between uncorrected and corrected profile of soil water content at the same point as panel A. Correction is based on the empirical model of Yamanaka et al. (2003).

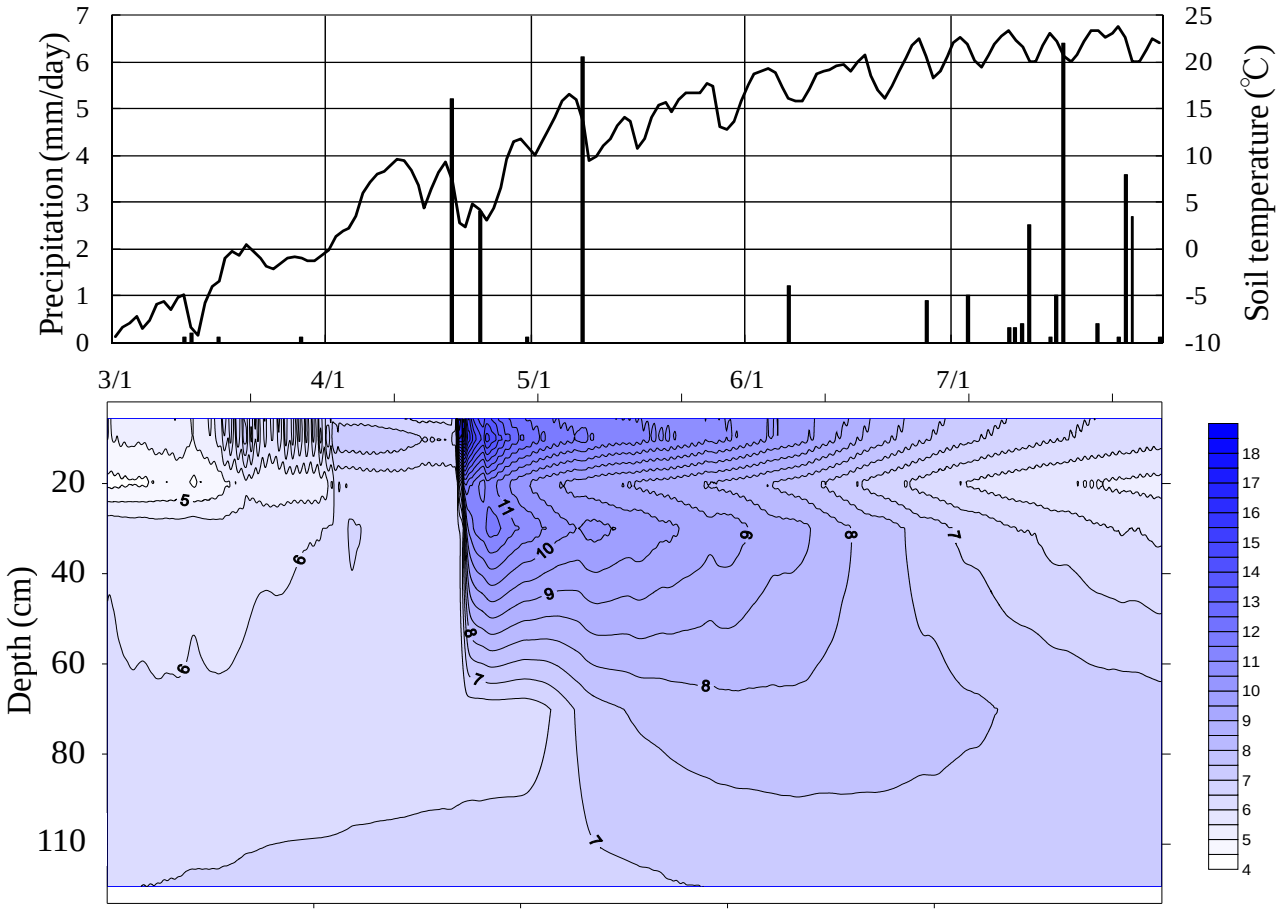

Figure 20 Relation of daily precipitation and soil temperature from May through July 2009 (top) and isopleths of volumetric soil water content (bottom). Soil water content increased significantly after the rainfall on April 19th.

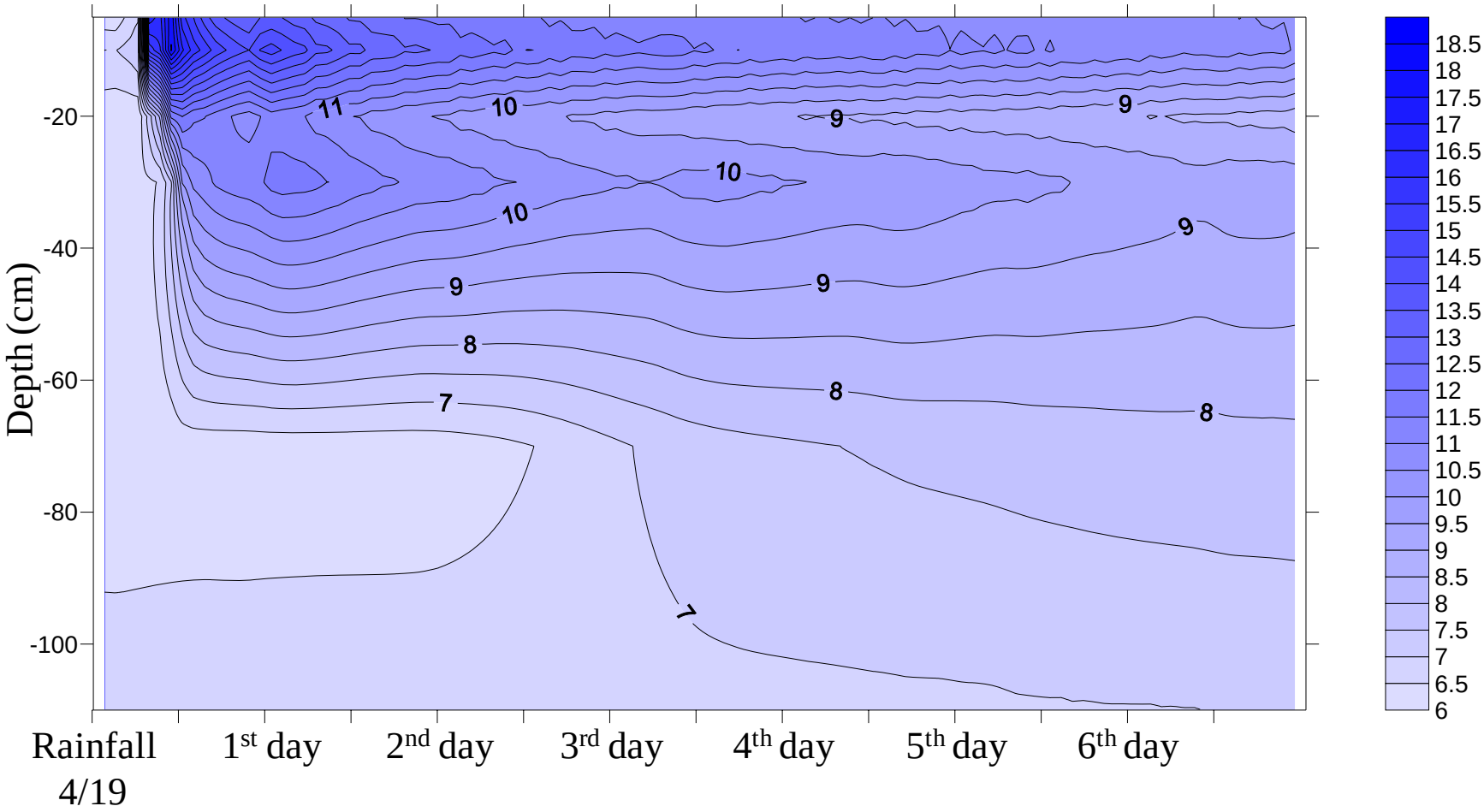

Figure 21 Close-up of isopleths of volumetric soil water content measured by MG1 station after the rain fall on April 19th, 2009.

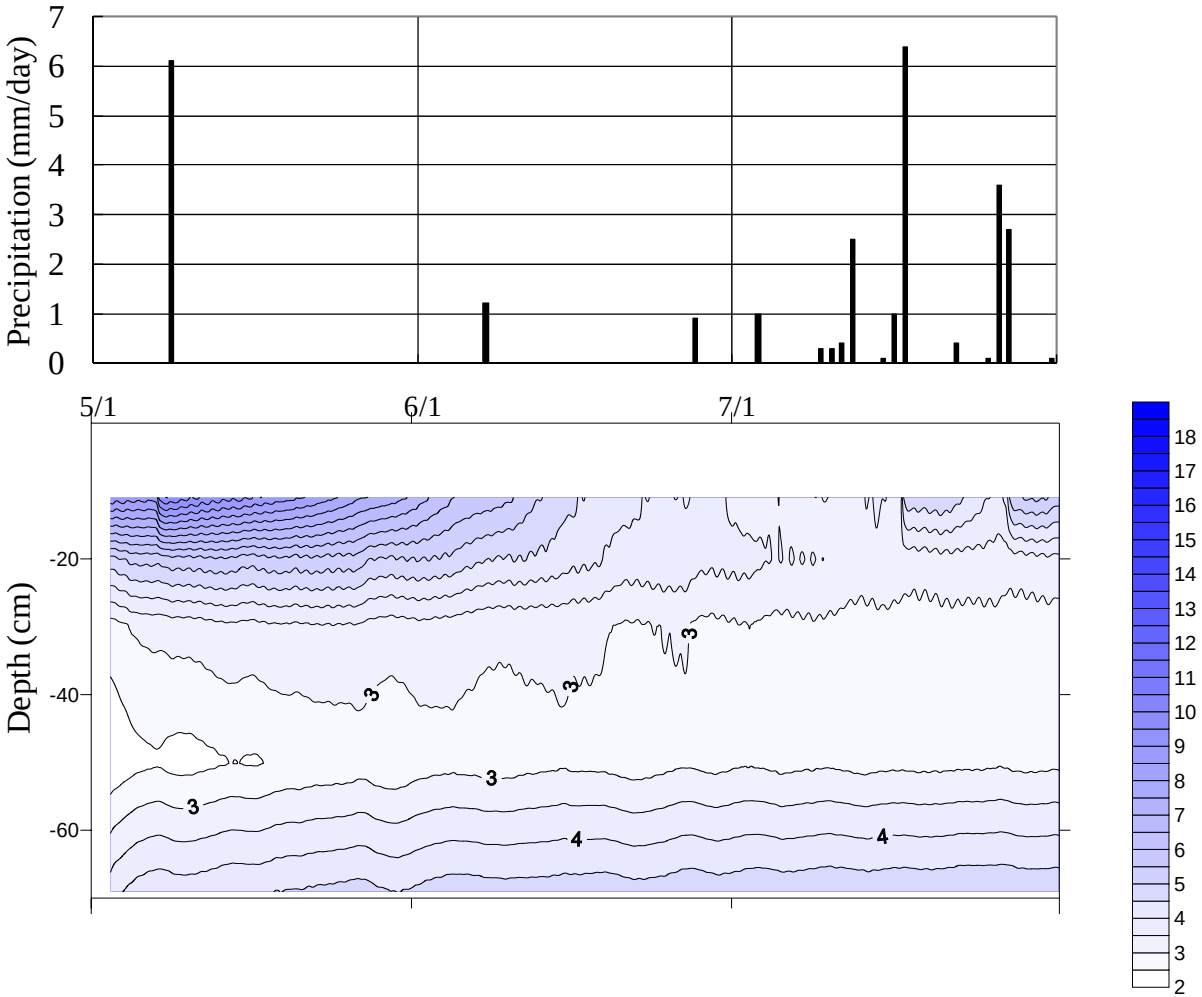

Figure 22 Relation of daily precipitation and soil temperature from May through July 2009 (top) and isopleths of volumetric soil water content measured by MG2 station (bottom)

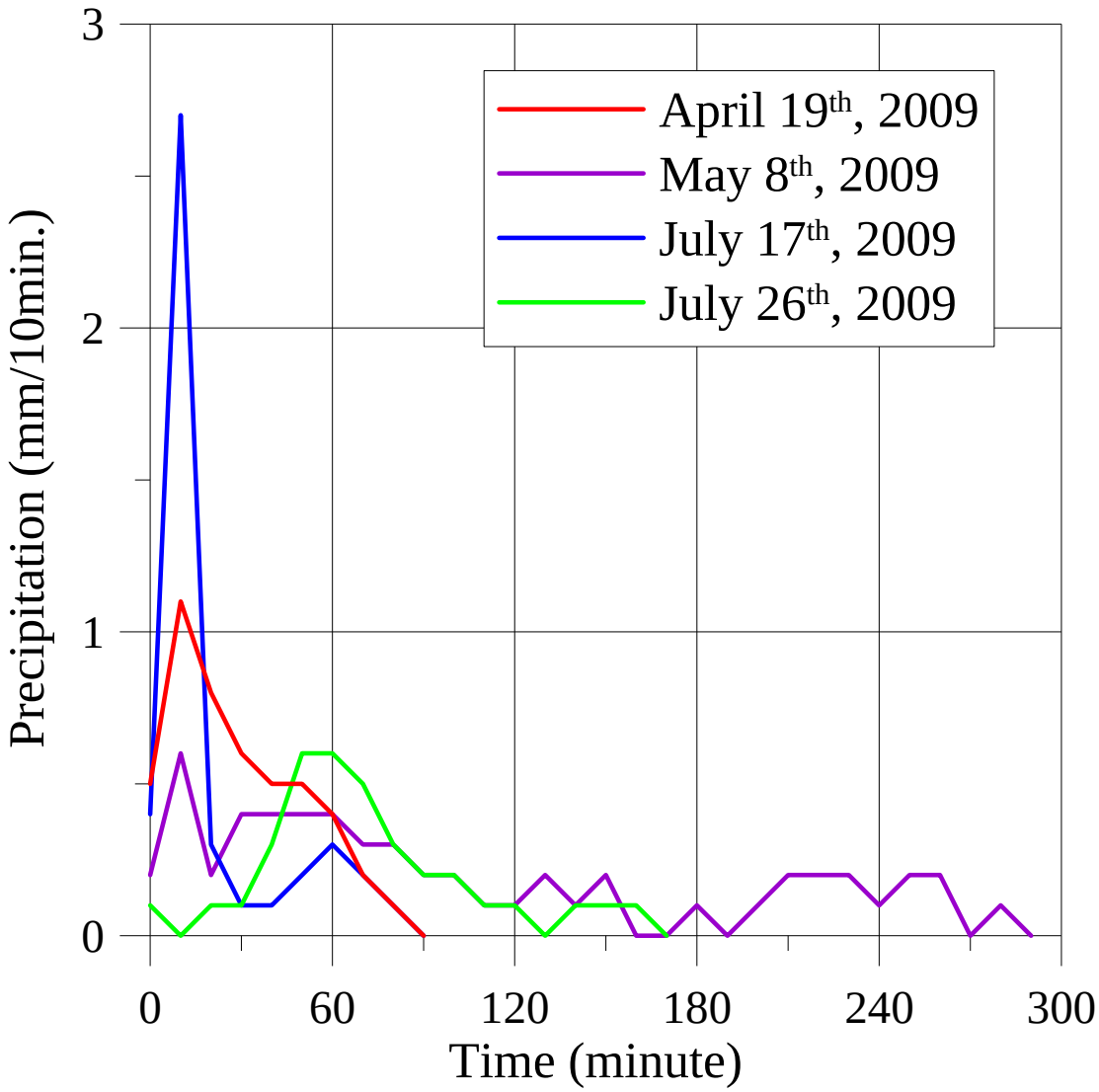

Figure 23 Time variance of heavy rainfall occurred from April through July, 2009.

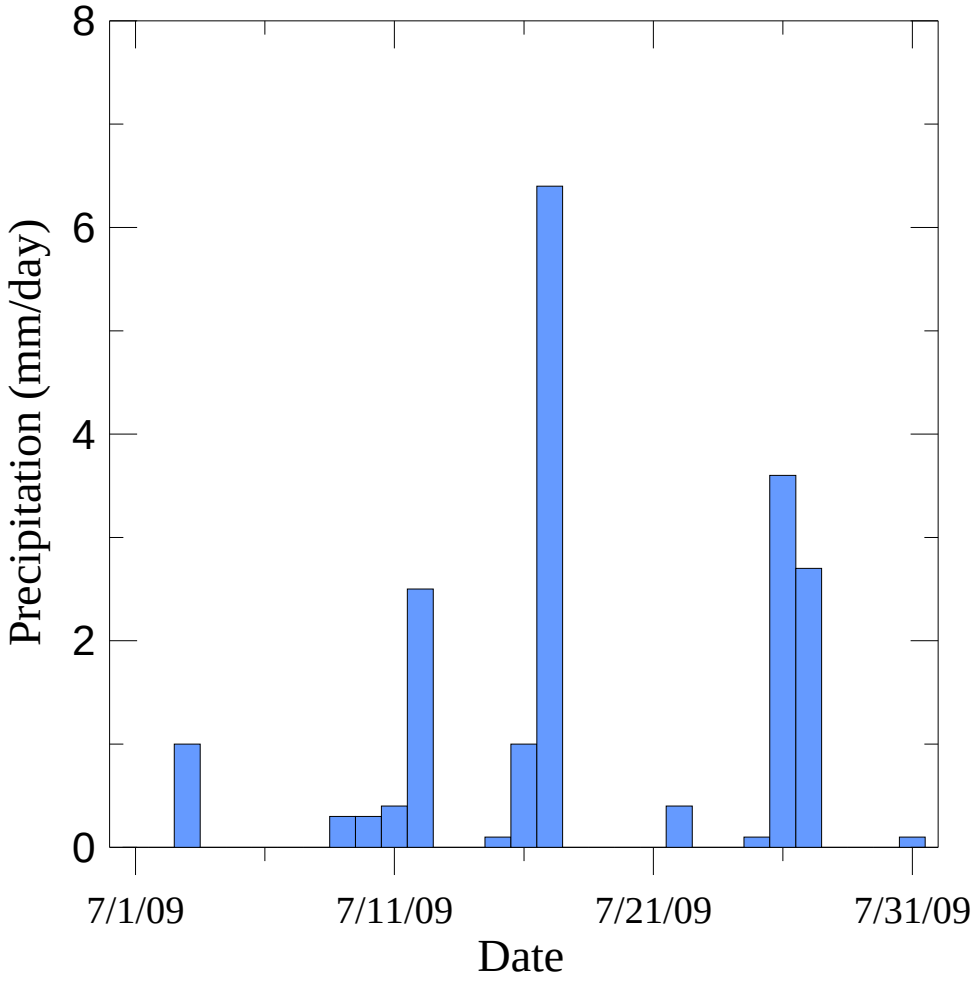

Figure 24 Daily precipitation on July, 2009.

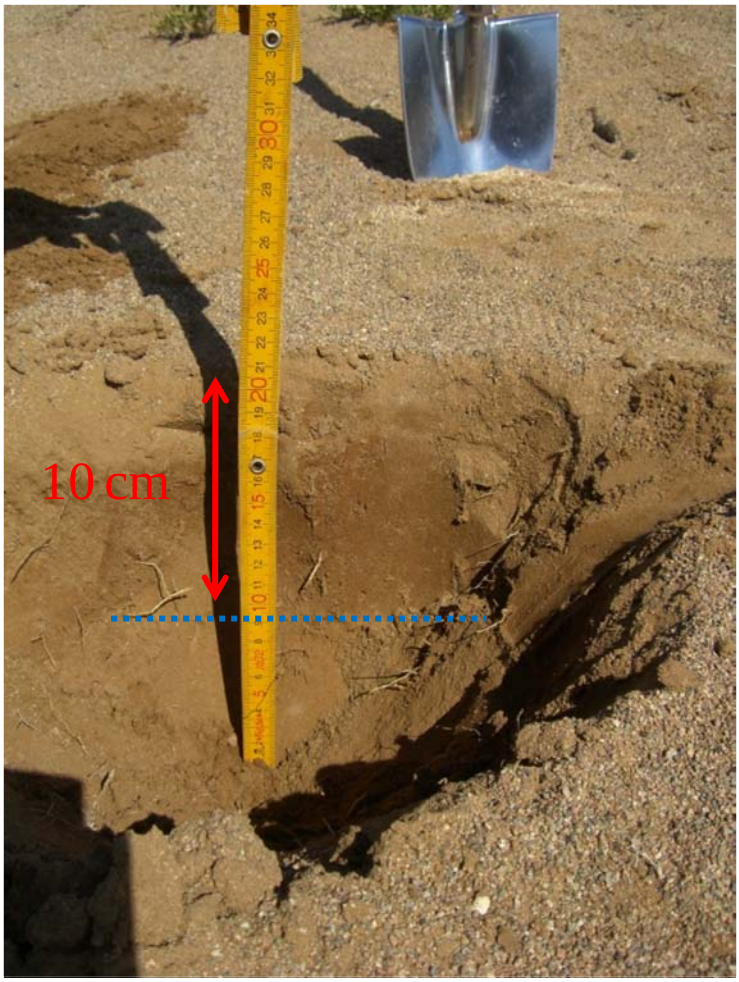

Figure 25 The wet soil observed after the rainfall on July 17th.

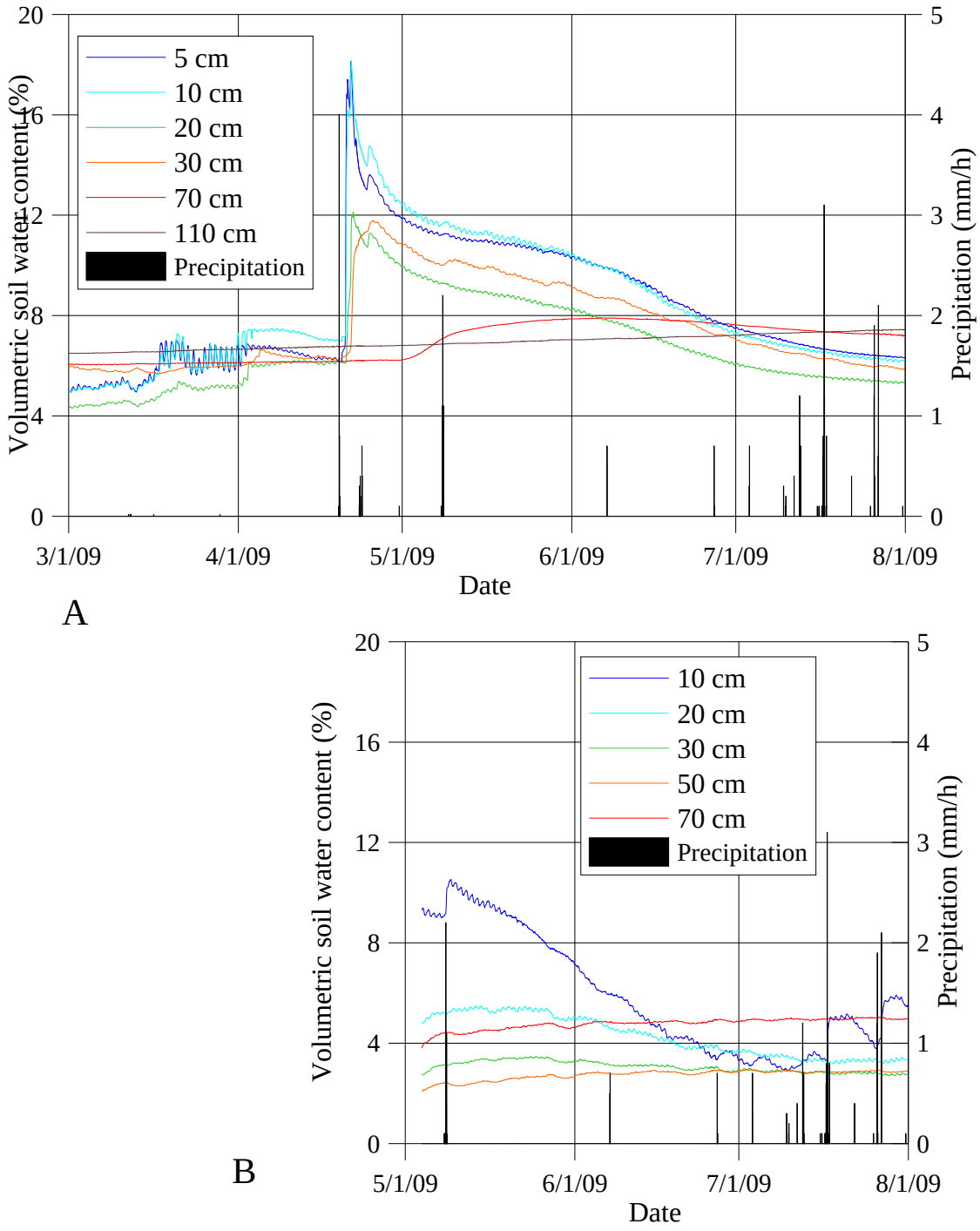

Figure 26 Relation between daily precipitation and volumetric soil water content measured by the TDR. A: TDR data from the MG1 station. B: TDR data from the MG2 station.

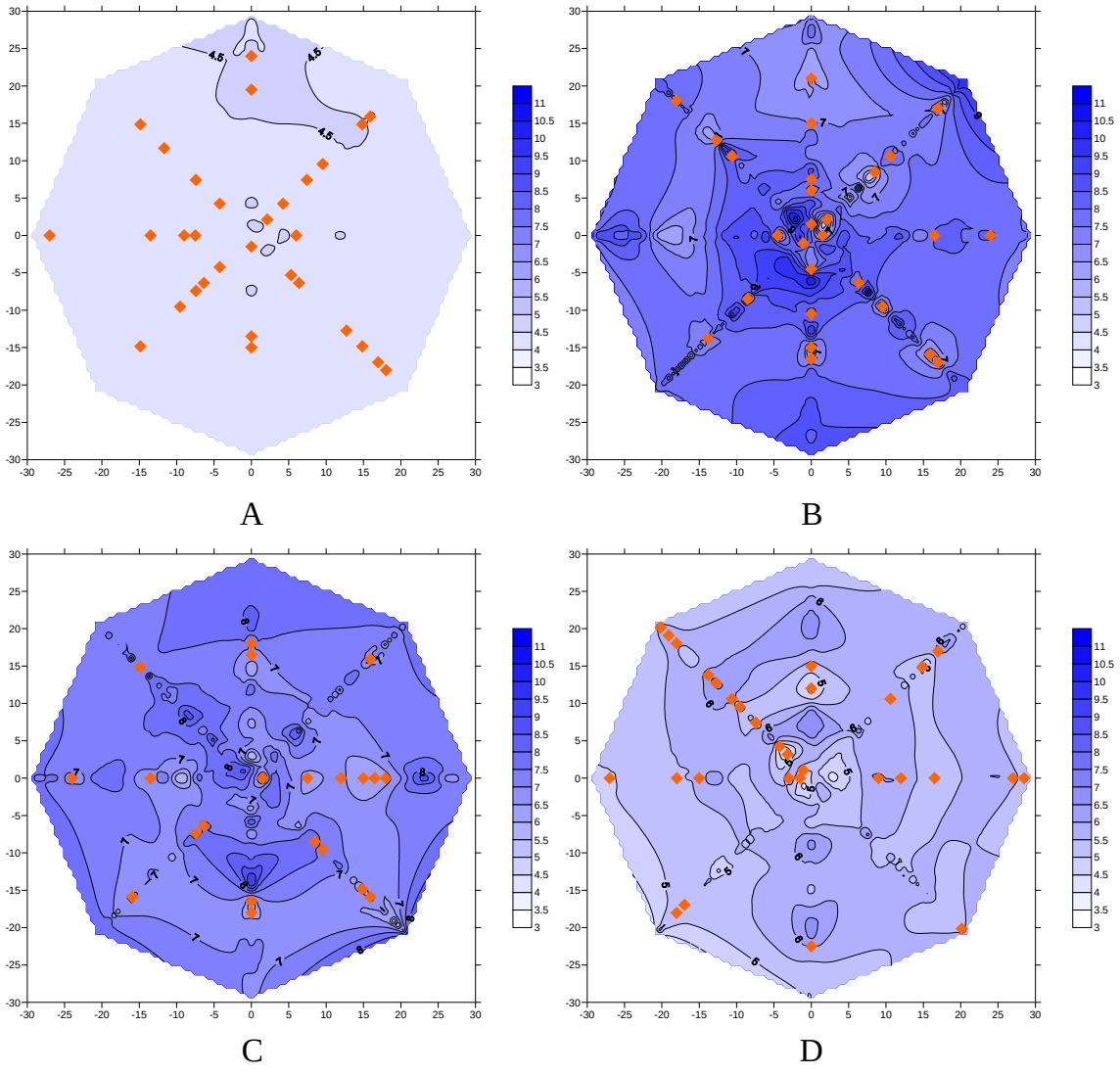

Figure 27a Horizontal distribution of volumetric soil water content at soil surface on July, 2009. Orange rhomboids indicate the point which was measured on the mounds formed by the shrubs. A: 10th B: 17th C: 18th D: 21st.

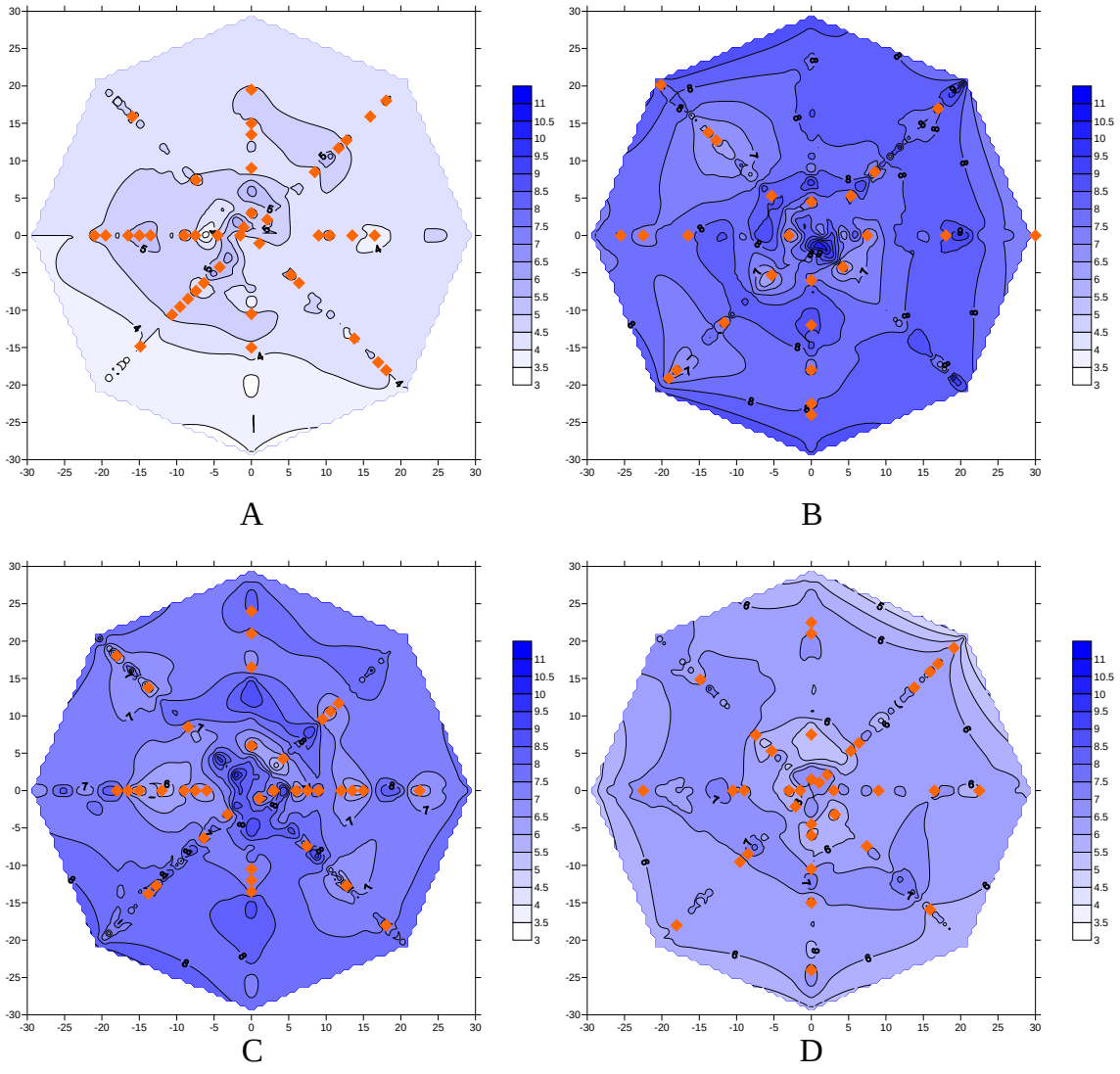

Figure 27b Horizontal distribution of volumetric soil water content at soil surface on July, 2009. Orange rhomboids indicate the point which was measured on the mounds formed by the shrubs. A: 25th B: 26th C: 27th D: 31st.

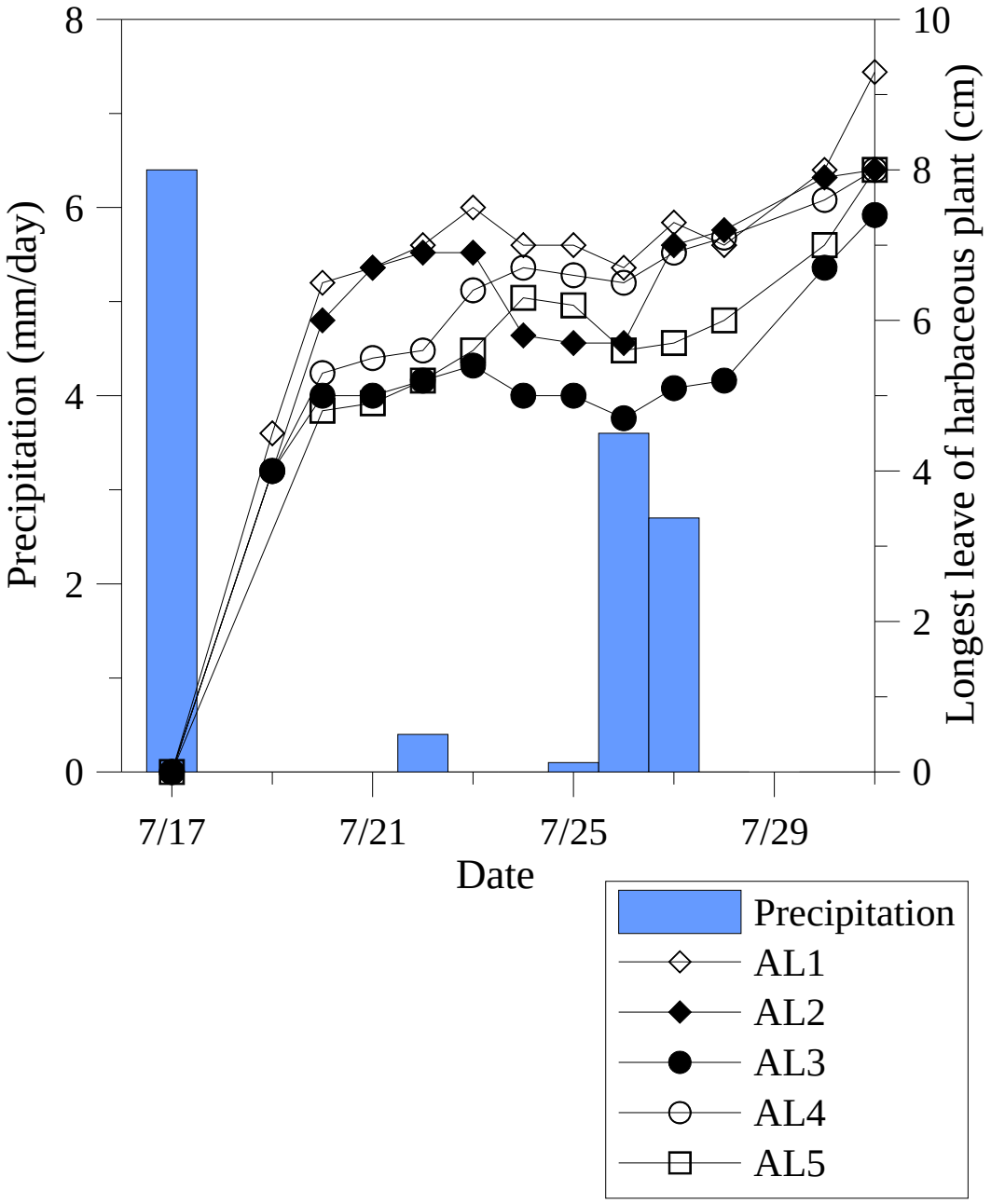

Figure 28 Relation between daily precipitation and the length of the longest leave of each herbaceous plant at each site.

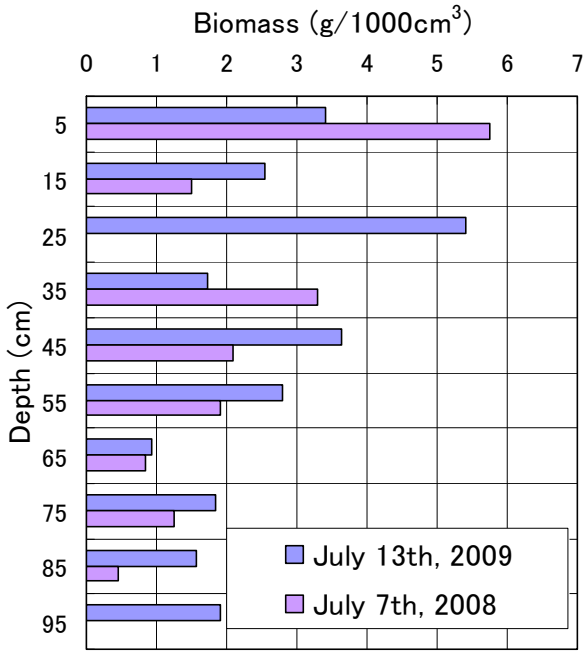

A

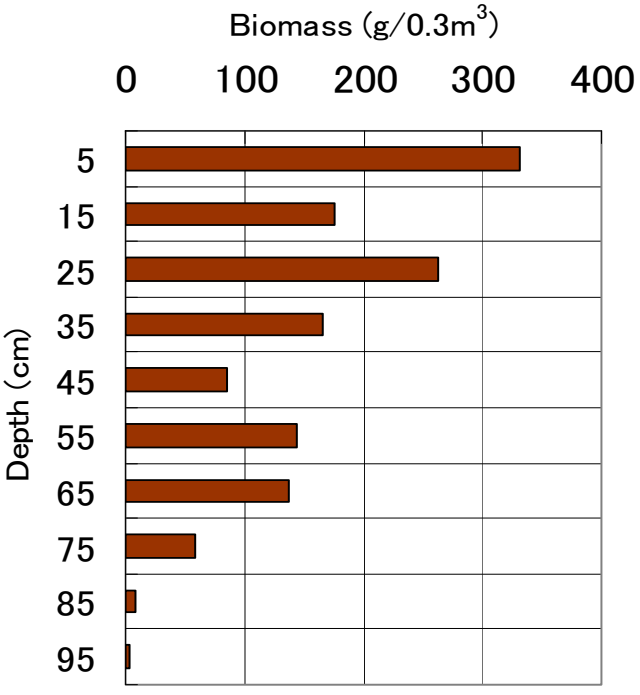

B

Figure 29 Profiles of below ground biomass. A: Small sized root distribution and B: Large sized root distribution. Small sized root biomass of 20-30 cm and 90-100 cm sampled on 2008 are missing values.

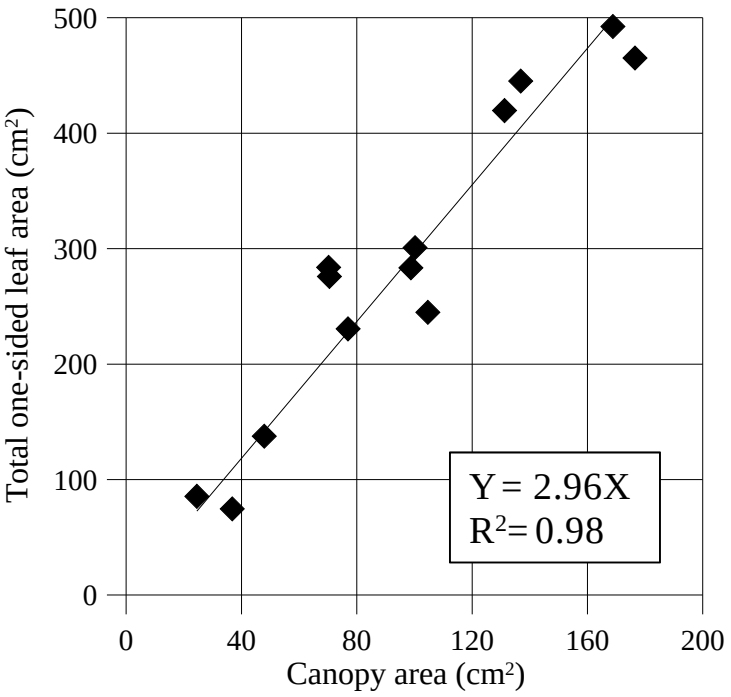

A

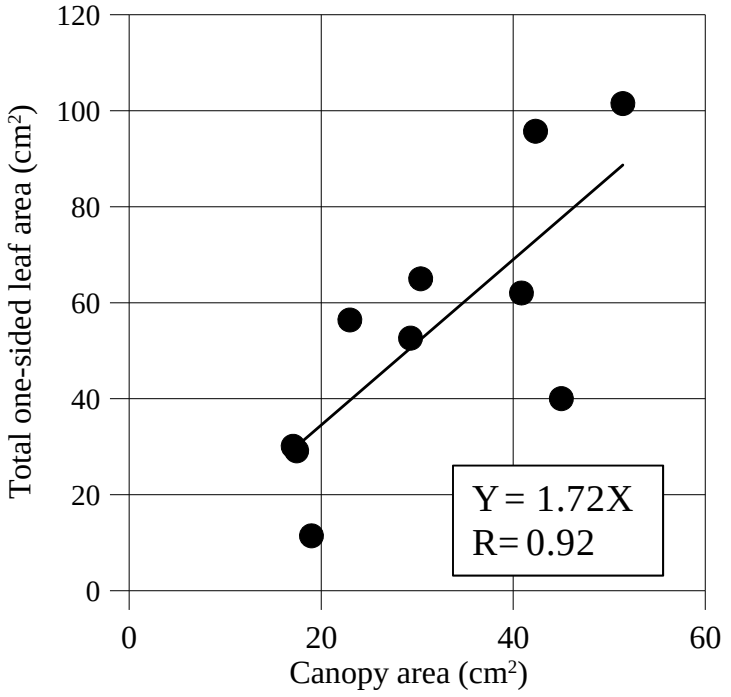

B

Figure 30 Correlation between vegetation coverage area (canopy area) and total upper leaf area of *Caragana microphylla* (A) and *Allium polyrrhizum* (B).

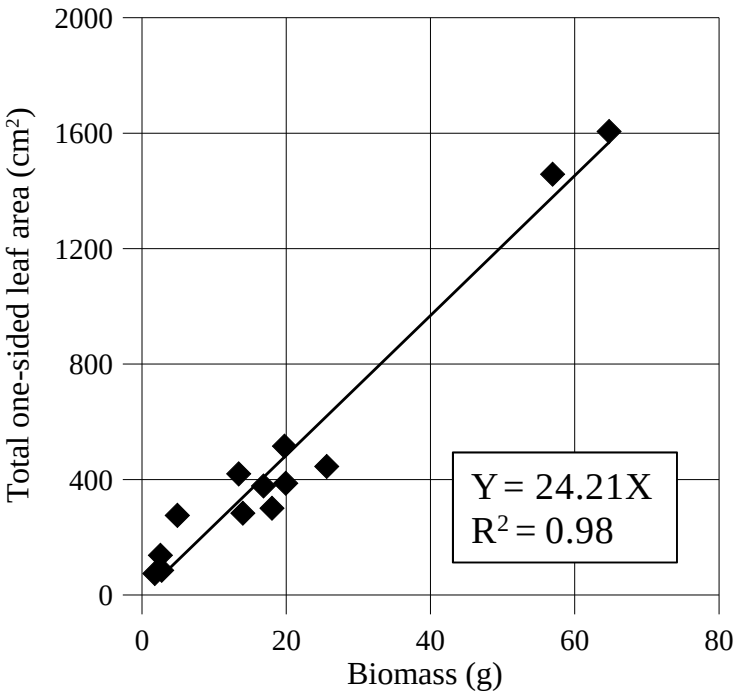

A

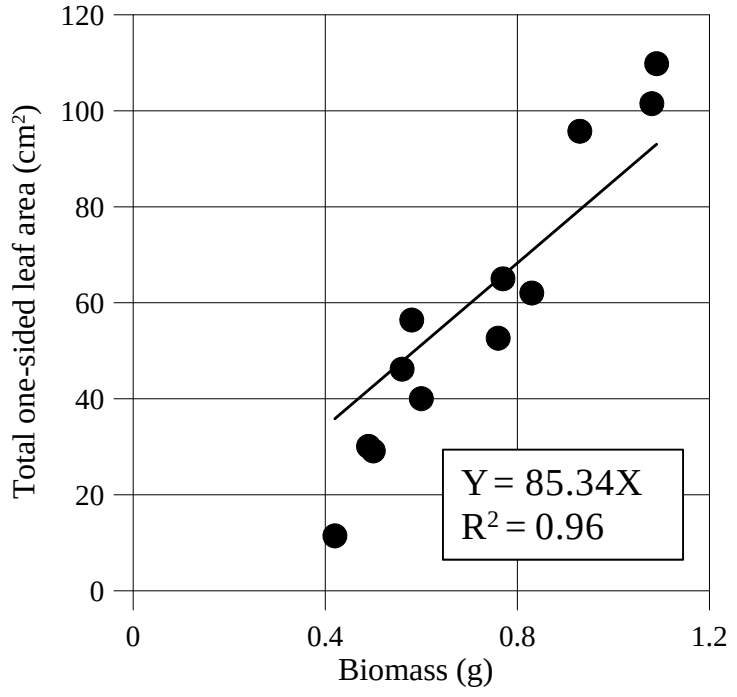

B

Figure 31 Correlation between Canopy area and total upper leaf area of *Caragana microphylla* (A) and *Allium polyrrhizum* (B).

A

B

Figure 32 Profile of the trench (A) and the side-wall (B) of the trench. Blue dashed line indicates the border of the sand layer and the Calcic horizon.

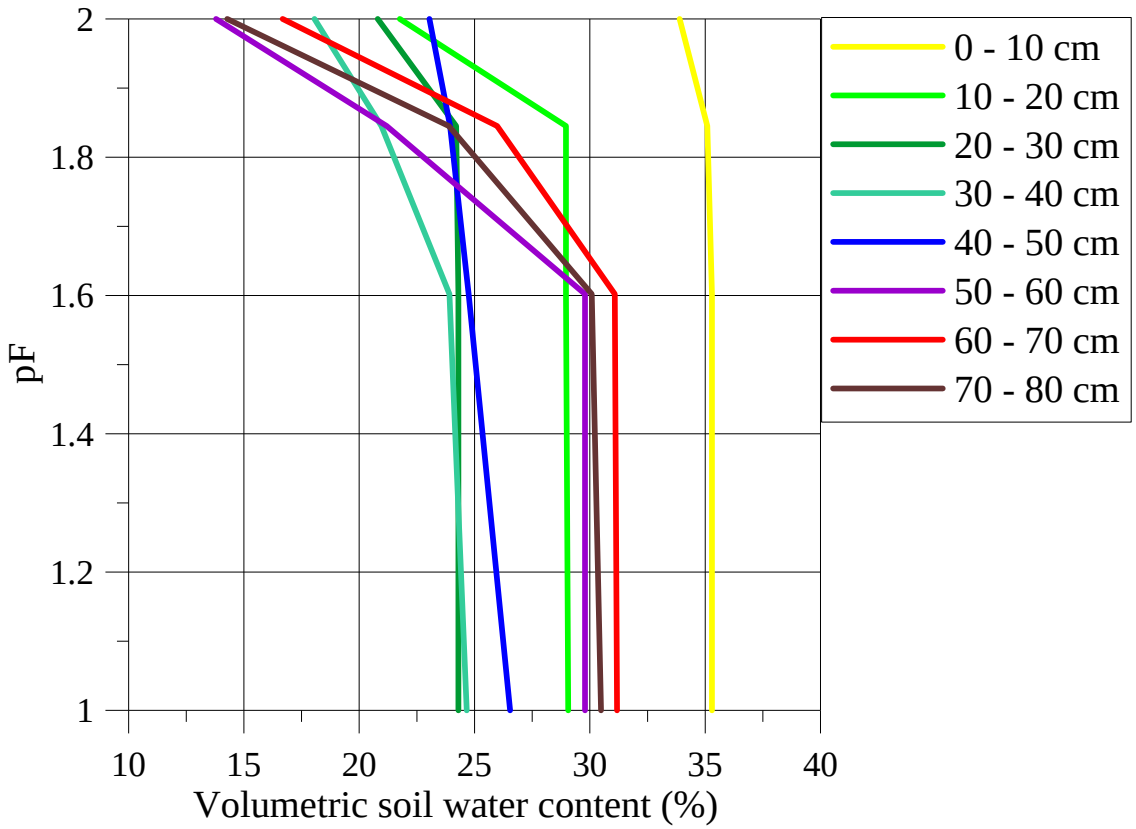

Figure 33 Relation between volumetric soil water content and pF value.

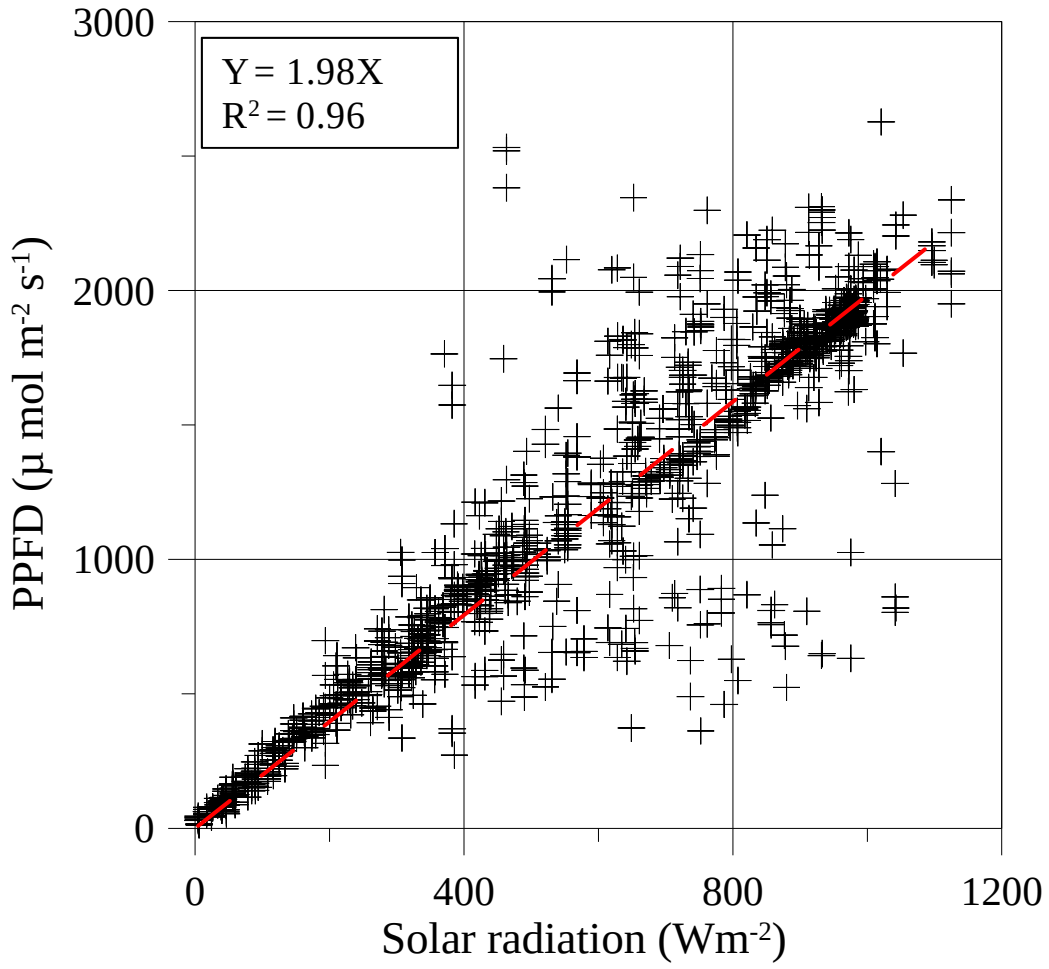

Figure 34 Relation between solar radiation measured by the MG1 station and PPFD measured by quantum sensor.

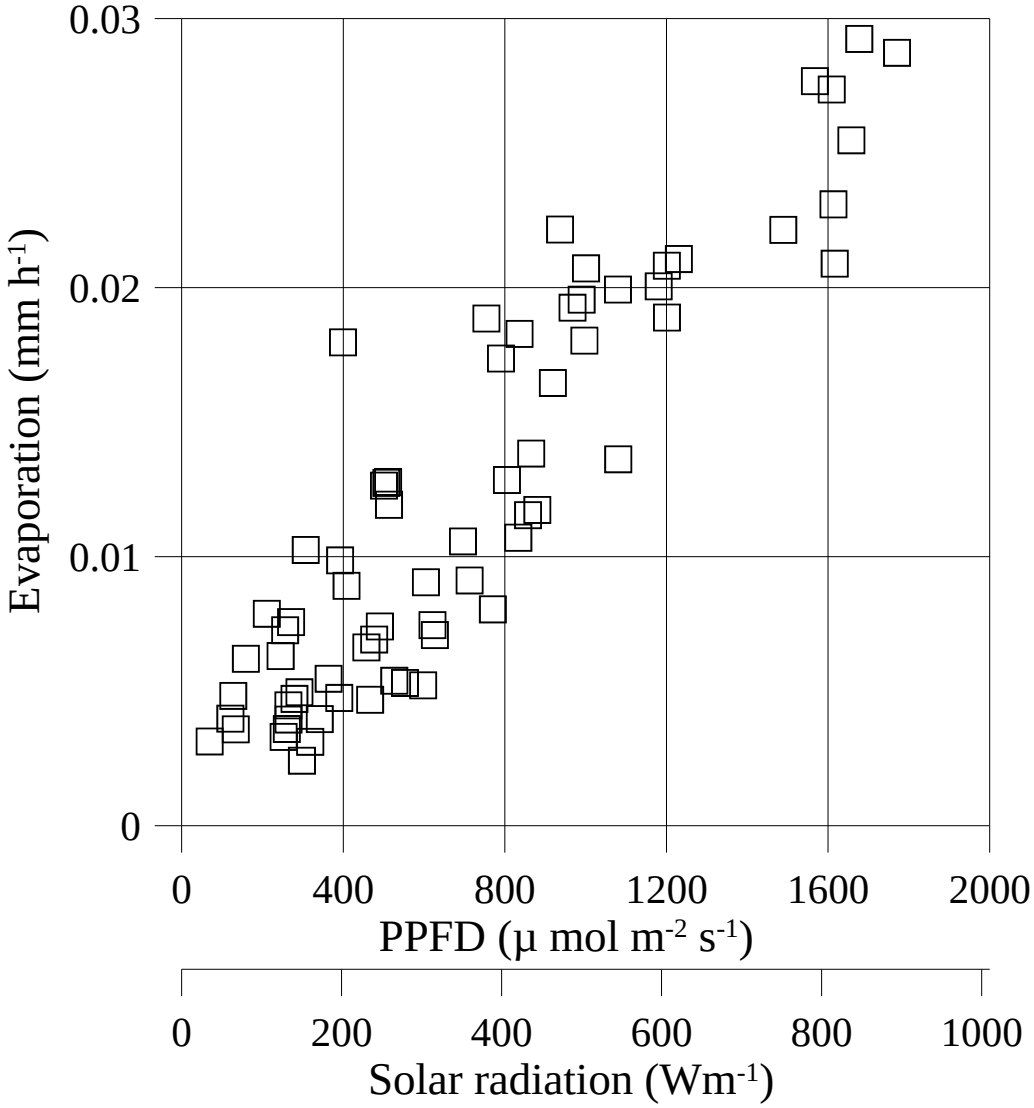

Figure 35 Relation between solar radiation and EV on June 1st to 4th.

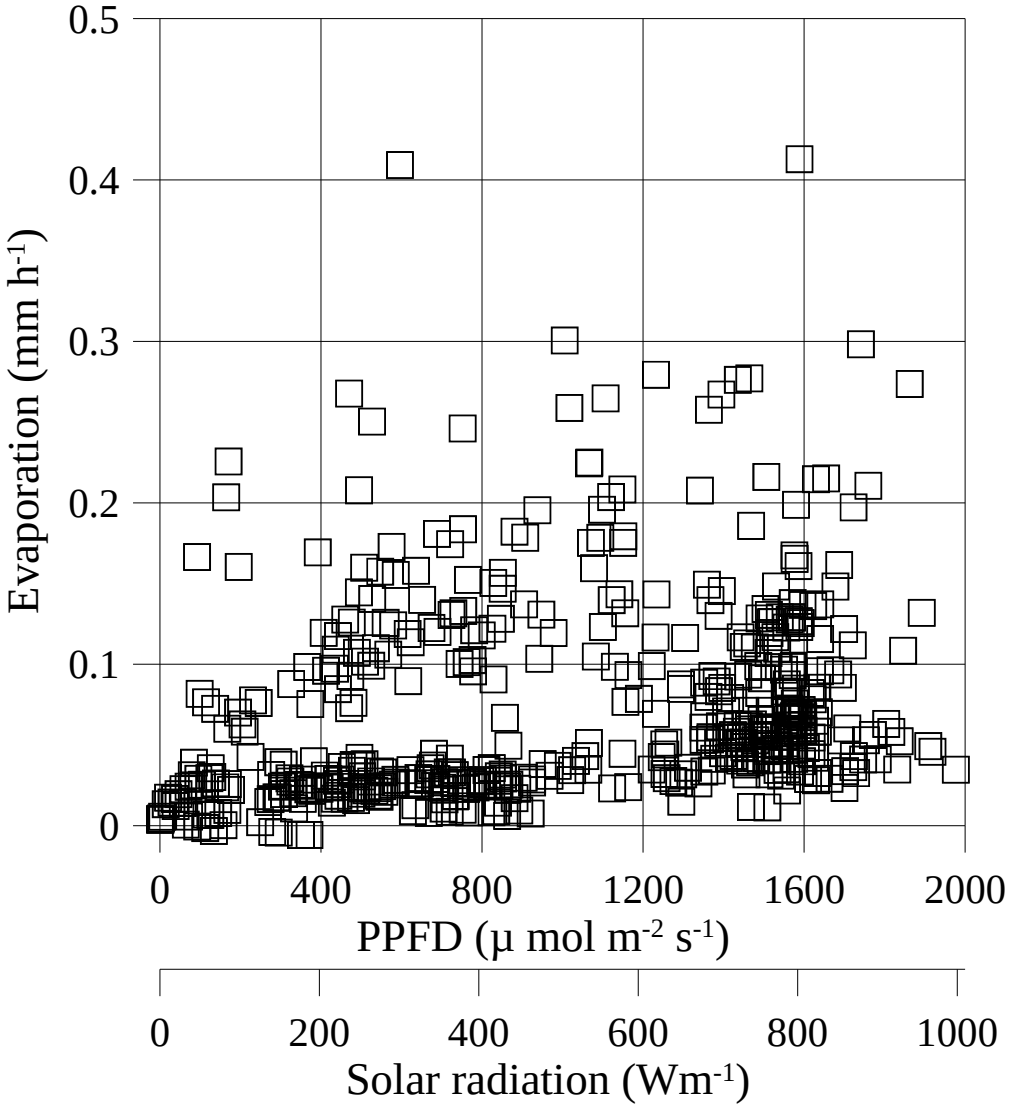

Figure 36 Relation between solar radiation and EV of whole chamber measurement covered on bare soil from July 11th through 31st, 2009.

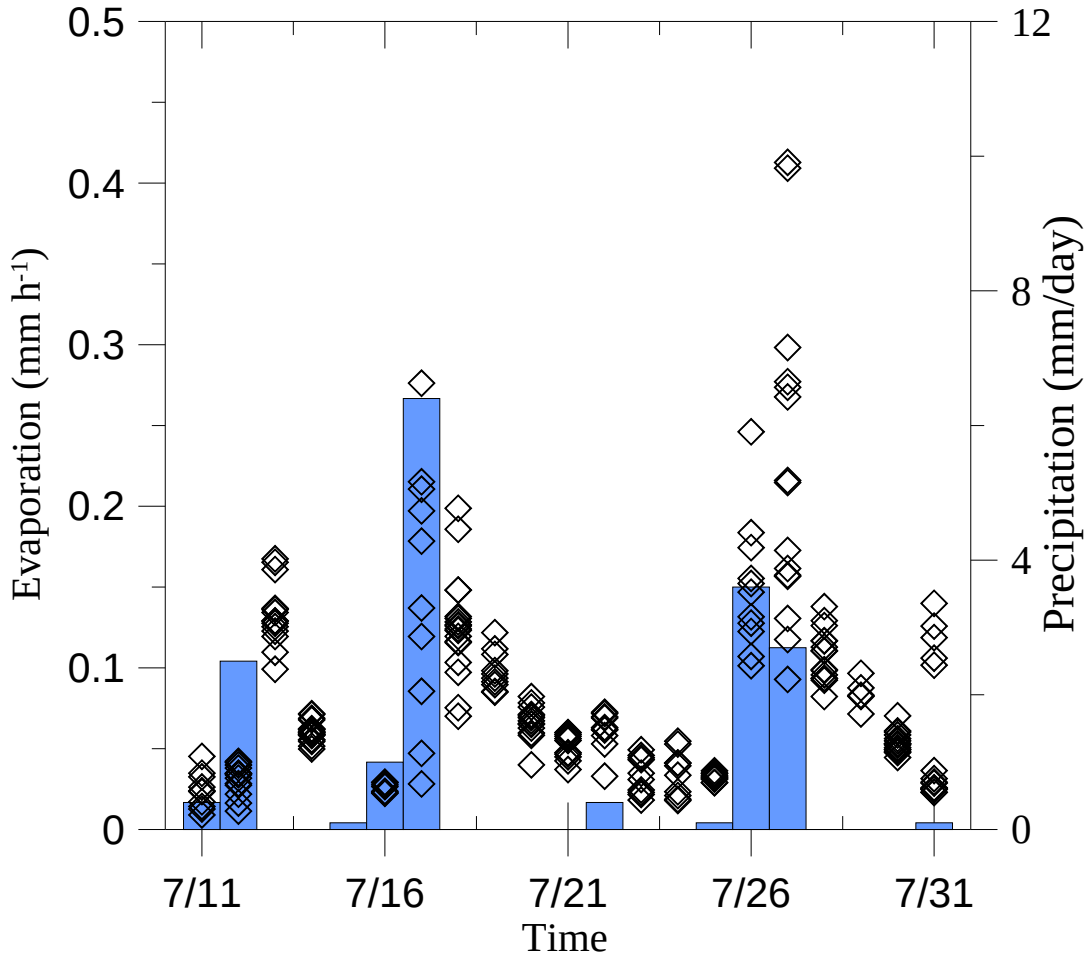

Figure 37　Relation between EV measured within 11:00 to 15:00 when the solar radiation was largest of each day and daily precipitation.

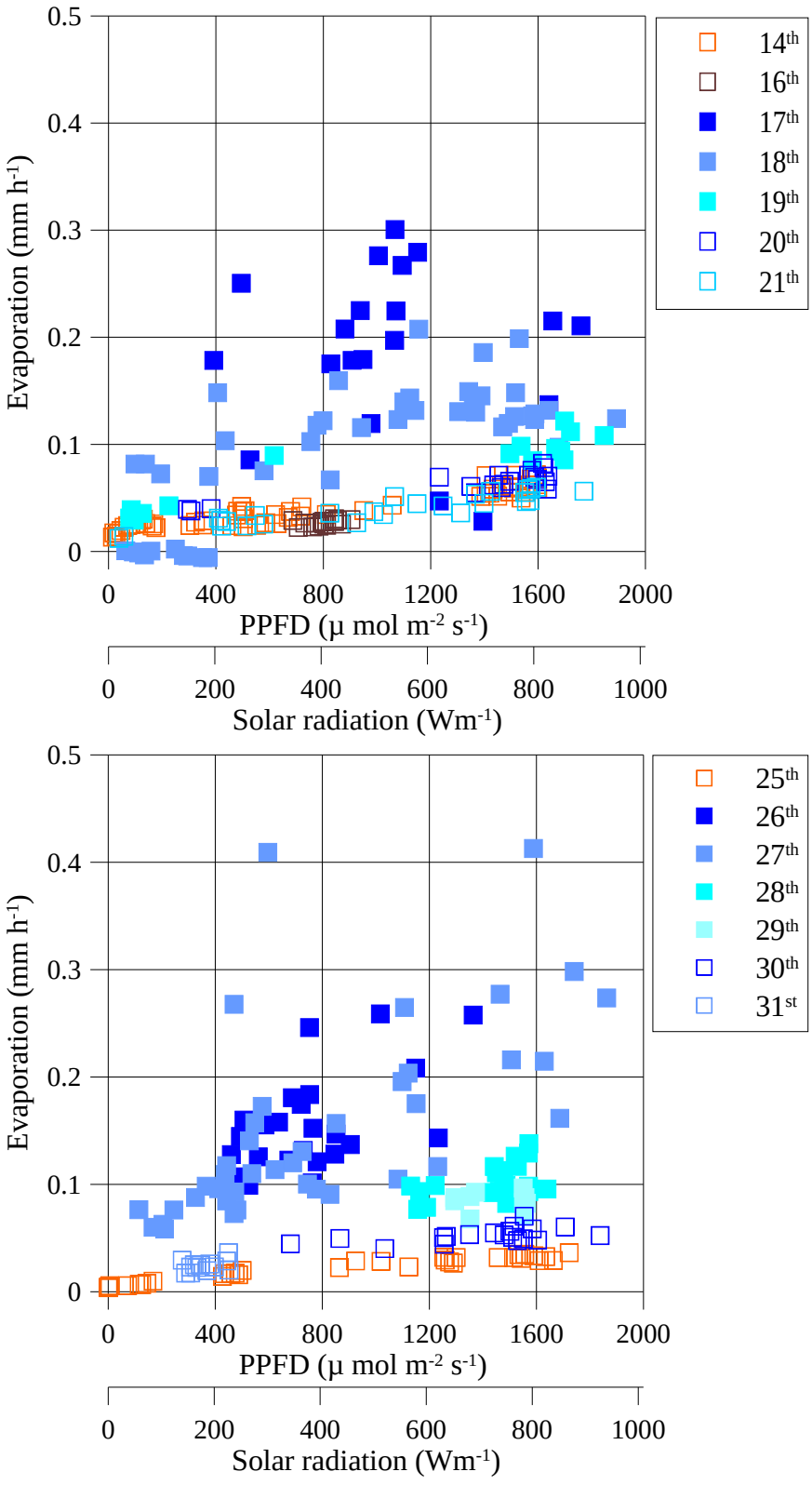

Figure 38 Relation between solar radiation and the EV on the vicinity of the rainfall event on July 17th and 27th 2009.

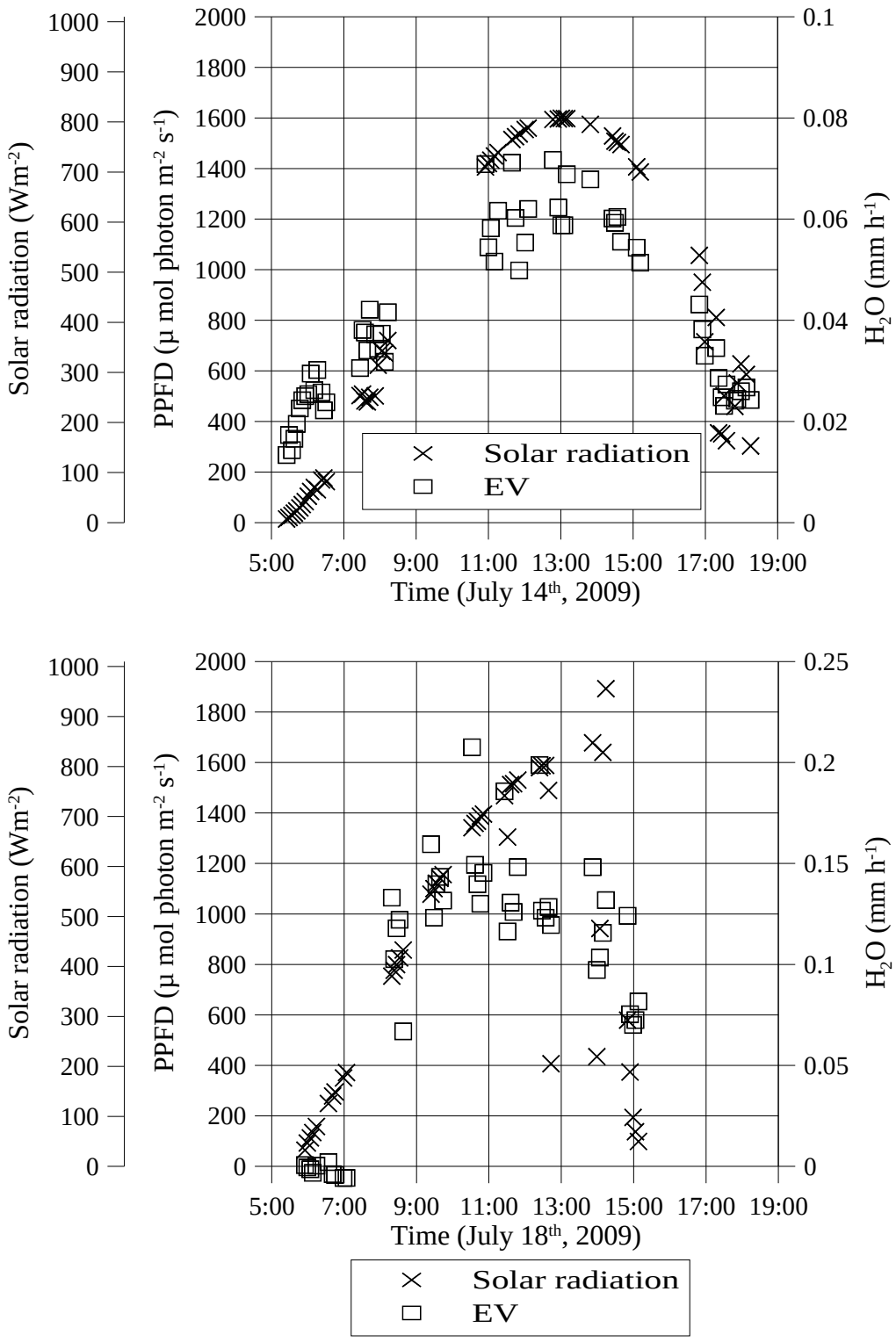

Figure 39 Example of time variations of solar radiation and EV before and after the rainfall on July17th, July 14th and 18th respectively.

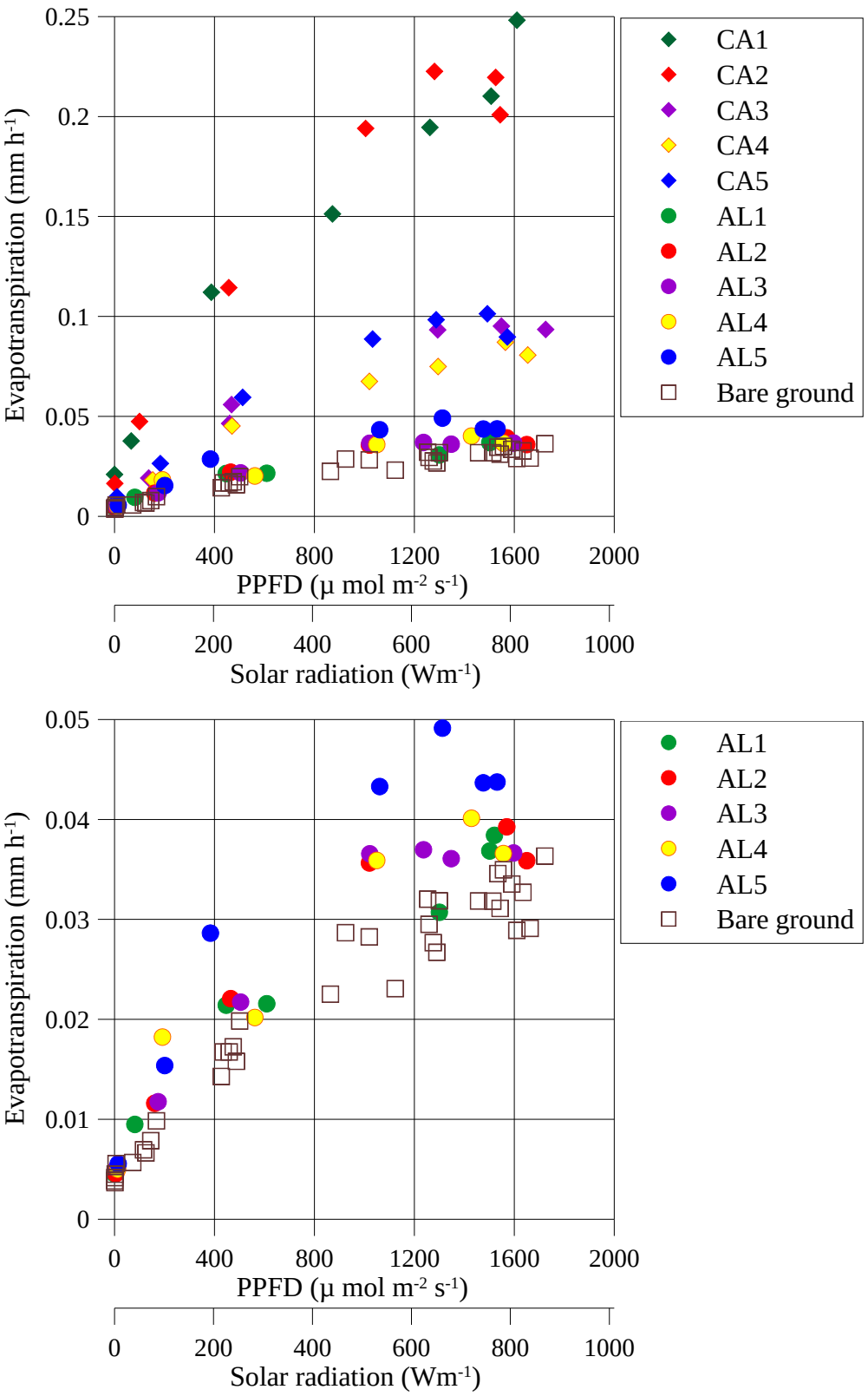

Figure 40 Relationship between PPFD and ET on July 25th, 2009 where CA represents sites including *Caragana microphylla* and AL represents sites including *Allium polyrrhizum* (Top). The EV from bare ground is shown for comparison. Bottom graph shows enlarged graph focusing on EV from AL sites.

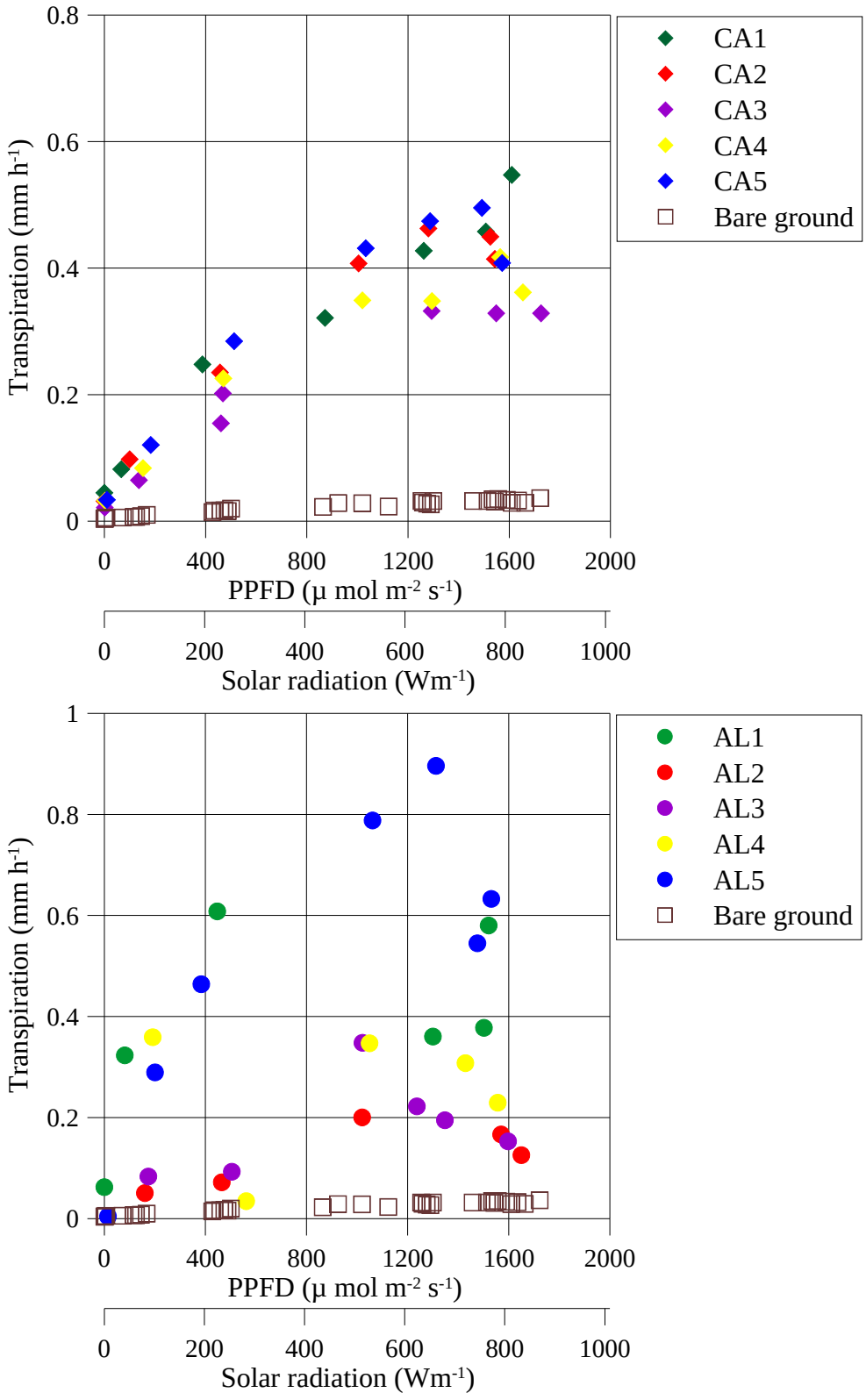

Figure 41 Relationship between PPFD and TR on July 25th, 2009 where CA represents sites including *Caragana microphylla* and AL represents sites including *Allium polyrrhizum*. The TR from bare ground is shown for comparison (Top). Bottom is enlarged for AL sites.

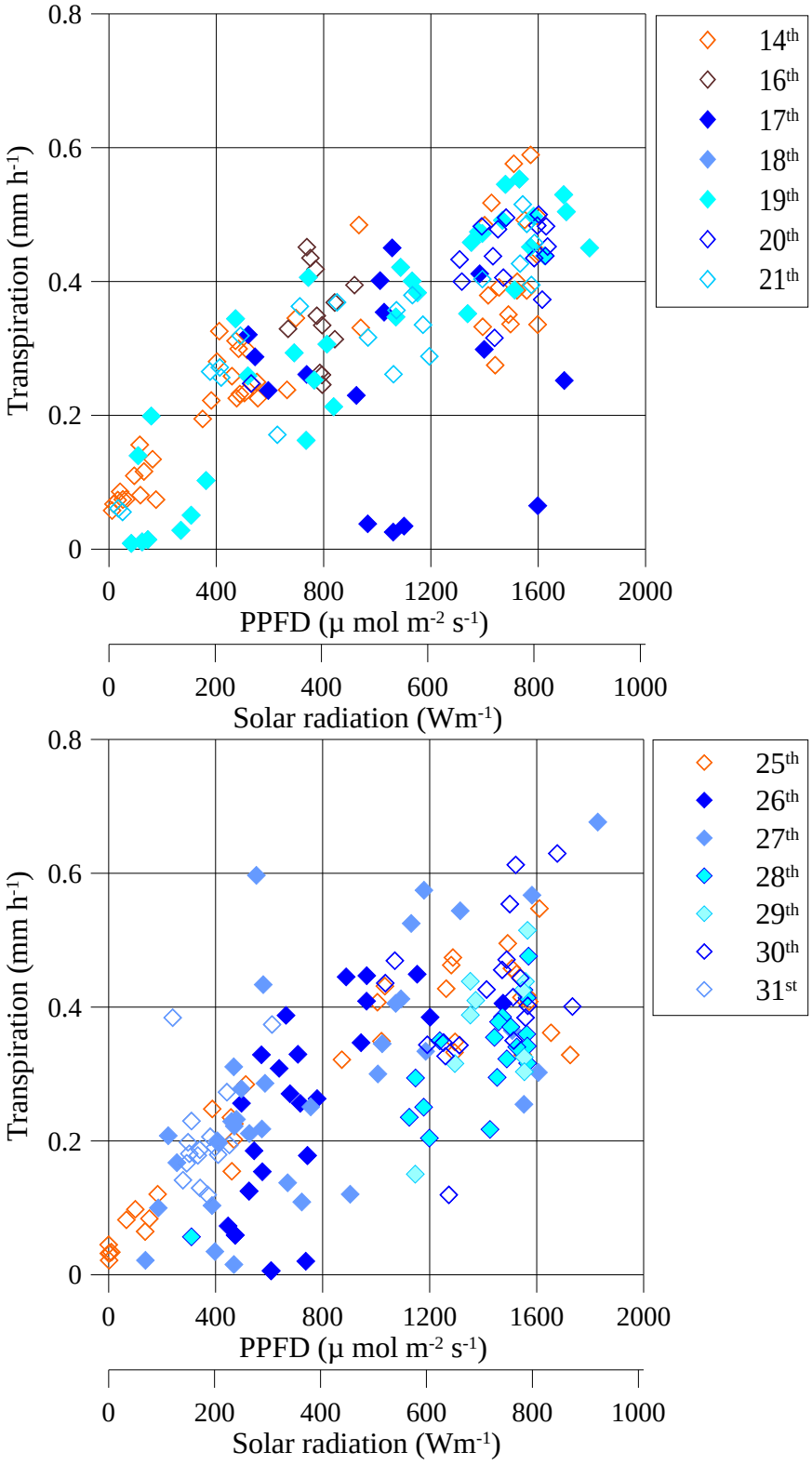

Figure 42 Relation between PPFD and the TR from shrubs on the vicinity of the rainfall event on July 17th and 27th 2009.

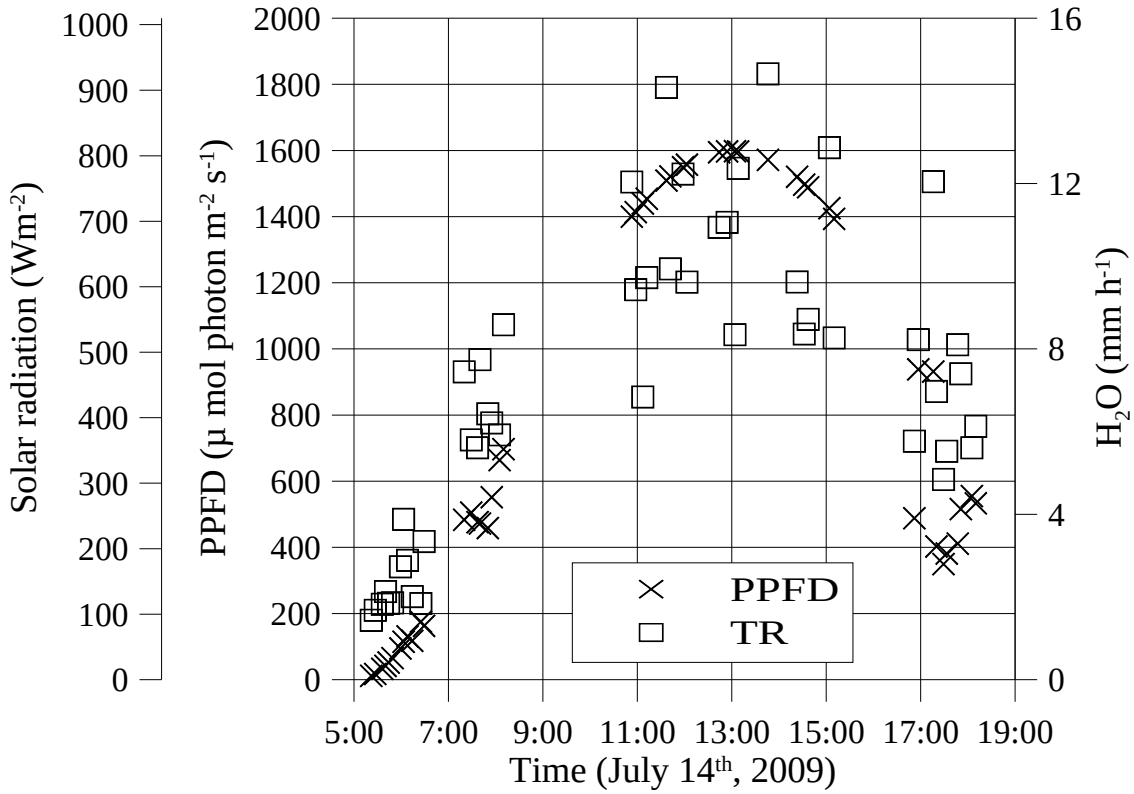

Figure 43 Time variations of solar radiation and TR of shrubs on July 14th.

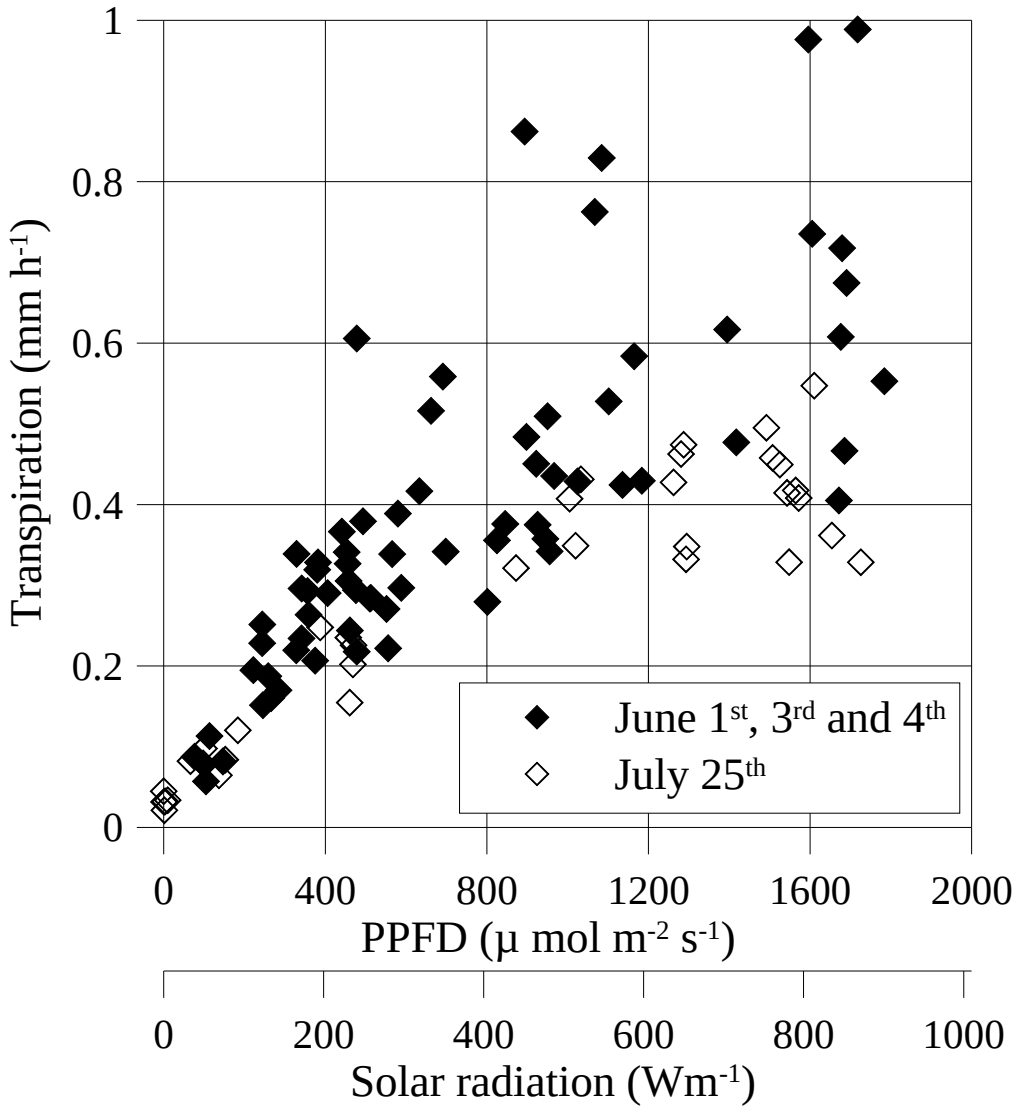

Figure 44 Relation between PPFD and TR of shrubs on June 1st, 3rd and 4th.

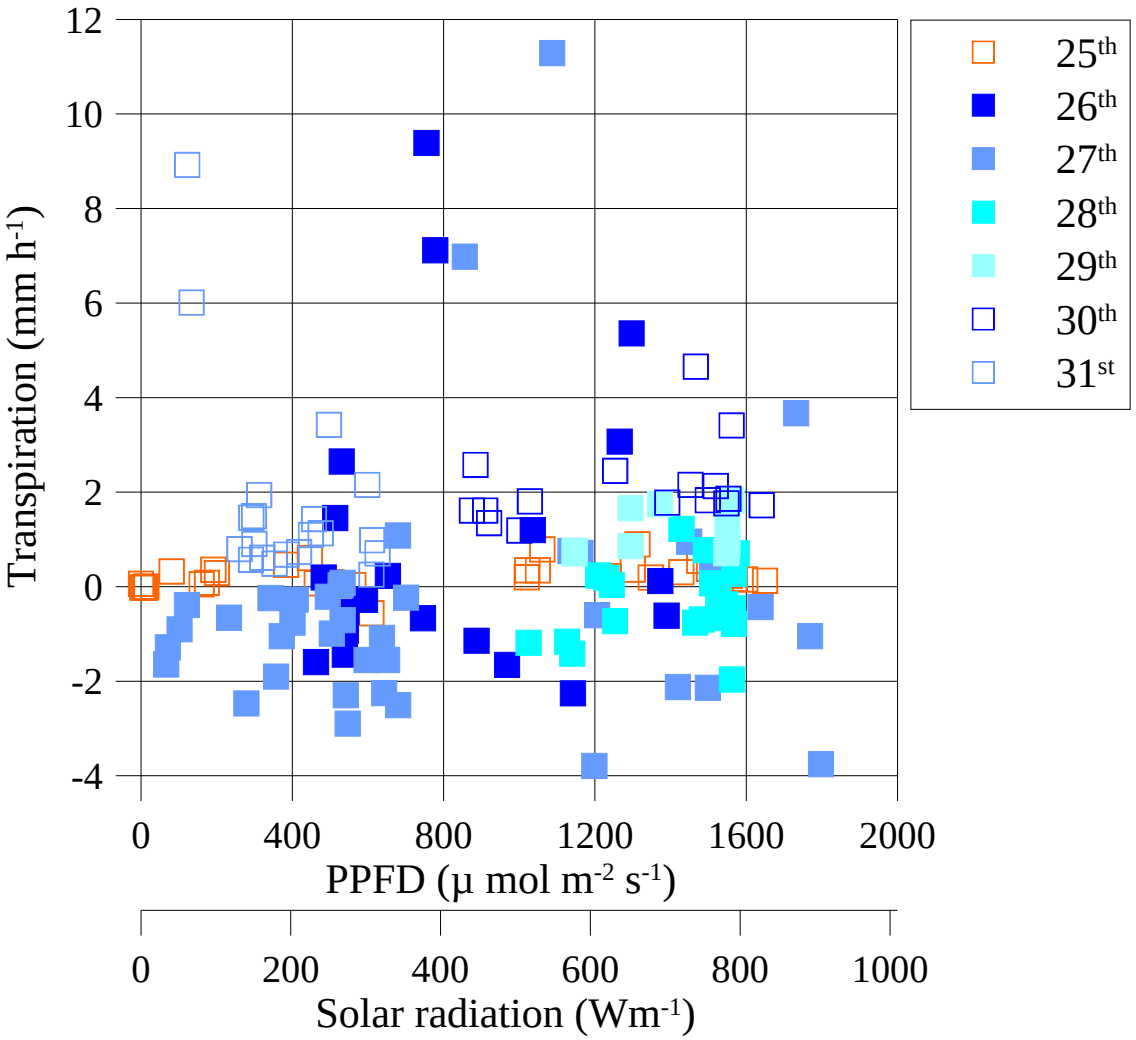

Figure 45 Relation between PPFD and the TR of herbaceous plants on the vicinity of the rainfall event on July 27th, 2009.

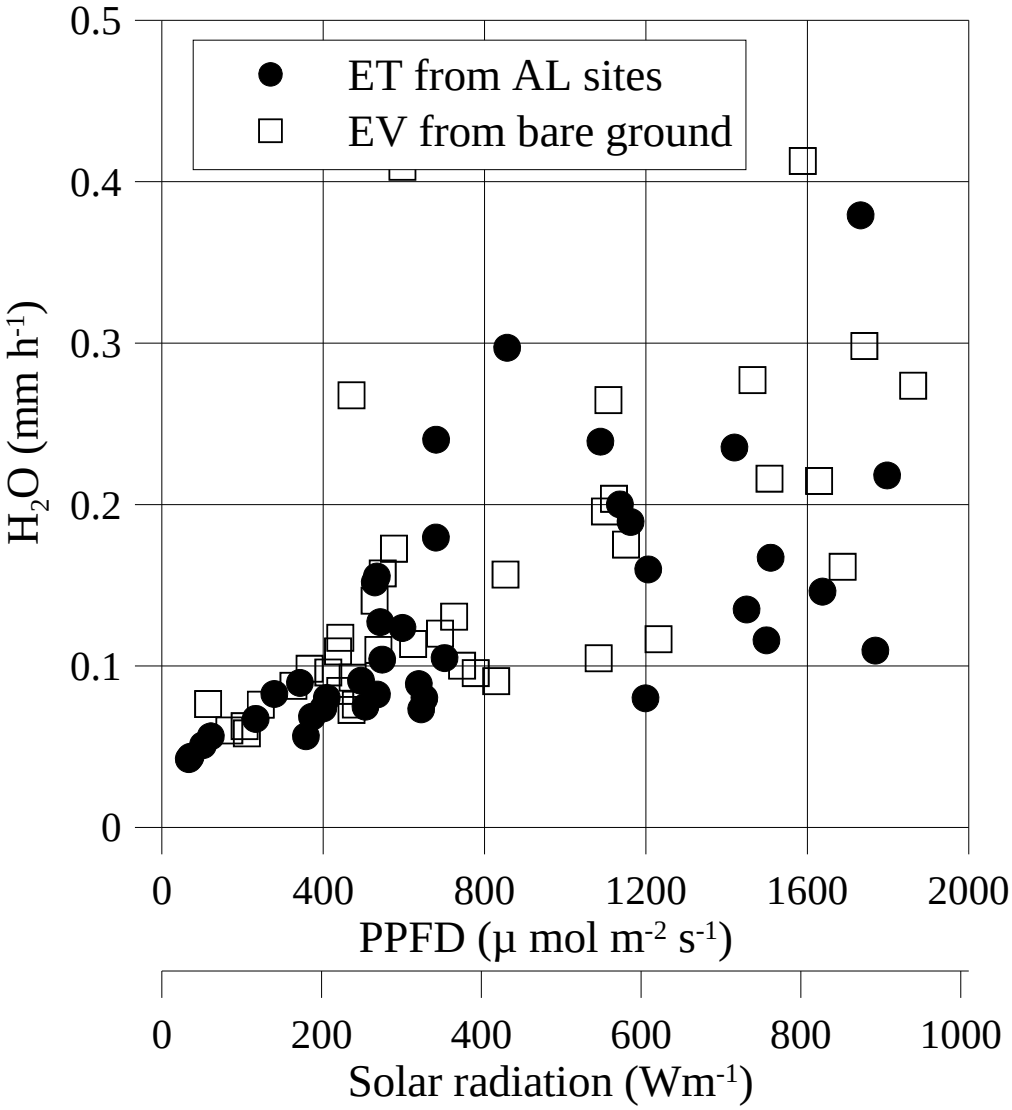

Figure 46 Relationship between solar radiation or PPFD and EV from bare ground and ET from AL sites on July 27th, 2009.

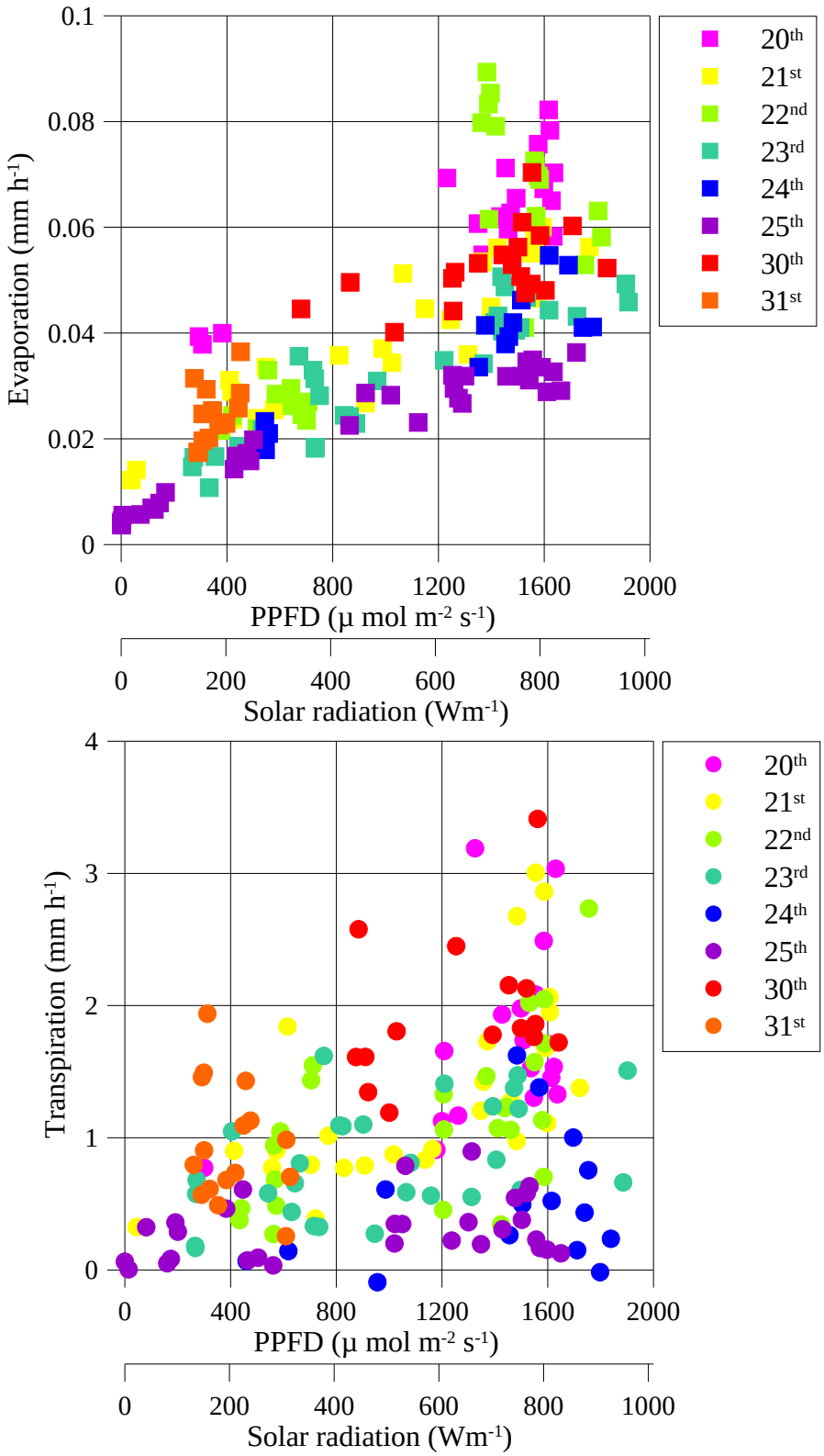

Figure 47　Relationship between solar radiation and EV form bare soil (top) and PPFD and TR from herbaceous plants (bottom) on dry period.

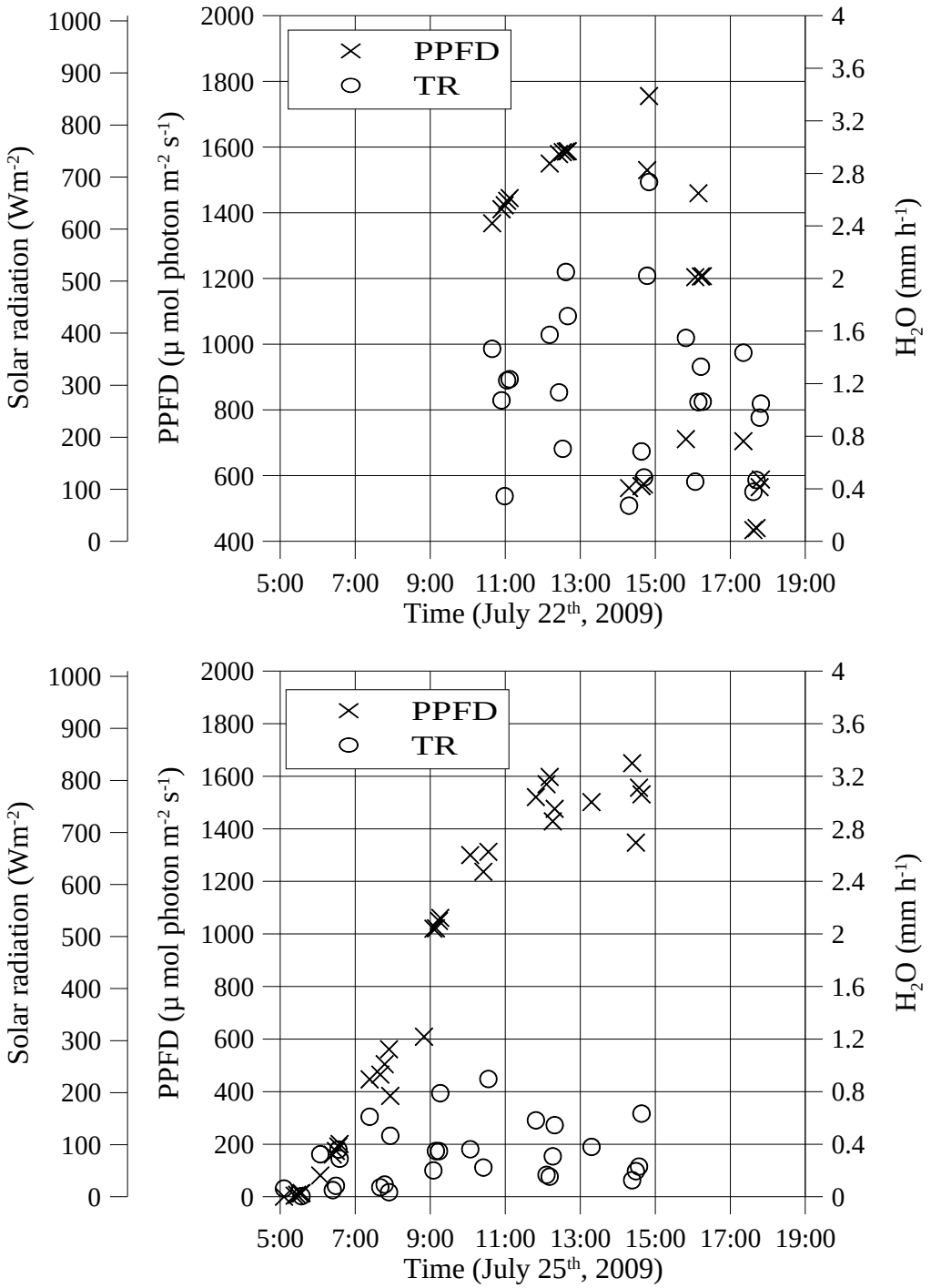

Figure 48 Time variance of PPFD and TR from herbaceous plants.

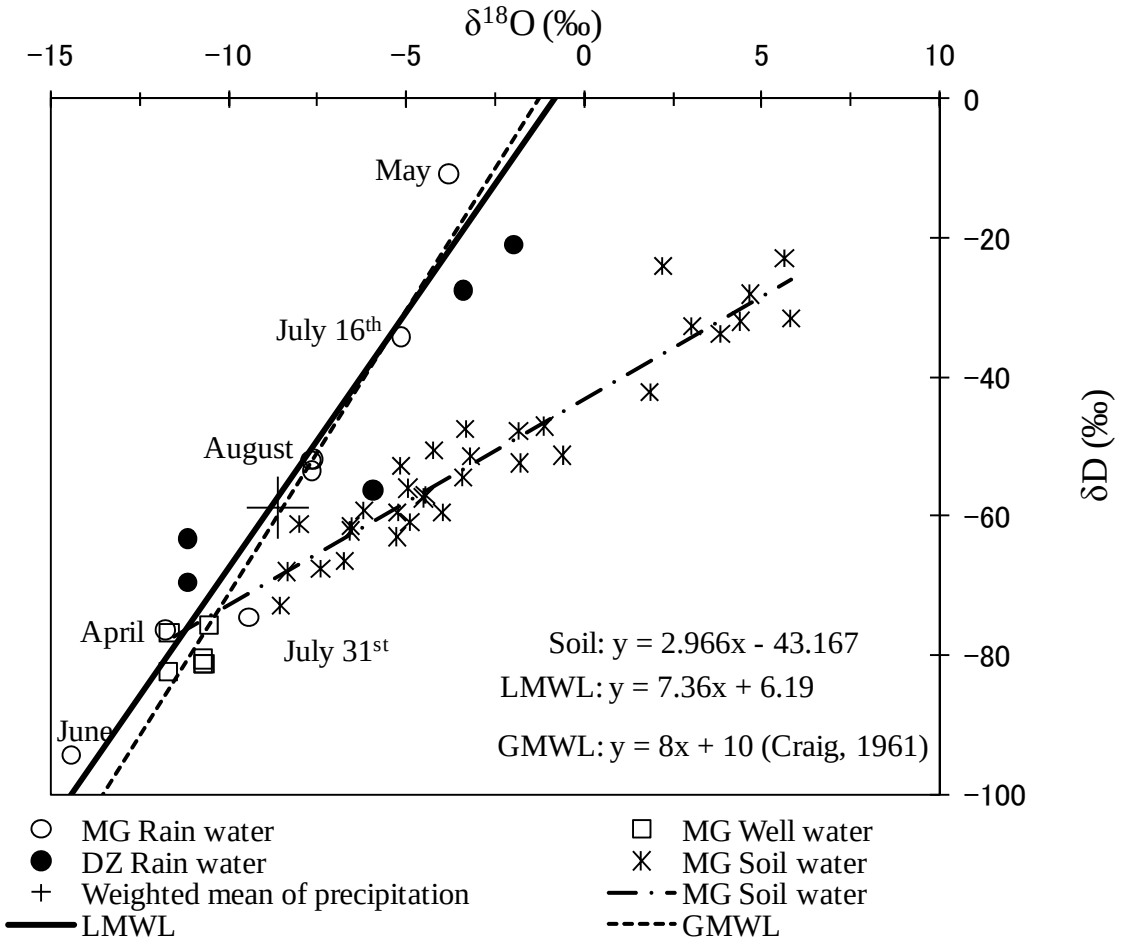

Figure 49 Relation between $\delta^{18}O$ and δD.

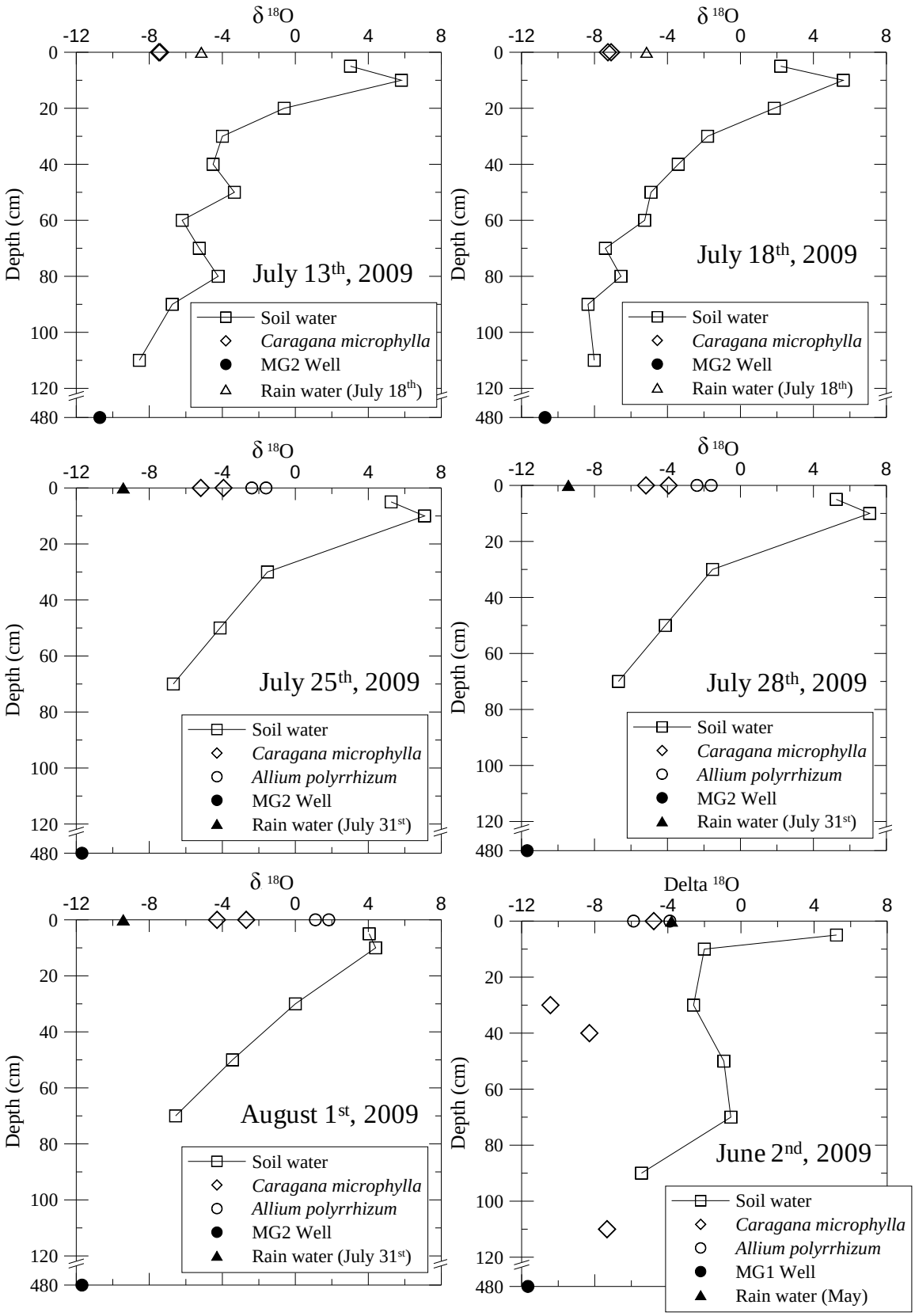

Figure 50 Vertical profiles of the $\delta^{18}O$ in soil water with the $\delta^{18}O$ of well water and in xylem sap of shrubs and herbaceous plants.

4. Discussion

4. 1 Evaporation variations

Good correlations were found between solar radiation and evaporation (EV) for each day under circumstances of steady wind speed. However, daily variations of EV differed significantly in the vicinity of rainfall events. There was rapid increase in EV shortly after the rainfall events and then gradually decreased in about three days. To investigate the driving force on daily variation of EV, a multiple regression analysis was applied by using the data from the chamber measurement and from the measurement of the MG1 station and the MG2 station. Six independent variables were used for the analysis, which is [1] air temperature, [2] air temperature inside the chamber, [3] soil temperature at 10 cm depth at the MG1 station, [4] volumetric soil water content at 10 cm depth at the MG2 station, [5] estimated solar radiation and [6] specific humidity. A stepwise method was used with F statistic of 2.5 to select the independent factors. The solar radiation used for the analysis was estimated from a PPFD instead of using the MG1 station data because the PPFD was measured every second while the MG1 station had collected only ten minute average data of the solar radiation. As a result, [1] air temperature, [3] soil temperature at 10 cm depth, [4] volumetric soil water content at 10 cm depth and [6] specific humidity were chosen. The equation was derived as follows:

$$EV_{hour} = -0.01507T_s + 0.01739q + 0.00554T_a + 0.01406\theta + 0.08096 \quad (11)$$

where EV_{hour} represents evaporation per hour (mm h^{-1}), T_s represents soil temperature at 10 cm depth (°C), q represents specific humidity (g kg^{-1}), T_a represents air temperature (°C) and θ represents volumetric soil water content at 10 cm depth (%). Partial correlation for each variables were T_s: -0.41, q: 0.41, T_a: 0.32 and θ: 0.23. Relation between observed and estimated EV are shown in Figure 51. There was a good agreement when the EV was smaller and a lesser agreement was found for larger EV range. The EV was overestimated when the EV was smaller. On the other hand, when the EV was larger it was underestimated.

However, from the result of chamber measurement, EV had correlation with solar radiation especially on the day before and after several days from the rainfall event but it was not chosen by the above multiple regression analysis. Thus, multiple regression analysis was also applied to those days whose EV was not affected by rainfall with the same condition as above. As a result, only [5] estimated solar radiation was chosen:

$$EV_{hour} = 4.7 \times 10^{-5} R_s + 0.0121 \quad (12)$$

where R_s represents solar radiation (Wm^{-2}). Figure 52 shows the relation between observed and estimated EV. The profile was similar to the relation derived from using whole data that it was underestimated when the observed EV was large.

4. 2 Transpiration variations

4. 2. 1 Transpiration from shrubs

The behavior of transpiration (TR) was different between shrubs and herbaceous plants. TR of shrubs did not change during July in spite of the sufficient rainfalls on July 17th and 16th–17th under the condition of steady wind speed. This was because shrubs were utilizing the water from around 70 cm to 90 cm depth with relatively high volumetric soil water content (Figure 53). The stable isotope ratio analysis of $\delta^{18}O$ indicated that shrubs are utilizing the water from about 70 cm to 90 cm depth. This could be also confirmed from the presence of the roots found by a below ground biomass observation. TDR data show that this soil layer has relatively high volumetric soil water content than the surface layer. This layer was also not affected by the rainfall events in July. This is the reason why TR of shrub did not change among the rainfall events. The TR difference between June and July could also be explained from the volumetric soil water content at those depths. June TR was larger than July while volumetric water content at depth around 70 cm to 90 cm was higher in June than July. A Multiple regression analysis with stepwise method was used with F statistic of 2.5 to select the independent factors for TR of shrubs. As a result, only PPFD was chosen for the TR variance.

$$TR_{hour} = 2.14 \times 10^{-4} R_p + 0.102 \quad (13)$$

where TR_{hour} represents TR per hour (mm h^{-1}) and R_p represents PPFD (μ mol m^{-2} s^{-1}). Figure 54 shows the relation between observed and estimated TR of shrubs through whole measurements took place in July, 2009. They correlate better than EV estimation described above, although they tend to overestimate when the TR was large.

4. 2. 2 Transpiration from herbaceous plants

The TR of herbaceous plants varied depending on volumetric soil water content and its growth. Figure 55 shows the relation between TR of herbaceous plants when PPFD was larger than 1400 (μ mol m^{-2} s^{-1}), length of tallest leaf in each site, precipitation and volumetric soil water content at 10 cm dept measured by the MG2 station. After the rainfall event on July 17th, volumetric soil water content started to decrease on July 20th and at the same time TR also

started to decrease. Three days later, herbaceous plants partly started to die which is reflected on the length of the tallest leaf. Those plants started to grow again after the rainfall event on July 26th and 27th which cultivate soil surface. This herbaceous plants reaction to the rainfall event corresponds to those plants behavior observed near Mandalgobi by Hirata et al. (2009). The TR also increased after the event. These TR variations could be explained from physiological activity of herbaceous plants. After the rainfall, herbaceous plants start to produce sugar to encourage its growth. As a result, TR increases shortly after the rainfall. When the volumetric soil water content depletes after several days from the event, plants experience water stress. Under this circumstance, plants close their stoma to keep the water inside the plants. Although those plants try to prevent water loss, vapor would be lost through cuticle (Chapin, 2002: Larcher, 2003). This lost water was reflected to the TR on dry period. Stable isotope analysis indicates that this water utilized for physiological activity of herbaceous plants came from the soil water from the layer close to the soil surface.

In conclusion, shrubs transfer the soil water at around 70 - 90 cm depth to the atmosphere regardless of the rainfall events. The PPFD was mainly responsible for the variation of daily transfer through TR when the wind speed variation is not considered. On the other hand, herbaceous plants accelerate the vapor transfer from soil surface to the atmosphere shortly after the rainfall due to the physiological activity. Subsequently, transportation capability of those plants declines with depletion of volumetric soil water content at surface layer of the soil.

4. 3 Soil water behavior

Soil water recharge had started at the end of March when the soil temperature exceeded 0 °C by melting the soil water or solid water over the soil surface. The results from the TDR at the MG1 station show that soils were saturated on April 19th when there was rainfall of 4.7 mm in one hour and twenty minutes. Although there also was strong rainfall on May and July, only the TDR at shallower depths responded to those rainfalls. However, the result of stable isotope analysis on hydrogen and oxygen indicated that source of the soil water was the rainfall of April or the underground water. Therefore, by comparing these results from TDR observation and isotope ratio, the source of the soil water could be determine as the rain fall of April 19th. This soil water recharge behavior was similar with the study of Tsujimura et al. (2007a) which determined that the recharges of ground water occur only on relatively large rainfall events. The relatively rapid depletion of volumetric soil water content at around 20 cm could be explained from water retaining capacity and stable isotope analysis. The downward water loss could be explained from relatively smaller water retaining capacity of soil depth at 20 – 50 cm than the other layers (Figure 33). The upward water loss could be

explained by stable isotope analysis. The isotopic compositions of the soil water shallower than 20 cm deviate significantly from the LMWL than the other layer (Figure 49) so that it indicates that soil water over 20 cm depth was strongly affected by evaporation. These two process, evaporation and the difference of water retaining capacity, caused the low volumetric soil water content at around 20 cm depth. There was no depletion observed at the depth around 70 – 90 cm depth, although stable isotope analysis showed that shrubs were utilizing water from those depths.

4. 4 Estimation of ET considering vegetation coverage

EV per unit area and TR per unit vegetation coverage area were determined by the chamber measurement. By combining these plot measurement by the chamber and the vegetation coverage of shrubs in the study area, the ET of the study area was estimated. As shown in sections 4.1 and 4.2, it was found that only PPFD was responsible for TR regardless of rainfall events, and that the only solar radiation which can be estimated from PPFD was responsible for EV in the dry period. Therefore, it is possible to estimate ET of the study area just by using PPFD. For estimation, dried day before sufficient rainfall on July 17th, 2009 with no herbaceous plants (July 14th, 2009), shortly after the rainfall event (July 21st, 2009) and dried day after a week from the rainfall event (July 25th, 2009) was chosen to estimate landscape scale ET. Fitted curve was derived from the measurement of EV and TR individually (Figure 56). The regression line derived from the multiple regression analysis was not employed because by calculating the regression line from each day measurement would enable to obtain more precise estimation. Fit curve was derived by least square regression. The type of the fit curve was determined when they had the largest value of R-square. The same equation for TR from shrubs was used for those three days estimation because TR from shrubs did not change among July. The equation for TR of shrubs was obtained as follows:

$$TRs_{hour} = R_p^{0.454} \times 0.0147 \quad (14)$$

where TRs_{hour} represents the TR from shrubs per hour (mm h^{-1}). On the other hand, TR from herbaceous plants and EV were determined for each day because its values varied. For July 14th, EV was determined as follows:

$$EV_{hour} = 5.39 \times 10^{-5} R_s + 0.0183 \quad (15)$$

For July 21st equations of TR and EV from herbaceous plants were obtained as:

$$TRh_{hour} = 7.085 \times 10^{-7} R_q{}^2 - 7.436 \times 10^{-4} + 0.9361 \quad (16)$$

$$EV = 2.018 \times 10^{-9} R_s^2 + 4.732 \times 10^{-5} R_s + 0.0146 \quad (17)$$

where TRh_{hour} represents TR from herbaceous plants per hour (mm h^{-1}). And for July 25th:

$$TRh_{hour} = -3.313 \times 10^{-7} R_q^2 + 7.042 \times 10^{-4} R_s + 0.0447 \quad (18)$$

$$EV = -2.758 \times 10^{-8} R_s^2 + 5.783 \times 10^{-5} R_s + 0.00423 \quad (19)$$

The TR at night time was assumed as zero because in general C_3 plants close their stomata during the night time to stop TR. The EV during night was estimated as 0.00423 - 0.0183 (mm h^{-1}) from the equation. This amount approximately agrees with the night time evaporation (0.011 mm h^{-1}) measured at 140 km northern from the Mandalgobi by Nakano et al. (2007). To estimate the daily variation, the solar radiation from the MG1 station was used because it was observed every 10 minutes all the day. A PPFD was estimated from the solar radiation by the equation (5). Subsequently, the ET of the study area was derived from equation:

$$ET_{day} = \int_0^{144} \left[\frac{aTR + (1-a)EV}{6} \right] dt \quad (16)$$

where a represents the vegetation coverage and ET_{day} represents ET per day (mm day^{-1}). To derive daily ET, integration was performed from 0 to 144 because the solar radiation data was measured 10 minutes interval by the MG1 station. The shrub vegetation coverage of 0.0312 determined from July 11th observation was substituted into the equation for July 14th. For July 21st and 25th, the vegetation coverage determined from July 29th observation was substituted which were 0.0386 for shrubs and 0.00689 for herbaceous plants. The results are shown in Figure 57, Figure 58 and Figure 59 with TR, EV and ET as a function of time variation. The amounts of vapor transferred from each component are listed on Table 8. ET was derived as about 0.6 - 1.00 mm per day from vegetated surface into the atmosphere. The ratio of TR to EV changed among each day. The result indicates that although the TR was

about larger than the EV on per unit area of vegetation coverage and bare soil, respectively, EV exceeds TR when it was considered with vegetation coverage. This ratio of TR to EV was smaller than that reported in other studies which took place under relatively similar climate conditions. For example, Yepez et al. (2003) determined that the TR accounted for 85% of ET during dry period of post-monsoon in semiarid savanna woodland. Tsujimura et al. (2007b) found the rate was 35-59% in semiarid grassland of north eastern Mongolia. On the shrub land of southern Arizona, Stannard and Weltz (2006) determined that the TR consists 84% of the ET. The difference of the TR-EV ratio between current study and the other would probably be result from the difference of the vegetation coverage in each study site. Indeed, the TR contributing ratio per one percent of vegetation coverage to the ET agreed well between current study and Stannard and Weltz (2006) had derived. The TR from one percent of vegetation coverage of shrub contributed about 5% for the ET in current study, while Stannard and Weltz (2006) found that TR from one percent vegetation coverage of desert zinnia contributed 4% of the total ET in landscape scale. Also, the elapse days from the rainfall event would change the TR-EV ratio. In this study, EV from bare soil increased significantly after the shortly after the rainfall events wile TR from shrubs did not change. This indicates that contribution ratio of TR from shrubs to ET would be much smaller shortly after the rainfall event.

Suppose there was no vegetation on the study area, the ET component would only be consisted of EV. The ET under this situation could be estimated by calculating the equation by substituting $a = 0$. The result was $ET_{day} = 0.87$ mm for July 14th, 2009. On the other hand, suppose the surface was all covered with shrubs ($a = 1$), the ET would be estimated as $ET_{day} = 4.94$ mm. This result indicates that the absence of shrubs probably not affects much in the total ET in this area. On the other hand, increase of shrubs significantly accelerates the ET by consuming the water at relatively deep soil layer.

Table 8 Information of the landscape scale TR, EV and ET.

Date	TR from shrubs (mm/day)	TR from herbaceous plants (mm/day)	EV (mm/day)	ET (total) (mm/day)
July 14th, 2009	0.150 (15%)		0.846 (85%)	1.00
July 21st, 2009	0.169 (18%)	0.121 (13%)	0.653 (69%)	0.943
July 25th, 2009	0.185 (31%)	0.0279 (5%)	0.382 (64%)	0.594

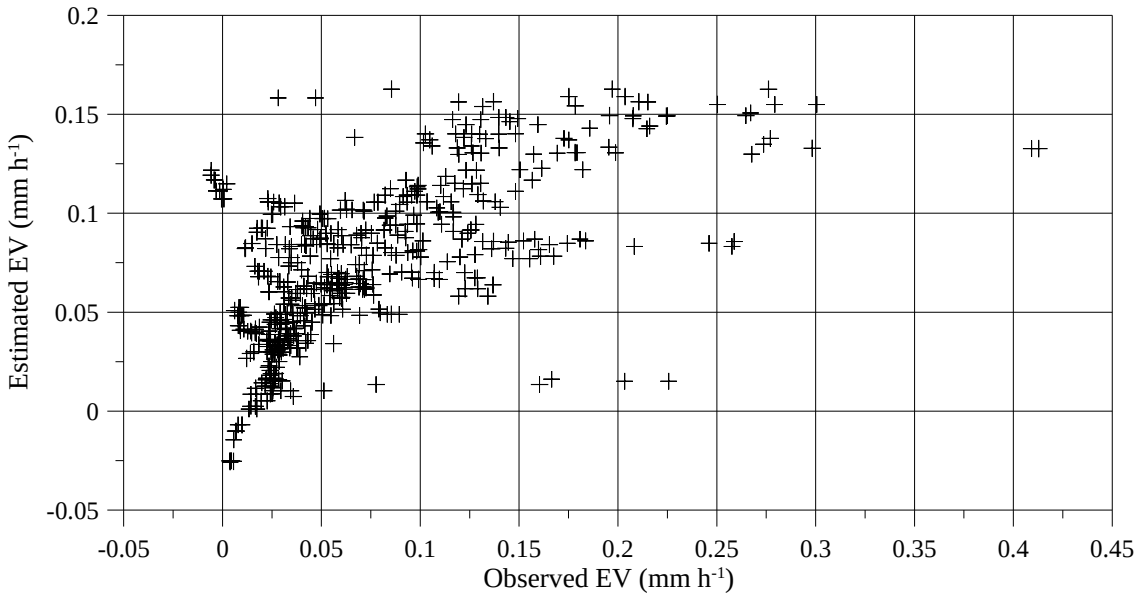

Figure 51 Relation between observed EV and Estimated EV from multiple regression analysis.

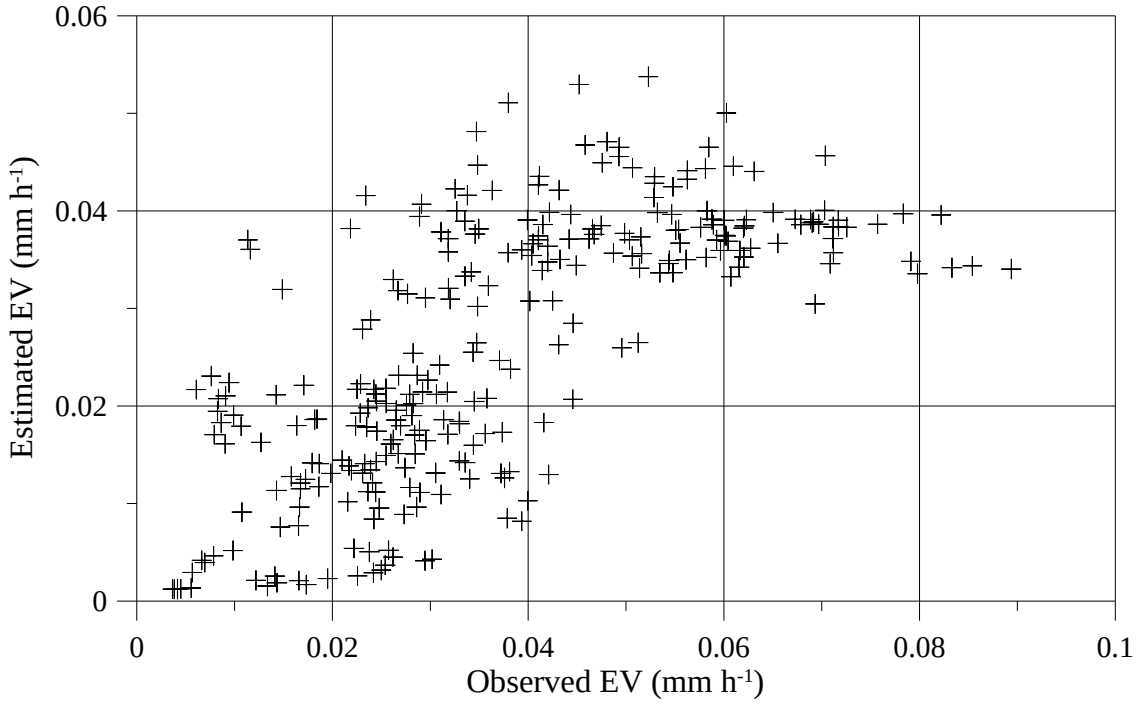

Figure 52 Relation between observed EV and Estimated EV from multiple regression analysis only on dry period with no effect of rainfall events.

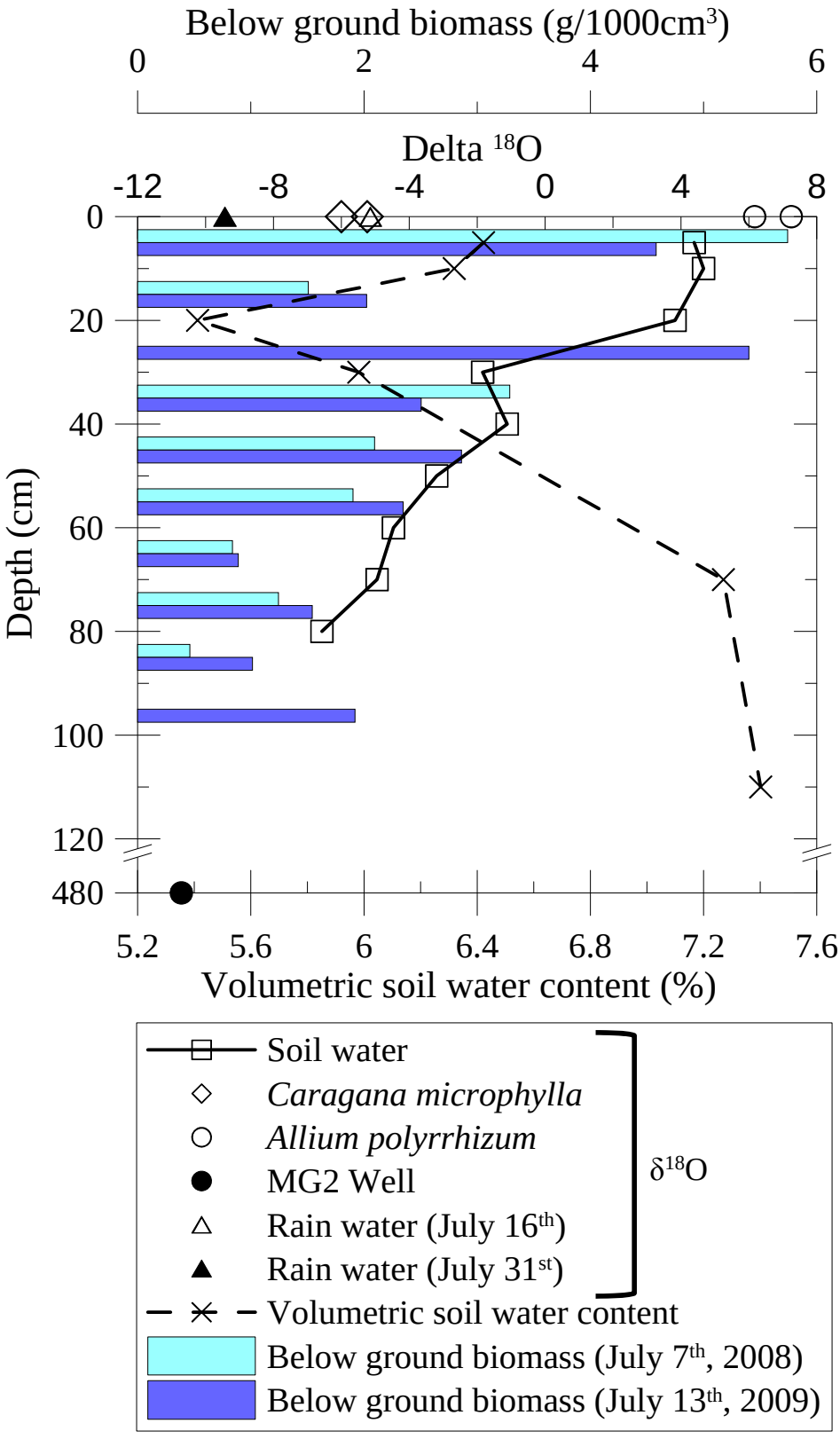

Figure 53 Vertical profile of $\delta^{18}O$, volumetric soil water distribution and below ground biomass of small sized roots.

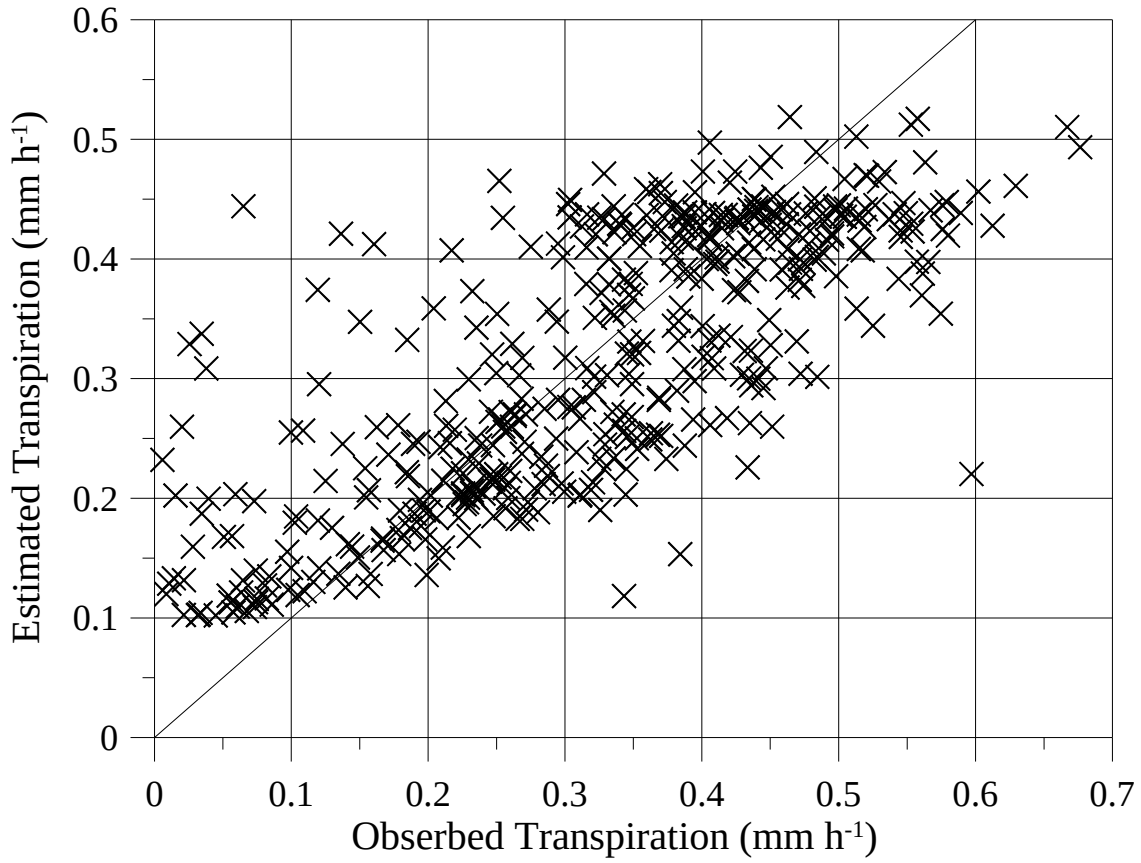

Figure 54 Relation between observed TR from shrubs on chamber measurement and estimated TR by multiple regression analysis.

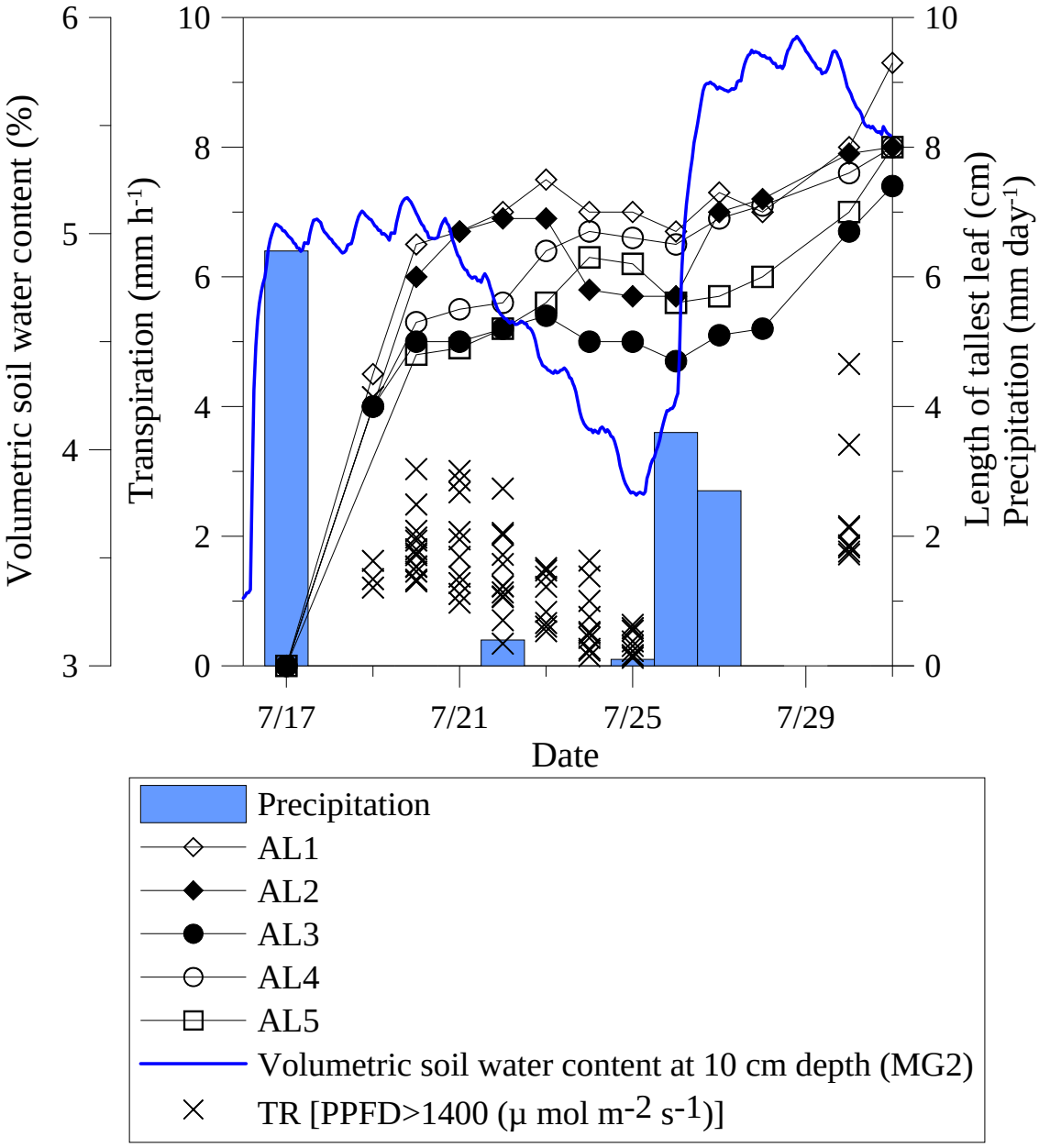

Figure 55 Relations between daily precipitation, volumetric soil water content at 10 cm depth measured on the MG2 station, TR from herbaceous plants when the PPFD was over 1400 (μ mol m^{-2} s^{-1}) and the length of tallest leaf in each AL sites.

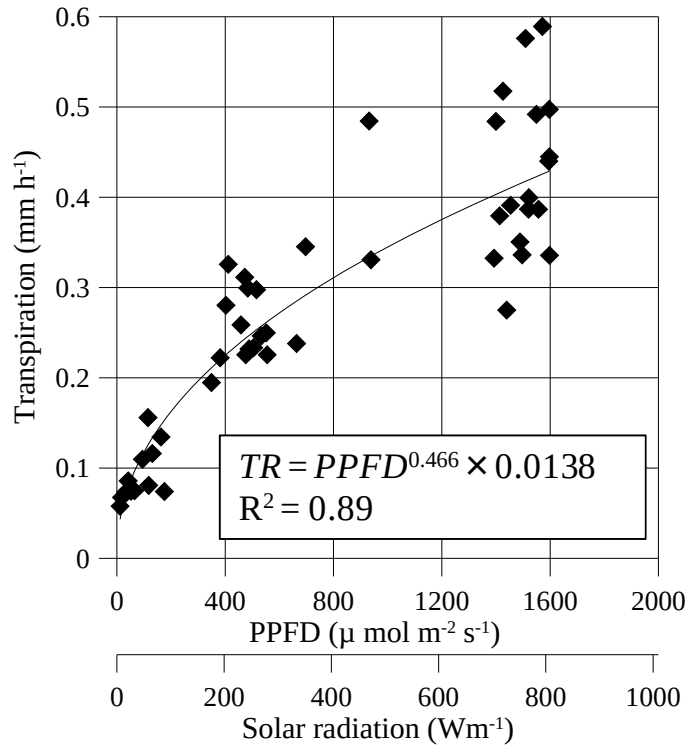

A

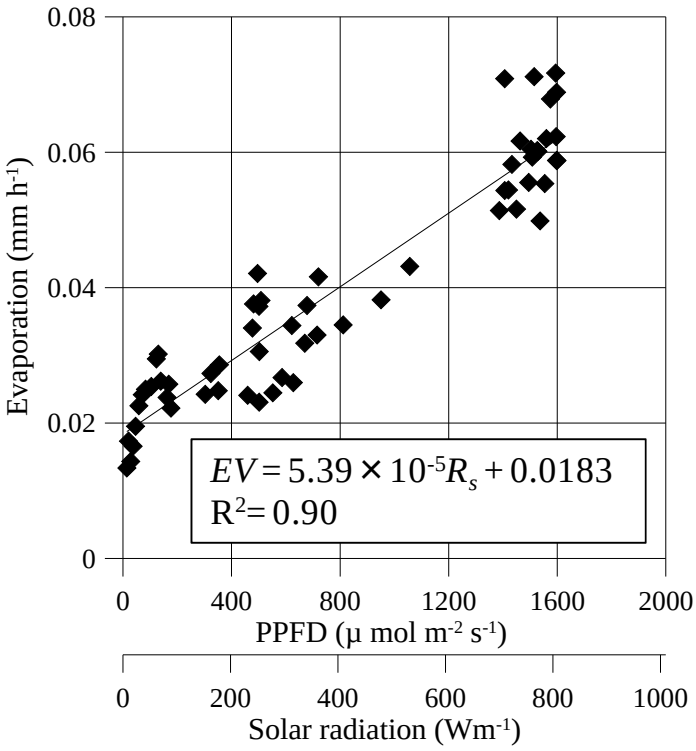

B

Figure 56 A: Relation between PPFD and TR from shrubs. B: Relation between solar radiation and EV. Both plots are measured on July 14th, 2009. Solid line indicates best fitted regression line.

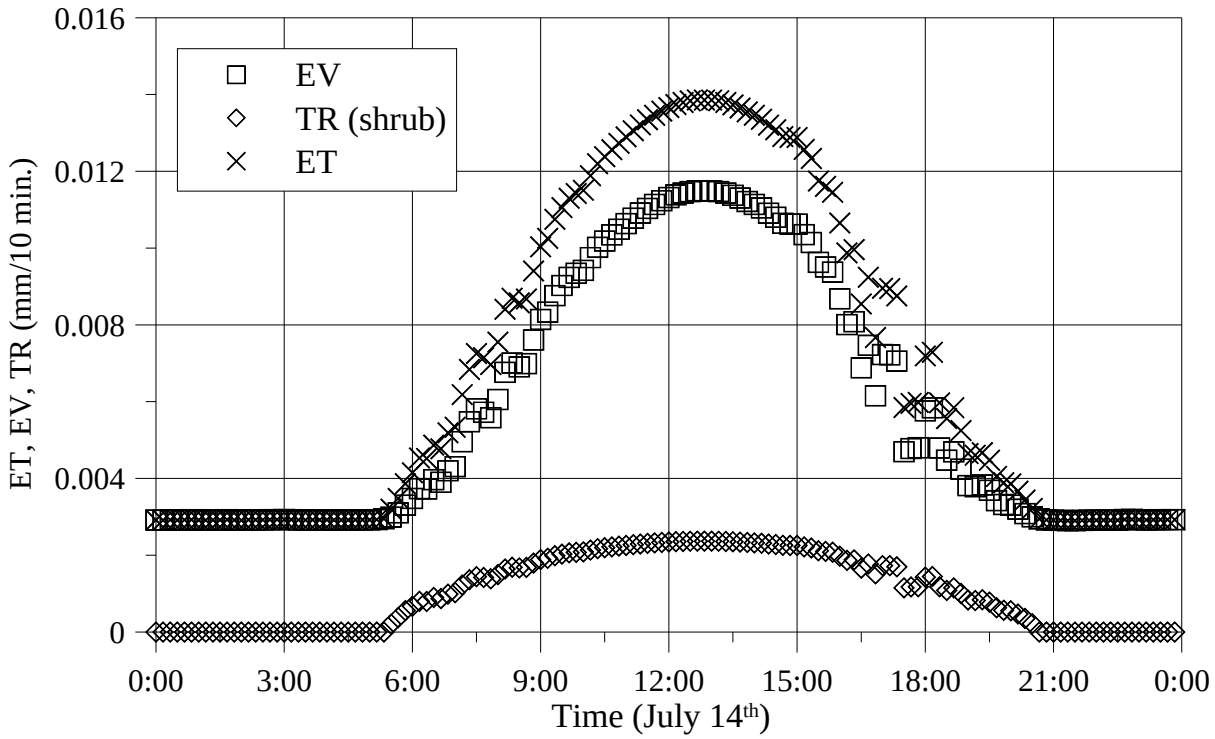

Figure 57 Time variation of estimated EV, TR and ET on July 14th, 2009.

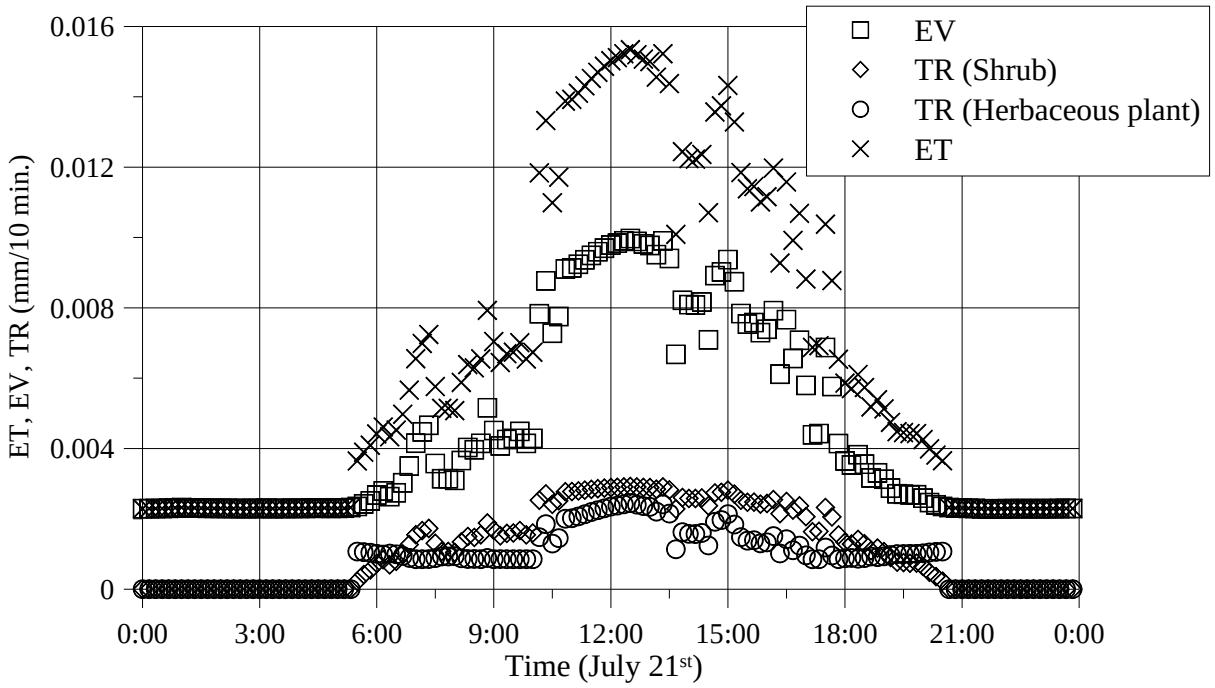

Figure 58 Time variation of estimated EV, TR (shrubs and herbaceous plants) and ET on July 21st, 2009.

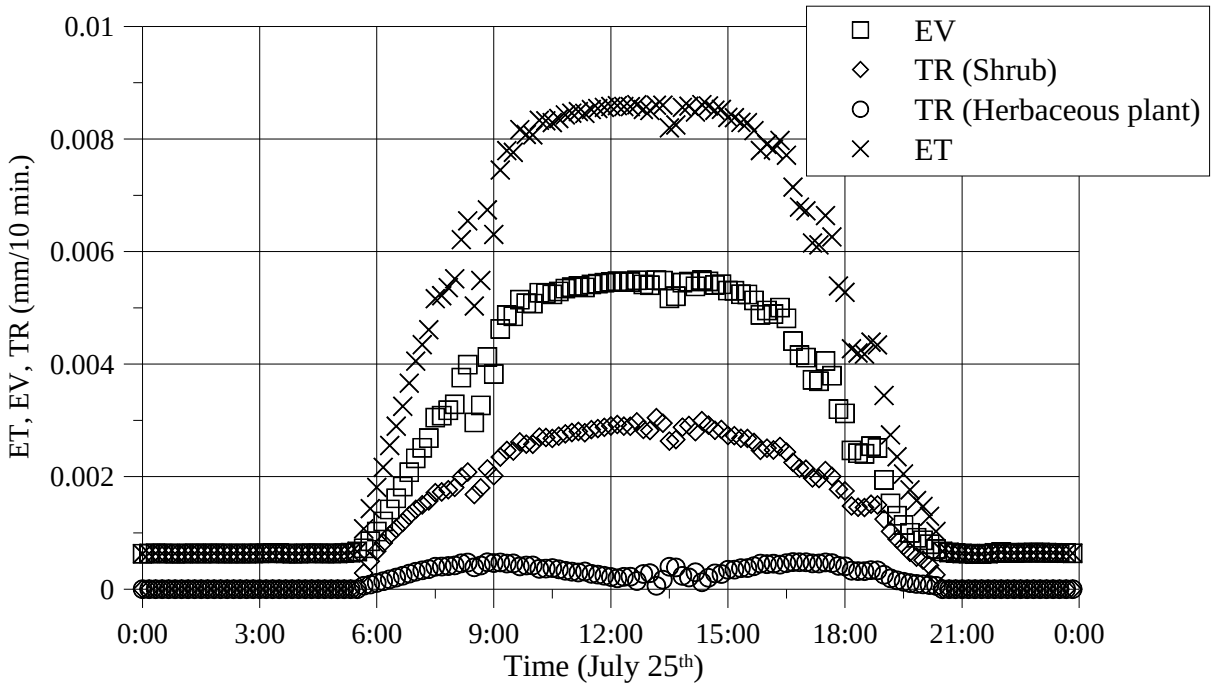

Figure 59 Time variation of estimated EV, TR (shrubs and herbaceous plants) and ET on July 25th, 2009.

5. Conclusion

The study was conducted in order to clarify the characteristics of vegetated surface-atmosphere water vapor transfer processes with consideration of soil water behavior and plant activity in an arid region of central Mongolia, using chamber measurement and stable isotope analysis of oxygen and hydrogen.

The results in the study are summarized as followings:

1. The evaporation increased rapidly shortly after the rainfall events. Contributing factor for the evaporation shortly after the rainfall was soil water temperature at 10 cm depth, specific humidity, air temperature and volumetric soil water content at 10 cm depth under the circumstance of steady wind speed. On the other hand, only the solar radiations are responsible for the EV on the dry period.
2. Shrubs transfer the water from around 70 to 90 cm depth soil water into the atmosphere before the rainfall event. After sufficient rainfall event, shrubs gradually shift the source of the soil water they utilize to the shallower depth. The transpiration changes with the volumetric soil water content at those depths. The PPFD is responsible for diurnal alteration of the TR from shrubs.
3. Herbaceous plants accelerate the vapor transfer from soil surface into the atmosphere shortly after the rainfall due to its physiological activity. Subsequently, capability of transportation declines with the depletion of soil water at the surface layer of the soil.
4. Stable isotope analysis indicates that shrubs and herbaceous plants compete with each other for the soil water even when the soil surface was sufficiently cultivated.
5. It will probably be difficult for herbaceous plants to grow in the future if climate condition followed the scenario of Sato et al. (2007) which predicts decrease of soil moisture on July due to the less precipitation and more evaporation.
6. Requires intense and heavy rainfall to cultivate soil water at deeper depth. In other words, most of the precipitation returns to the atmosphere immediately by evaporation and transpiration.
7. The ratio of transpiration to evapotranspiration is 15% on dry condition with only shrubs existing. This ratio is very small compared to other studies in similar climate condition.

Acknowledgments

The author wishes to express his sincere gratitude to his academic adviser, Professor Michiaki Sugita for his continuing guidance and encouragement.

Special thanks are expended to Dr. Tsutomu Yamanaka, Dr. Maki Tsujimura, Dr. Jun Asanuma, Professor Norio Tase, Mr. Tadaaki Urano Dr. Yuki Tosaki and Mr. Yutaka Abe for their guidance and helpful comments.

The author gives his thanks to Mr. Shintaro Yoshizawa, Mr. Yuich Morinaga, Mr. Ishgaldan Byambakhuu, Dr. Gombo Davaa, Dr. Dambaravjaa Oyunbaatar and others at Institute of Meteorology and Hydrology, Mongolia and Mongolian people who helped him in the field work.

This research was partly supported by the Research Institute for Humanity and Nature (project number D-04).

References

Byambakhuu, I. (1997): Assessment of regional land cover fraction of Mongolian semiarid and arid area based on multi-channel radiance data. Master thesis, Graduate School of Life and Environmental Sciences, University of Tsukuba. 86p.

Chapin, F. S. III., P. A. Matson and H. A. Mooney (2002): Principles of terrestrial ecosystem ecology. Springer. 90p.

Cohen, Y., M. Fuchs, V. Falkenflug and S. Moreshet (1988): Calibrated heat pulse method for determining water uptake in cotton. *Agronomy J*., **80**, 298-402.

Coplen, T. B., J. D. Wildman and J. Chen (1991): Improvements in the gaseous hydrogen-water equilibration technique for hydrogen isotope ratio analysis. *Anal. Chem.*, **63**, 910-912.

Craig, H. (1961): Isotopic variations in meteoric waters. *Science*, **133**, 1702-1703.

Davaa, G., D. Oyunbaatar and M. Sugita (2006): Surface water of Mongolia. モンゴル環境保全ハンドブック, 見聞社, 大阪, 55-68

Ehleringer, J. R., S. L. Philips, W. S. F. Schuster and D. R. Sandquist (1991): Differential utilization of summer rains by desert plants. *Oecologia*, **88**, 430-434.

Fu, H., S. Pei, Y. Chen and C. Wan (2007): Influence of shrubs on soil chemical properties in Alxa desert steppe, China. *USDA Forest Service RMRS-P-47*, 117-122.

Gat, J. R. and P. L. Airey (2006): Stable water isotopes in the atmosphere/biosphere/lithosphere interface: Scaling-up from the local to continental scale, under humid and dry conditions. *Global Planet. Change*, **51**, 25-33.

Gibson, J. J., S. J. Birks and T. W. D. Edwards (2008): Global prediction of δ_A and δ^2H-$\delta^{18}O$ evaporation slopes for lakes and soil water accounting for seasonality. *Global Biogeochem. Cycles*, **22**, GB2021.

Gochis, D. J., E. R. Vivoni and C. J. Watts (2009): The impact of soil depth on land surface energy and water fluxes in the North American Monsoon region. *J. Arid. Envr.*, In Press, Corrected Proof, 1-8.

Hirata, M., S. Kishikawa, A. Kondoh, T. Yamanaka, I. Kaihotsu, B. Damdin and A. Hongo (2009): Effects of some environmental factors on the plant growth in the central Mongolian Plateau. *Journal of Arid Land Studies*., **19-2**, 403-411 (in Japanese).

Heijmans, M. M. P. D., W. J. Arp and F. S. Chapin III (2004): Carbon dioxide and water vapour exchange from understory species in boreal forest. *Agric. For. Meteorol.*, **123**, 135-147.

Iizuka, S., T. Yamanaka and T. Tanaka (2004): Extraction of water from a plant for isotopic

measurement – pot experiments -. *Bull. Terr. Environ. Res. Ctr., Univ. Tsukuba*., **5**, 81-86 (in Japanese).

Kurc, S. A., and E. E. Small (2004): Dynamics of evapotranspiration in semiarid grassland and shrubland ecosystems during the summer monsoon season, central New Mexico. *Water Resour. Res.*, **40**, W09305.

Larcher, W. (2003): Physiological plant ecology: ecophysiology and stress physiology of functional groups. Springer. 513p

Li, S.-G, J. Asanuma, A. Kotani, G. Davaa and D. Oyunbaatar (2007): Evapotranspiration from a Mongolian steppe under grazing and its enviromnental constraints. *J. Hydrol.*, **333**, 133-143.

Mori, S. (2003): For the desirable jointing with the market economy (市場経済との望ましい接合を求めて). *Kagaku*, **73**, 594-598 (in Japanese).

Nakano, T., M. Manabu and M. Shinoda (2007): Measurement of nighttime water vapor flux using a closed chamber technique. *J. Agric. Meteorol.*, **63**, 103-107 (in Japanese).

Romero-Saltos, H., L. da S. L. Sternberg, M. Z. Moreira and D. C. Nepstad (2005): Rainfall exclusion in an eastern Amazonian forest alters soil water movement and depth of water uptake. *Am. J. Bot.*, **93**, 443-455.

Saandar, M. and M. Sugita (2005): Digital atlas of Mongolian natural environments (1) vegetation, soil, ecosystem and water. *Bull. Terr. Environ. Res. Ctr., Univ. Tsukuba*., 5, 75-76.

Sasaki, L. (2004): A stable isotope ratio fluctuation process with hydrological cycle in Kherlen river basin, Mongolia (モンゴル・ヘルレン川流域における水循環に伴う安定同位体比変動プロセス). Master thesis, Graduate School of Environmental Sciences, University of Tsukuba. 58p (in Japanese).

Schwartz, F. W. and H. Zhan (2002): Fundamentals of ground water. Wiley, NJ., USA.

Smith, D. M., P. G. Jarvis and J. C. W. Odongo (1997): Source of water used by trees and millet in Sahelian windbreak systems. *J. Hydrol.*, **198**, 140-153.

Socki, R. A., C. S. Romanek and E. K. Gibson Jr. (1999): On-line technique for measuring stable oxygen and hydrogen isotopes from microliter quantities of water. *Anal. Chem.*, **71**, 2250-2253.

Stannard, D. I. and M. A. Weltz (2006): Partitioning evapotranspiration in sparsely vegetated rangeland using a portable chamber. *Water Resour. Res*., **42**, W02413.

Sato, T., F. Kimura and A. Kitoh (2007): Projection of global warming onto regional precipitation over Mongolia using regional climate model. *J. Hydrol.*, **333**, 144-154.

Stott, P. (1994): Savanna landscapes and global environmental change. In N. Roberts (ed.),

The Changing Global Environment. Blackwell Publishers, Cambridge, pp. 287-303.

Sugita, M. (2003): Interactions of water cycle processes and ecosystems (水循環プロセスと生態系との係わり). *Kagaku*, **73**, 559-562 (in Japanese).

Sugita, M., J. Asanuma, M. Tsujimura, S. Mariko, M. Lu, F. Kimura, D. Azzaya and T. Adyasuren (2007): An overview of the rangelands atmosphere-hydrosphere-biosphere interaction study experiment in northeastern Asia (RAISE). *J. Hydrol.*, **333**, 3-20.

Tamura, K. (2003): For the conservation of soils on Mongolian glassland (モンゴル草原の土壌保全にむけて). *Kagaku*, **73**, 541-544 (in Japanese).

Tsujimura, M., Y. Abe, T. Tanaka, J. Shimada, S. Higuchi, T. Yamanaka, G. Davaa and D. Oyunbaatar (2007a): Stable isotopic and geochemical characteristics of groundwater in Kherlen River basin, a semi-arid region in eastern Mongolia. *J. Hydrol.*, **333**, 47-57.

Tsujimura, M., L. Sasaki, T. Yamanaka, A. Sugimoto, S.-G.. Li, D. Matsushima, A. Kotanib and M. Saandar (2007b): Vertical distribution of stable isotopic composition in atmospheric water vapor and subsurface water in grassland and forest sites, eastern Mongolia. *J. Hydrol.*, **333**, 35-46.

Udo S. O. and T. O. Aro (1999): Global PAR related to global soral radiation for central Nigeria. *Agric. For. Meteorol.*, **97**, 21-31.

United Nations Development Programme (2004): Access to water and sanitation services in Mongolia. Mongolia: United Nations.

Weltzin J. F. and G. R. McPherson (1997): Spatial and temporal soil moisture resource partitioning by trees and grasses in a temperate savanna, Arizona, USA. *Oecologia*, **112**, 156-164.

Wilson, K. B., P. J. Hanson, P. J. Mulholland, D. D. Baldocchi and S. D. Wullschleger (2001) A comparison of methods for determining forest evapotranspiration and its components: sap-flow, soil water budget, eddy covariance and catchment water balance. *Agric. For. Meteorol*., **106**, 153-168.

World Water Assessment Programme (2009): The United Nations World Water Development Report 3: Water in a Changing World. Paris: UNESCO, and London: Earthscan. 150-159.

Xu, H. and Y. Li (2006): Water-use strategy of three central Asian desert shrubs and their responses to rain pulse events. *Plant and Soil.*, **285**, 5-7.

Yabusaki, S. and N. Tase (2007): Formation process of vertical profile of stable isotopes in soil water at TERC. *Bull. Terr. Environ. Res. Ctr., Univ. Tsukuba.*, **8**, 17-16 (in

Japanese).

Yamanaka, T., M. Daigo and M. Hirota (2010): Competition for water alters root water up take profile of plants.

Yamanaka, T., I. Kaihotsu and D. Oyunbaatar (2003): Temperature effect on soil water content measured by time domain reflectometry and its correction using in situ data. *Bull. Terr. Environ. Res. Ctr., Univ. Tsukuba*., **16**, 246-254 (in Japanese).

Yamanaka, T. and J. Shimada (1997): Simple but reliable method to extract soil water for stable isotope analysis. *J. Japan Soc. Hydrol. & Water Resour*., **10 (2)**, 181-184 (in Japanese).

Yamanaka, T., M. Tsujimura, D. Oyunbaatar, and G. Davaa (2007a): Isotopic variation of precipitation over eastern Mongolia and its implication for the atmospheric water cycle. *J. Hydrol.*, **333**, 21-34.

Yamanaka, T., I. Kaihotsu, D. Oyunbaatar, T. Ganbold (2007b): Summertime soil hydrological cycle and surface energy balance on the Mongolian steppe. *J. Arid Envr.*, **69**, 65-79.

Yasunari, T. (2003): How did Mongolian grassland maintained? : Preface of ecological climatology (モンゴル草原はどう維持されてきたか？：生態気候システム学的序説). *Kagaku*, **73**, 555-558 (in Japanese).

Yepez, E. A., D. G. Williams, R. L. Scott and G. Lin (2003): Partitioning overstory and understory evapotranspiration in a semiarid savanna woodland from the isotopic composition of water vapor. *Agric. For. Meteorol*., **119**, 53-68.

Yepez, E. A., T. E. Huxman, D. D. Ignace, N. B. English, J. F. Weltzin, A. E. Castellanos and D. G. Williams (2005): Dynamics of transpiration and evaporation following moisture pulse in semiarid grassland: A chamber-based isotope method for partitioning fluc components. *Agric. For. Meteorol.* **132**, 359-376.

Zenchich, S. J., R. H. Froend, J. V. Turner and V. Gailitis (2002): Influence of groundwater depth on the seasonal sources of water accessed by *Banksia* tree species on a shallow, sandy coastal aquifer. *Oecologia*, **131**, 8-19.